An Experimental and Numerical Analysis of Soluble Reactive Phosphorus Removal Mechanisms in Surface-Flow Constructed Stormwater Wetlands Using Soil Amendment Strategies

By

Kaitlin Elizabeth Vacca

Dissertation
Submitted to Department of Civil and Environmental Engineering
College of Engineering
Villanova University
in partial fulfillment of the requirements
for the degree of

DOCTOR OF PHILOSOPHY

In

Civil and Environmental Engineering

Water Resources

May, 2013

Villanova, Pennsylvania

UMI Number: 3560917

All rights reserved

INFORMATION TO ALL USERS
The quality of this reproduction is dependent upon the quality of the copy submitted.

In the unlikely event that the author did not send a complete manuscript
and there are missing pages, these will be noted. Also, if material had to be removed,
a note will indicate the deletion.

UMI 3560917

Published by ProQuest LLC (2013). Copyright in the Dissertation held by the Author.

Microform Edition © ProQuest LLC.
All rights reserved. This work is protected against
unauthorized copying under Title 17, United States Code

ProQuest LLC.
789 East Eisenhower Parkway
P.O. Box 1346
Ann Arbor, MI 48106 - 1346

Copyright © 2013 by Kaitlin Elizabeth Vacca
All Rights Reserved

STATEMENT BY AUTHOR

This dissertation has been submitted in partial fulfillment of requirements for the degree of Doctor of Philosophy at Villanova University and is deposited in the University Library to be made available to borrowers under rules of the Library.

Brief quotations from this dissertation are allowable without special permission, provided that accurate acknowledgement of source is made. Requests for permission for extended quotation from or reproduction of this manuscript in whole or in part may be granted by the head of the major department or the Associate Dean for Graduate Studies and Research of the College of Engineering when in his or her judgment the proposed use of the material is in the interests of scholarship. In all other instances, however, permission must be obtained from the author.

Acknowledgements

I have far too many individuals that I need to thank and acknowledge for having put up with my over the past several years. I could not possibly name them all. Without the constructive criticism, guidance, challenge, and support from each of my committee members (Dr. Traver, Dr. Wadzuk, Dr. Komlos, Dr. Gilbert-Jennings, and Dr. Davis), this research would not have come to fruition. I owe particular gratitude to Dr. Komlos who continually challenged me to be the best with everything I do and encouraged me throughout the entire process. To Dr. Traver who has always been on my side as a growing PhD candidate. He not only was able to find support for me financially, but put his faith in me as a leader and valued my opinions as I came into my own. My gratitude to him is limitless. I cannot thank my advisor, Dr. Wadzuk, nearly enough. You have put just as much effort into my dissertation as I have. You are tough and ask a lot, but you do it with grace and patience. I genuinely would not have finished this if you were not my advisor. Thank you for every late night email response, for every pep-talk, and for all the laughter and fun to make this more enjoyable.

I have to thank my friends and family, specifically my sister Rosemary, brother Josh, and brother Pat who never missed a moment to make fun of me for "putting water through dirt." I love you guys and am grateful that you are never impressed by anything I do because it keeps me humble and level-headed. Lastly, my parents are easily the people I need to thank the most. I have been a student for a very long time and they never told me not to follow through on what I set out to do. They always gave me emotional and financial support as I needed it. My mother came and helped me run soil tests or plant plants often without asking for anything in return. They are hands-down the best people I know and I will never be able to repay them, but I look forward to trying.

Dedication

This dissertation is dedicated to my Nana, whom I lost this past year. You are missed.

Table of Contents

List of Figures viii
List of Tables x
Nomenclature xiii
Abstract xiv
Chapter 1 Introduction 1
1.1 Background 1
1.2 Objectives of this Study 6
1.3 Organization of Report 6
Chapter 2 Literature Review 8
2.1 Urban Stormwater Runoff: Pollutants 8
2.2 Phosphorus 9
2.3 Stormwater Control Measures 10
2.4 Removal Mechanisms of SRP and Soil Amendments 13
2.5 Soil Amendments 16
2.6 Mesocosm Studies 19
Chapter 3 Research Methodology 21
3.1 Research Methods 21
3.2 Mesocosm Design and Construction 22
3.2.1 Phase I 22
3.2.2 Phase II 30
3.3 Pore Water Analysis 39
3.4 Soil Analyses 42
3.4.1 Chemical Characteristics of Soil Matrices 43
3.4.2 Physical Characteristics of Soil Matrices 50
3.5 Statistical Analyses 52
Chapter 4 Phase I Analysis Examining Fate and Transport of SRP 53
4.1 Pore Water Analysis Results and Discussion 54
4.2 Soil Chemical Analysis Results and Discussion 65
4.3 Summary 67
Chapter 5 Phase II Results and Discussion of Soil Amendment Experimental Runs 70
5.1 Preliminary Soil Chemical Analysis Results 70
5.2 Pore Water Analysis Results and Discussion 73
5.3 Soil Analysis Results and Discussion 97

5.3.1 Chemical Analysis 98
5.3.2 Physical Analysis 107
5.4 Aluminum WTR 5% Mix 112
5.5 Summary and Conclusions 113
Chapter 6 Vertical and Horizontal Flow Mechanisms 116
Chapter 7 Conclusions and Future Work 126
7.1 Summary and Conclusions 126
7.2 Future Work 133
Works Cited 135
APPENDIX A: Phase I Raw Data 143
APPENDIX B: Phase II 150
APPENDIX C: Model Results 173

List of Figures

Figure 1.1. Phosphorus storages and transfers in the wetland environment. 3
Figure 2.1. Speciation diagram of phosphoric acid 10
Figure 2.2. Rhizosphere oxygenation. 18
Figure 3.1. Experimental set-up in greenhouse during phase I. 24
Figure 3.2. Photographs and technical sketch of non-vegetated, 15.2 cm mesocosm. 27
Figure 3.3. Typical port construction in phase I. 28
Figure 3.4. Photographs and technical sketch of vegetated, 25.4 cm mesocosm.. 29
Figure 3.5. Typical port construction in phase II. 30
Figure 3.6. Phase II experimental set-up in Villanova's research greenhouse. 32
Figure 3.7. Phase II plants. 33
Figure 3.8. Peristaltic pump orientation for phase II experimental design.. 34
Figure 3.9. Phase II iron (III) coated sand soil mixture. 37
Figure 3.10. Soil core extraction method. 47
Figure 4.1. Phosphorus and chloride concentrations from the non-vegetated mesocosm pore water results 56
Figure 4.2. Mass SRP removed and percent SRP removal values of all eight, 24-hr, test simulations. 58
Figure 4.3. Results of the seven day analysis where four days of SRP and chloride dosed water was followed by three days of no surface flow. 59
Figure 4.4. Phosphorus and chloride concentrations from the vegetated mesocosm pore water results 61
Figure 4.5. Contour plot of chloride C/C_o values from the vegetated mesocosm at t=24 hrs in phase I. 61
Figure 4.6. Trend of SRP retention over the course of eight 24-hr tests in the vegetated mesocosm. 63
Figure 4.7. Results from P leaching analysis in the vegetated mesocosm. 64
Figure 5.1. P sorption isotherm for control mesocosm soil. 71
Figure 5.2. A typical flow regime for all wetland mesocosm studies. 74
Figure 5.3. Mass SRP and percent removal values shown each week over a 4 week duration. 76
Figure 5.4. Mass SRP and percent removal values shown each week over the duration of each extended study. 77
Figure 5.5. Average Fe (II) concentrations including both 3 and 8 cm samples 79
Figure 5.6. Ferrozine assay results for Control mesocosm over 10 weeks. 82
Figure 5.7. Ferrozine assay results for Control and FeP mesocosms over 10 weeks.. 85
Figure 5.8. Fe (II) concentrations for control, FeP, and Fe mesocosms over 10 weeks. .. 86
Figure 5.9. Photographs of Fe soil after a 10 week experimental run. 87
Figure 5.10. Comparison of soil between the Fe and FeP mesocosms. 87
Figure 5.11. P sorption capacity compared to percent removal of SRP 100
Figure 5.12. Oxalate extractable P, Fe, and Al in initial soil sample. 101
Figure 5.13. Oxalate extractable P. All final soil samples were taken at the 4 weeks. 104
Figure 5.14. Typical grain size distribution of mesocosm soil. 108
Figure 6.1. Modeling snapshots from HYDRUS 2-D numerical model. 119
Figure 6.2. Control mesocosm study of chloride tracer and SRP fate and transport. 122

Figure 6.3. FeP mesocosm study of chloride tracer and SRP fate and transport 125
Figure B.1. Temperature and relative humidity data from phase II study. 163
Figure B.2. P sorption isotherm data for the control, FeP, and Fe mesocosms. 164
Figure B.3. P sorption isotherm data for the Al 2 and Al 2D mesocosms. 165
Figure B.4. P sorption isotherm data for the Al 5D and Al 8 mesocosms. 166
Figure B.5. Chloride tracer study, 3D graphs showing equilibrium had fully been reached by week two for the control mesocosm. 167
Figure B.6. Chloride tracer study, 3D graphs showing equilibrium had fully been reached by week two for the FeP mesocosm. 167
Figure B.7. Chloride tracer study, 3D graphs showing equilibrium had fully been reached by week two for the Fe mesocosm. 168
Figure B.8. Chloride tracer study, 3D graphs showing equilibrium had fully been reached by week two for the Al 2 mesocosm. 168
Figure B.9. Chloride tracer study, 3D graphs showing equilibrium had fully been reached by week two for the Al 5D mesocosm. 169
Figure B.10. Chloride tracer study, 3D graphs showing equilibrium had fully been reached by week two for the Al 8 mesocosm. 169
Figure B.11. Chloride tracer study, 3D graphs showing equilibrium had fully been reached by week two for the Al 5 mesocosm. 170
Figure B.12. Typical flow rates for all mesocosm studies over respective durations. ... 171
Figure B.13. Results from the hydrometer and grain size analysis for each mesocosm initial soil sample. 172
Figure C.1. Contour plot of actual SRP and chloride concentrations at each port location over a four week period for the Fe mesocosm. 174
Figure C.2. Contour plot of actual SRP and chloride concentrations at each port location over a four week period for the Al 2 mesocosm. 175
Figure C.3 Contour plot of actual SRP and chloride concentrations at each port location over a four week period for the Al 2D mesocosm. 176
Figure C.4. Contour plot of actual SRP and chloride concentrations at each port location over a four week period for the Al 5D mesocosm. 177
Figure C.5 Contour plot of actual SRP and chloride concentrations at each port location over a four week period for the Al 8 mesocosm. 178
Figure C.6. Contour plot of actual SRP and chloride concentrations at each port location over a four week period for the Al 5 mesocosm. 179

List of Tables

Table 1.1. Forms of phosphorus 2
Table 3.1. Summary of phase I flow values, consisting of eight-24 hour experimental runs in each mesocosm. 24
Table 3.2. Summary of phase I flow values, reflecting the seven day study. 26
Table 3.3. Mesocosm identification, description of study, and length in weeks. 31
Table 3.4. Average flow rates, standard deviations, and n values for each mesocosm over the entire duration of each experimental run. 35
Table 3.5. The mass of wetland soil and respective amendments. 39
Table 3.6. Characteristic depths of soil plugs. 46
Table 3.7. Oxalate Extraction Samples 47
Table 3.8. Results from soil pH study in phase II. 49
Table 3.9. Summary of mass of soil matrix mixture, mass of amendment added (kg), and resulting effective porosity. 51
Table 4.1. Average flow rates of non-vegetated and vegetated mesocosms. 53
Table 4.2. Influent concentrations of SRP in non-vegetated mesocosm. 54
Table 4.3. Mass SRP input and output values for all eight 24-hr test simulations in the non-vegetated mesocosm. 57
Table 4.4. Mass SRP summary of eight, 24 hr experimental runs in phase I vegetated mesocosm. 60
Table 4.5. Mass SRP input and output values for all eight 24-hr test simulations in the vegetated mesocosm study. 63
Table 4.6. Results from oxalate extraction in phase I. 66
Table 4.7. Summary of oxalate extractions after all eight, 24 hr dosing experiments were completed. 66
Table 5.1. Average inlet concentrations of SRP, P sorption capacity at average inlet concentrations 72
Table 5.2. Average flow rates of all mesocosms.. 73
Table 5.3. Influent concentrations of SRP and chloride, mass of SRP input per week 75
Table 5.4. Summary table for all mesocosms reported at 4 weeks. 78
Table 5.5. Summary table for control mesocosm. 80
Table 5.6. Results of control pore water analysis. 81
Table 5.7. Summary table for of influent SRP and chloride values 83
Table 5.8. Results of FeP pore water analysis. 83
Table 5.9. Summary table of influent SRP and chloride values, shown for the control, FeP, and Fe mesocosms.. 85
Table 5.10. Summary of pore water SRP removal in control, FeP, and Fe mesocosms over a four and 10 week duration. 88
Table 5.11. Summary table of iron (III) coated sand mesocosm study in comparison with the control. 89
Table 5.12. Influent SRP and chloride values, mass SRP input, and influent flow rates presented for the control, Al 2, and Al 2D mesocosm. 90
Table 5.13. Summary of mass SRP removal in the control, Al 2, and Al 2D mesocosms over a four week study. 91

Table 5.14. Influent SRP and chloride values, mass SRP input, and influent flow rates are presented for the control, Al 2, Al 2D, and Al 5D mesocosm 92
Table 5.15. Summary of mass SRP removal in the control, Al 2, Al 2D, and Al 5D mesocosms over the durations noted.. 93
Table 5.16. Influent SRP and chloride values, mass SRP input, and influent flow rates are presented for the control, Al 2, Al 2D, Al 5D, and Al 8 mesocosm 94
Table 5.17. Summary of mass SRP removal in the control, and all Al WTR mesocosms over the durations noted.. 95
Table 5.18. Summary of phase II results for t=4weeks. 95
Table 5.19. Summary of pore water analyses in control and Al WTR amended mesocosms. 96
Table 5.20. Average inlet concentrations of SRP, P sorption capacity at average inlet concentrations, and mass removal values are reported for all mesocosms 99
Table 5.21. Oxalate extractable P, Fe, and Al from each mesocosm.. 100
Table 5.22. Results of the P sorption analysis and oxalate extraction are presented 102
Table 5.23. Oxalate extraction for all mesocosms over a four week study.. 103
Table 5.24. Comparison between dry mass of amendments. 106
Table 5.25. USDA classification of each soil mixture 109
Table 5.26. Porosity, organic matter, and percent SRP removal values. 110
Table 5.27. Saturated hydraulic conductivity values in m hr^{-1} (K_{sat}) 111
Table 5.28. Summary of mass SRP input, output, removed, and percent removal values for all mesocosms with the inclusion of Al 5.. 112
Table 5.29 Summary of Al added via Al WTR for all mesocosms 113
Table 5.30. P sorption results showing all mesocosms 113
Table 5.31. Summary of mass SRP input, output, removed, and percent removal values for all mesocosms with the inclusion of Al 5.. 113
Table 6.1. Physical soil characteristics, including projected and actual hydraulic conductivity values 116
Table 6.2. HYDRUS parameters. 118
Table A.1. Non-vegetated raw SRP concentrations all tests 1-8. 144
Table A.2. Non-vegetated raw SRP concentrations by horizontal port location 145
Table A.3. Non-vegetated raw SRP concentrations by vertical port location 146
Table A.4. Vegetated raw SRP concentrations all tests 1-8 147
Table A.5. Vegetated raw SRP concentrations by vertical port location 148
Table A.6. P sorption isotherm values for t=24hrs and t=48hrs. 149
Table A.7. Raw data from oxalate analysis in phase I. 149
Table B.1. Raw SRP data for control mesocosm study. 151
Table B.2. Raw SRP data for FeP mesocosm study. 151
Table B.3. Raw SRP data for Fe mesocosm study. 152
Table B.4. Raw SRP data for Al 2 mesocosm study. 152
Table B.5. Raw SRP data for Al 2D mesocosm study 153
Table B.6. Raw SRP data for Al 5D mesocosm study 153
Table B.7. Raw SRP data for Al 8 mesocosm study. 154
Table B.8. Raw SRP data for Al 5 mesocosm study. 154
Table B.9. Fe (II) concentrations for control mesocosm over a 12 week study. 155

Table B.10. Fe (II) concentrations for FeP mesocosm over a 12 week study. 155
Table B.11. Fe (II) concentrations for Fe mesocosm over a 12 week study..... 156
Table B.12. Raw data from oxalate extractions in control mesocosm study. 157
Table B.13. Raw data from oxalate extractions in FeP mesocosm study. 158
Table B.14. Raw data from oxalate extractions in Fe mesocosm study. 159
Table B.15. Raw data from oxalate extractions in Al 2 mesocosm study. 160
Table B.16. Raw data from oxalate extractions in Al 2D mesocosm study. 160
Table B.17. Raw data from oxalate extractions in Al 5D mesocosm study. 161
Table B.18. Raw data from oxalate extractions in Al 8 mesocosm study. 162

Nomenclature

A	Area
Al	Aluminum
Al WTR	Aluminum Water Treatment Residual
Al_{ox}	Oxalate extractable Al content of dried soil
C	Concentration at port location
CSW	Constructed Stormwater Wetland
Fe (III)	Iron III
Fe_{ox}	Oxalate extractable Fe content of dried soil
G_s	Specific gravity
h	head
k	A constant related to the bonding energy
K_{sat}	Saturated hydraulic conductivity
K_{satl}	Latitudinal saturated hydraulic conductivity
K_{satv}	Vertical saturated hydraulic conductivity
L	length of sample
OM	Organic matter
PO_4-P	Phosphate measured as Phosphorus
P_{ox}	Oxalate extractable P content of dried soil
PP	Particulate Phosphorus
Q	Flow rate at port location
S	Total amount of P retained
S’	P retained by the solid phase
SCM	Stormwater Control Measure
S_{max}	P sorption maximum
S_o	P originally sorbed on the solid phase (previously adsorbed P)
SP	Soluble Phosphorus
SRP	Soluble Reactive Phosphorus
t_i	Duration of experimental run
TP	Total Phosphorus
w	Moisture content
γ_d	Dry unit weight
γ_t	Unit weight of soil
γ_w	Unit weight of water
η	Porosity

Abstract

Constructed stormwater wetland (CSW) systems were previously reported to be effective for phosphorus (P) removal in the stormwater control community. However, recent studies have found that CSWs are no longer valuable P retention tools past a certain point in their lifetime especially when the dominant form of P is soluble. It is the soluble inorganic form of P (soluble reactive P or SRP) that causes excessive algae growth, which leads to eutrophication, diminished macrophyte, periphyton, benthic, and fish communities, and depleted oxygen levels.

The results presented in this research focused on the fate and transport of soluble reactive phosphorus (SRP) in a surface-flow constructed stormwater wetland. A two-phased laboratory mesocosm approach was used to study SRP fate and transport. The phase I objective was to observe and measure SRP pathways through a surface-flow CSW soil profile through a nonvegetated and vegetated mesocosm. Pore water samples were taken at various vertical depths (0, 3, and 8 cm) and horizontal locations throughout the soil profile, analyzed for SRP, and in some instances, chloride. Results from phase I showed there were both horizontal and vertical flow characteristics that ultimately affected SRP movement through the soil profile. Surface water had not fully infiltrated all horizontal and vertical depths prior to the end of the 24 hr experimental replicates. More SRP removal was observed at the inlet region of the mesocosm and within the top 3 cm. There was mass SRP removed within both the nonvegetated and vegetated mesocosms, indicating that sorption processes were the main mechanism of SRP removal as opposed to plant uptake.

Phase II consisted of soil amendments mixed into wetland soil taken directly from Villanova University's CSW. Two soil amendments were used in phase II: Iron [Fe (III)] coated sand and Aluminum Water Treatment Residuals (Al WTR). Mesocosms were constructed similarly to phase I. Seven mesocosm studies were employed in phase II: a control, 5% iron coated sand by dry mass WITH plants (FeP), 5% iron coated sand by dry mass WITHOUT plants (Fe), and 2%, 2% duplicate, 5%, and 8% mix by dry mass of Al WTR. A P sorption isotherm analysis determined that the P sorption capacity of the control mesocosm (390 mg kg^{-1}) was within the range of both the FeP and Fe mesocosms (380 mg kg^{-1}), suggesting SRP removal would be comparable between these three mesocosms. Conversely, the P sorption capacity increases as more Al WTR was added to the original wetland soil (590 mg kg^{-1} ~ 900 mg kg^{-1}), suggesting mesocosms amended with Al WTR will provide the greatest SRP removal based on its chemical characteristics.

Overall, the mesocosms amended with Fe (III) coated sand provided the largest mass of SRP removal amongst all added amendments. The pore water analysis for the mesocosms amended with Al WTR showed that the WTR provided less SRP removal than the control although the initial P sorption capacities were greater in the amended soil than the control. It was thought that the physics are inhibiting the chemical reaction from occurring. A similar conclusion can be made for the soil amended with Fe (III) coated sand: SRP removal using soil amendments is not solely dependent upon the amendment's chemical characteristics, but is also dependent upon its physical and subsequently hydraulic characteristics.

Chapter 1 Introduction

1.1 Background

Urbanization contributes to increased stormwater runoff due to decreased pervious surfaces (NRC, 2008; Rosenquist, et al., 2010). As more runoff is transmitted to surrounding bodies of water, hydrologic and ecologic patterns are altered. Runoff carries large amounts of sediments, nutrients, metals, and hydrocarbons that impact stream and aquatic health (USEPA, 2005). Depending on climate, geography and water body uses, different pollutants may be considered a priority for removal. In many areas, such as the Chesapeake Bay watershed and urban environments, the necessary control of nonpoint source nutrients nitrogen (N) and phosphorus (P) has been identified (Barth, 1995; Boesch, et al., 2001).

With an ever pressing concern for management and treatment of stormwater runoff, stormwater control measures (SCMs) are being recommended and implemented throughout the urban landscape to help meet water quality requirements. These engineered, ecological systems are used in place of conventional stormwater infrastructure and can assist with both flood mitigation and water quality control. Urban streams have some of the highest N and total P levels observed (only second to agricultural streams) and are often found to be as high as those in agricultural areas (Barth, 1995). In surplus, these nutrients can cause excessive biotic growth in natural waterways. Therefore, maintaining safe levels of each nutrient is critical for the prevention of eutrophication, protection of macrophyte, periphyton, benthic, and fish

communities, and sustaining oxygen levels for aquatic life (USEPA, 2005; Sharpley, et al., 1999).

One nutrient, phosphorus (P), is often considered the limiting nutrient in freshwater ecosystems, and if found in excess, P contributes to eutrophication through algal blooms (as a result of depleting the dissolved oxygen, thus wreaking havoc on the aquatic ecosystem). Atmospheric deposition, fertilizers, failing septic systems, pet wastes, and collection of organic matter are possible sources of P in urban stormwater runoff (Ann, Y. et al., 2000). Phosphorus exists in two forms: insoluble (particulate) P (PP) and soluble P (SP) (Table 1.1); of which there are three main mechanisms of removal: sedimentation through adsorption, precipitation of insoluble phosphates, and binding of P within organic matter (Figure 1.1). Soluble organic P and all insoluble forms of P are generally not available for plant uptake; however, it is possible that these forms, depending on how they are bound within the soil layer, can transform into the soluble inorganic form that is biologically available for plant growth. These transformations and existence of the element within a sedimentary cycle make it difficult to quantify and understand this nutrient's fate and transport within a natural ecosystem (Odum, 1988).

Table 1.1**.** Forms of phosphorus (adapted from Mitsch and Gosselink, 2000).

	Organic	Inorganic
Soluble	Dissoved Organics	Orthophosphates Polyphosphates Ferric Phosphate Calcium Phosphate
Insoluble	P bound in organic matter	Clay-Phosphate Complexes Metal Hydroxide Phosphates Minerals

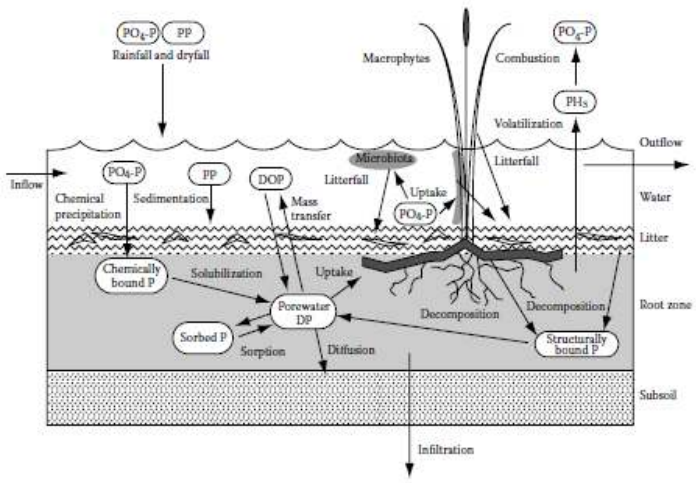

Figure 1.1. Phosphorus storages and transfers in the wetland environment. PO_4–P = orthophosphate; PP = particulate phosphorus; DP = dissolved phosphorus; DOP = dissolved organic phosphorus; PH_3 = phosphine. PP may consist of all the forms shown in the root zone. (Kadlec, Knight, 1996).

The soluble inorganic form of P has been shown to directly affect algal growth, consequently causing eutrophic conditions (Fozzard, et al., 1999; Fisher, 1992). More specifically, it is the biologically available form of P (orthophosphate), measured analytically as soluble reactive phosphorus (SRP), that must be managed and removed from urban stormwater runoff to prevent the aquatic depletion of natural bodies of water (Mitsch and Gosselink, 2000).

Several SCMs show positive SRP and reactive P (RP) removal efficiencies (bioretention: Hsieh, et al., 2007; sub-surface constructed stormwater wetlands (CSW): Forbes, et al., 2004; RP, surface-flow CSW: Wadzuk, et al., 2010). One such SCM, a surface-flow CSW, shows potential for being a P sink, much like their natural counterparts (Mitsch and Gosselink, 2000). Sorption and burial of P has long been considered as the main P retention pathway for wetlands causing accumulation of P in sediments (Reddy, et al.,

1999; Jin, et al., 2005; Zhang, et al., 2007). Previous studies have stated that CSWs are no longer valuable P retention tools past a certain point in their lifetime as soil reaches its maximum P saturation capacity (Richardson, 1985; Vohla, et al., 2007; Forbes, et al., 2004). As a result, enhancement of soil sorption capacity is one possible way for increasing P sorption capabilities in wetland soils.

Soil has a maximum P sorption capacity (through adsorption and precipitation); however, chemical soil amendment strategies can provide additional P sorption benefits to wetland soil, thus extending the lifetime of these engineered systems. Chemical soil amendments are relatively easy to apply in various forms, and possess a high potential for rendering P inactive within the soil profile (Ann, et al., 2000; Pant and Reddy, 2003). Phosphorus ions tend to be attracted to calcium (Ca), manganese (Mn), iron (III) (Fe), and aluminum (Al) and will form chemical and ionic bonds with these metals, rendering them insoluble. In basic soils P is attracted to Ca and Mn and in neutral to acidic soils (pH < 7), P has a stronger affinity towards Al^{3+} and Fe^{3+} (Hsu, 1975).

Soil amendments high in iron (III) and aluminum can be used to encourage P sorption through adsorption and precipitation. Two soil amendments are studied in this research: Iron [Fe (III)] coated sand and Aluminum Water Treatment Residuals (Al WTR). When Fe (III) is present in wetland soil, it attracts the strongly electronegative SRP species, thus removing SRP from solution and rendering it immobile. However, in environments where oxidation and reduction processes are prevalent, as in wetland soils, Fe (III) may reduce to Fe (II) at which point sorbed SRP may be released back into solution. This research uses emergent wetland plants as a method of creating and sustaining oxidized

regions within the soil profile with the intention of inhibiting the advancement of reduced conditions.

The second amendment used was Al WTR (drinking water residuals), which has been shown to have large P sorption capacities as a result of high aluminum contents. These residuals are readily and freely available from water treatment plants (Makris, et al., 2004; Elliott, 2002). Studies have shown WTRs to "dramatically reduce soluble P" through a soil profile as a result of their large P sorption capacities and are suggested as methods for immobilizing P in P-sensitive ecosystems (Makris, K. et al., 2004). Babatunde, et al. (2009) verified that the application of Al WTR within wetland sediment via a vertical column study experiment successfully removes P from the water column, and deemed the residuals fit for field-application. However, Babatunde et al.'s (2009) research merely assumes, and does not verify, that the Al WTR will behave similarly when placed in a wetland environment where vertical and lateral flow pathways are present.

The results presented in this research focus on the fate and transport of soluble reactive phosphorus (SRP) in a surface-flow constructed stormwater wetland (CSW) when soil amendments are employed. Villanova University's existing CSW is used as the baseline for this study and informed the design of bench-scale laboratory mesocosms. The mesocosms used in this research replicate similar ecology, hydrogeology, and nutrient loadings seen in the existing wetland. With sedimentation processes controlling the long-term P removal capability of a wetland (Faulkner and Richardson, 1989), it has become increasingly more important to: (1) understand the fate and transport of SRP through the

vertical and lateral soil profile in a CSW; and (2) engineer these wetland systems for maximum SRP removal capabilities through the use of soil amendment strategies. This will solidify CSWs as effective SRP retention SCMs.

1.2 Objectives of this Study

Understanding the effects of vertical and horizontal flow components on SRP fate and transport could inform more effective removal strategies, maintenance techniques, and ultimately provide wetland scientists, urban planners, water resources engineers, and water quality modelers with more accurate lifetime estimates for CSWs. Additionally, soil amendments could provide supplementary benefits towards SRP removal.

The objectives of this research were:

1. To observe and measure pathways of SRP fate and transport through a surface-flow constructed stormwater wetland (CSW) soil profile.
2. To quantify pore water SRP mass removal associated with two soil enhancement strategies (Al WTR and iron (III) coated sand).
3. To analyze physical and chemical characteristics of soil matrices that may relate to SRP mass removal seen in pore water analyses.
4. To verify horizontal sub-surface flow mechanisms through a 2-D numerical model (HYDRUS) and to demonstrate implications of vertical and longitudinal flow pathways in phases I and II.

1.3 Organization of Report

The report has been divided into six chapters:

Chapter 1 Introduction: This chapter provides background and introductory remarks for the research completed herein.

Chapter 2 Literature Review: A literature review was completed to show the current knowledge and gaps in knowledge about SRP and its mechanisms of removal within a surface flow CSW and to illuminate possible areas of physical, chemical, and biologic methods for enhanced SRP removal.

Chapter 3 Research Methodology: This chapter provides a complete description of the research methods in phase I and II of this research.

Chapter 4 Phase I Analysis Examining Fate and Transport of SRP: Two horizontal-flow wetland mesocosms (a non-vegetated and vegetated system) were used in phase I to complete objective 1. Pore water samples were taken and tested for SRP, while pore water transport through each mesocosm was observed.

Chapter 5 Phase II Results and Discussion of Soil Amendment Experimental Runs: Phase II consisted of seven mesocosm studies using various soil enhancement strategies: Fe (III) coated sand and Al WTR. Pore water was extracted and analyzed for SRP concentrations to determine mass removal amongst soil amendments. Additionally, soil chemical and physical characteristics were found.

Chapter 6 Vertical and Horizontal Flow Mechanisms: Flow pathways are discussed for chloride and SRP concentrations through each mesocosm soil.

Chapter 7 Summary and Future Research: Conclusions and suggested research for future

Chapter 2 Literature Review

2.1 Urban Stormwater Runoff: Pollutants

Urbanization contributes to increased stormwater runoff due to decreased pervious surfaces (NRC, 2008; Rosenquist, et al., 2010). Runoff carries large amounts of sediments, nutrients, metals, and hydrocarbons that impact stream and aquatic life health (USEPA, 2005). With an ever pressing concern for management and treatment of runoff, especially nutrients nitrogen (N) and phosphorous (P), stormwater control measures (SCMs) are being recommended and implemented throughout the urban landscape to help meet water quality requirements.

One nutrient, phosphorus (P), is often considered the limiting nutrient in freshwater ecosystems, and if found in excess, P contributes to eutrophication through algal blooms, which subsequently deplete the amount of dissolved oxygen (Makris, K. et al., 2004). The soluble form of P has been shown to directly affect algal growth (Fozzard, et al., 1999; Fisher, 1992). More specifically, it is the biologically available form of P (orthophosphate), measured analytically as soluble reactive phosphorus (SRP), that must be managed and removed from urban runoff to prevent the depletion of natural bodies of water (Mitsch and Gosselink, 2000).

Stormwater control measures (SCMs) are being studied for their ability to manage and treat runoff in urban areas. One such SCM, a surface-flow CSW, shows potential for being a P sink, much like their natural counterparts (Mitsch and Gosselink, 2000). However, given the complexity of a CSW environment, it is difficult to quantify and

predict a CSW's water quality performance. The purpose of this literature review is to show the current knowledge and gaps in knowledge about SRP and its mechanisms of removal within a surface flow CSW and to illuminate possible areas of physical, chemical, and biologic methods for enhanced SRP removal.

2.2 Phosphorus

Phosphorus is a naturally occurring nutrient in ecosystems and is governed by geologic, biologic, and hydrologic processes. In a freshwater ecosystem, P has been recognized as one of the limiting factors causing eutrophic conditions (Sharpley, A. et al., 1999). Phosphorous is present through a sedimentary cycle as opposed to a gaseous one (e.g. nitrogen), which makes the nutrient less mobile within the ecosystem and difficult to remove. Internal inputs, such as weathering of underlying rock and deposition of organic matter, affect the amount of P present in the sediment layer of a wetland (Mitsch and Gosselink, 2000). External inputs of P, such as atmospheric deposition, mineral fertilizers, animal fecal matter, and stormwater runoff, are primary contributors to a wetland ecosystem (Urbonas and Doerfer, 2004). Quantifying these inputs and outputs is problematic without first understanding P's various forms and respective removal mechanisms.

Phosphorus is found within the environment in various forms: soluble, insoluble, organic, and inorganic. Total P content is represented by the combination of particulate (insoluble) and soluble forms. Soluble P is defined as all compounds that are able to pass through a 0.45 μm pore diameter filter, while particulate P are those that do not (SERA-IEG, 2009).

Soluble inorganic P includes the ions PO_4^{3-}, HPO_4^{2-}, and $H_2PO_4^-$; the predominant form of which changes with pH (Figure 2.1). These three ions are defined as orthophosphates, make up the biologically available form of P, and are measured analytically as soluble reactive phosphorus (SRP) (Vymazal, 2007; Mitsch and Gosselink, 2000).

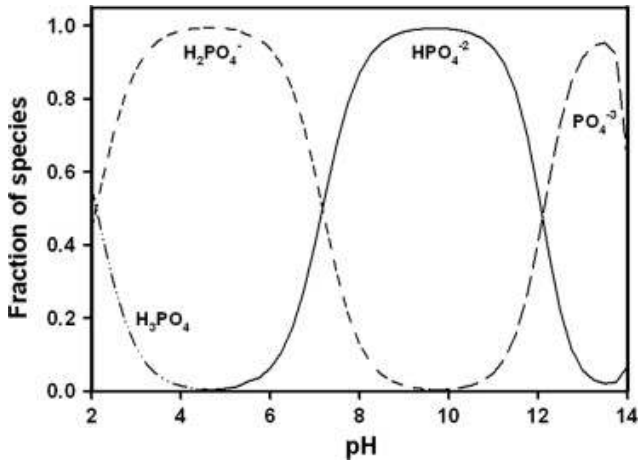

Figure 2.1. Speciation diagram of phosphoric acid (Kang, S. et al., 2011).

2.3 Stormwater Control Measures (SCMs)

Knowing the mechanisms of removal for SRP is valuable when trying to better design and engineer biologic stormwater control measures (SCMs). Stormwater control measures are being studied for their ability to manage and treat runoff in urban areas. The NRC (2008) issued a stormwater study documenting up and coming regulations set in place by the EPA to comply with the Clean Water Act. These regulations required industrial and construction agencies to implement stormwater pollution plans, while permits for municipal separate storm sewer systems (MS4s) required a stormwater management plan. Non-structural (low impact design) and structural (bioswales, rain gardens, green roofs, porous asphalt/concrete, constructed wetlands) SCMs were

suggested for use when addressing requirements for stormwater control; however, long-term results and limited information on the effectiveness of these SCMs has made state and local stormwater programs uncertain of the longevity of SCMs.

Constructed Stormwater Wetlands Natural wetlands have been known to improve water quality (Grant and Patrick, 1970; Odum, et al., 1977), but are complicated systems with their fluctuating aerobic/anaerobic conditions, hydraulic retention times, influent nutrient concentrations, water depths in various regions, vegetation, water chemistry, and soil matrices (Carleton and Montas, 2010; Mitsch and Gosselink, 2000; Kadlec and Knight, 1996). Constructed stormwater wetlands (CSWs) have been encouraged in recent years because natural wetlands would subsequently not be affected by nonpoint source pollution (Carleton, J. et al., 2000). These engineered wetland systems provide a multitude of benefits including wildlife habitats, reducing peak flow, recharging groundwater, and the successful attenuation of nutrients within urban nonpoint source pollution (Serra, et al., 2004; USEPA, 2005; Baker, 1992; Mitsch, 1992; Nairn and Mitsch, 2000; Mitsch and Gosselink, 2000; Kalin, et al., 2012). Specifically, CSWs have shown potential for being a P sink, much like their natural counterparts (Mitsch and Gosselink, 2000). As a result of P's strong affinity to soil, this nutrient generally moves downward through the soil column or horizontally via sub-surface interflow (Eghball, et al., 1990; Sims, et al., 1998).

The effects of varied hydraulic retention times (HRT) and periods of flooding on P retention have been studied in CSWs (Ann, et al., 2000; Chavan and Dennet, 2008;

White, et al., 2006). Longer HRTs result in greater removal of TP presumably caused by the settling of suspended solids. Slowing down surface flow and increasing the hydraulic residence time within a CSW allows finer sediments, such as clay particles, to settle out of solution (Chavan and Dennet, 2008). A strong correlation between TSS and TP removal has been seen in surface-flow CSWs (Chavan and Dennet, 2008; Wadzuk, et al., 2010). However, these studies do not specify what percentage of the TP is soluble or particulate. Given that the biologically used form of P is found in the soluble portion of the TP component, it is important to delineate how each form is predominantly removed and through which removal mechanism.

Flooding of wetland soils, which are sometimes associated with storm surges, have been shown to rapidly release P (Ann, Y. et al., 2000). These fluctuations in flow regimes can cause sediment to re-suspend itself within the water column, consequently transporting P downstream and ultimately negating the results of sedimentation (Novak, et al., 2004). Additionally, the potential for sediment-water interactions are limited attributable to the increase in water depth associated with storms (Forbes, M. et al., 2004).

Understanding the fate and transport of P is difficult when preferential flow conditions exist (Akhtar, M. et al., 2003) and near-ambient nutrient concentrations typical of nonpoint sources are present (Mitsch et al. 2004). The quantification of P retention is often unreliable because removal processes are complex, spatially heterogeneous (Carleton and Montas, 2010), and difficult when biogeochemical processes are not thoroughly studied (Lai and Lam, 2009).

2.4 Removal Mechanisms of SRP and Soil Amendments

There are three primary methods of rendering P unavailable for biological uptake: sedimentation through adsorption, precipitation of insoluble phosphates, and binding of P in organic matter.

(1) Sedimentation through adsorption

Considered the predominant method of P removal from a water column, sedimentation occurs through gravitational forces. Phosphates found in solution will adsorb or bind to suspended solids and mineral surfaces, which is due to the ionic attraction between the positively charged sediment particles within solution and the negatively charged phosphate ions. As phosphates adsorb to bonding sites on sediment particles, these particles become heavier and subsequently settle out of solution.

Several pools of P are available within the soil once P is sorbed to the sediments. Each pool reflects various bond strengths between the sediment and the P. Labile P is loosely bound to soil particles and prone to desorption. Fixed P represents P that is considered permanently bound within the sediment, although it is possible that the P can be desorbed and transferred back into solution. Desorption is undesirable because the P becomes available for plant use thus increasing the potential for excessive vegetative growth and consequently, eutrophication.

Every type of soil has a different potential for P retention. Phosphorus sorption isotherms represent the amount of P a soil can retain before reaching its saturation point. Batch

experiments are generally used to determine the P sorption capacity of a soil. The Langmuir, Freundlich, and Tempkin equations can describe the relationship between the amount of P sorbed to the soil and the P left in solution at an equilibrium point (SERA-IEG, 2009). Knowing a soil's P sorption capacity will allow engineers to make better estimates of a CSWs lifetime as a valuable P retention tool. Strong correlations have been seen between TSS and TP removal in a CSW (Chavan and Dennet, 2008; Wadzuk, et al., 2010); however, it is uncertain whether this strictly translates to the removal of particulate P or if soluble forms of P are removed as well (sub-surface CSW: Forbes, et al., 2004; surface-flow CSW: Wadzuk, et al., 2010). Additionally, other studies show SRP increase through a SCM after several years of performance or when flooding events occur (Ardon, 2010; Nairn and Mitsch, 2000; Novak, et al., 2004). As a result, studying the SRP fate and transport through wetland soils given the vertical and lateral hydraulic properties, could provide insight into the most probable removal mechanism.

(2) Precipitation of Insoluble Phosphates

Through precipitation, soluble reactants chemically bond to form insoluble products (complexes), which settle out of solution and accumulate within wetland sediments. Much like in sedimentation through adsorption, P has an affinity towards specific elements. Iron and aluminum attract P in acidic to neutral soils, while calcium and magnesium allow for complexation with P in alkaline soils (Mitsch and Gosselink, 2000).

While chemical bonds are more difficult to alter than ionic ones, insoluble precipitates may dissociate under altered conditions allowing P to transfer back into solution (Kadlec,

Knight, 1996). Changes to CSW hydrology are shown to encourage dissociation through the results of reduction/oxidation within the soil layer. Phosphorus that was once bound to Fe (III) is released when reduced to Fe (II) under anaerobic conditions (Mitsch and Gosselink, 2000). However, it is interesting to note that oxidation resulting from dry periods may cause a decrease in sorption potential of P (Baldwin, 1996). This contradiction may not be seen in surface-flow CSW environments where the soil is always inundated yielding more anaerobic environments, but it would be interesting to determine whether iron amended soil, in combination with an aerobic environment, would allow for additional SRP retention.

(3) Binding of P in Organic Matter

Binding of P in organic matter through the uptake by plants and organisms was originally acknowledged as an important mechanism for P removal within CSWs (Kuusemets and Mander, 2002). More recently, however, newer studies speculate that this may not be the case (Lucas and Greenway, 2008; Wadzuk, et al., 2010). Initially, as vegetation becomes established, biologic uptake of P is substantial, but as plants die and begin to decompose, they release the bound P back into the soil layer (Mitsch and Gosselink, 2000). As a result, it is unclear whether vegetation is a key component in the long-term removal of phosphorus from CSW environments, especially if plant harvesting is not completed annually (Vohla, C. et al., 2007).

If plants are not harvested each growing season, this P accretion over time will change the physical and biological characteristics of the soil (White, et al., 2006). Costs

associated with plant harvesting and the uncertainties of TP removal quantities make this option of removal undesired and seldom recommended (Kadlec, Knight, 1996). Therefore other removal mechanisms should be studied and employed (Vohla, C. et al., 2007).

Indirectly, CSW vegetation affects P reduction through impeding flow, which allows sedimentation of suspended solids (Carleton and Montas, 2010). Vegetation also assists with P retention by releasing oxygen into the rhizosphere, which can indirectly affect enzyme activity (Neori, 2000; Kong, et al., 2009). Kong, et al. (2009) was able to document a strong correlation between phosphatase (an enzyme emitted from plant roots), TP, and SRP removal. These indirect benefits provided by plants ultimately assist with the SRP removal within wetland sediments and will be further explored in this research.

2.5 Soil Amendments

While the three main mechanisms for P removal were described in the previous section, scientists have found the mechanisms removing the majority of the P within a CSW to be chemical adsorption and physical sedimentation (Guan, B. et al., 2009). The P adsorption capacity of wetland soil is dictated by the physical-chemical properties and as such, P removal depends mostly on physical-chemical properties of soil matrices (Tanner, et al., 1999; Drizo, et al., 1999). Chemical amendments have been suggested as preventative measures for potentially assisting with long-term P removal efficiencies (Pant and Reddy, 2003). As a result, soil amendment strategies have been employed to retain additional P.

Blast furnace slag, gravel-based soil, combinations of granite, river sand, shale, masonry sand, and chemical amendments have been studied in CSW environments (Ann, et al., 2000; Forbes, et al., 2004; Hu and Shan, 2009; Lai and Lam, 2009). Each study found these amendments to positively contribute to P retention. Two studies, Forbes (2004) and Ann et al. (2000), looked specifically at the effects of SRP retention in CSWs. Forbes (2004) compared the use of light-weight expanded shale and masonry sand in a sub-surface flow CSW laboratory experiment for P retention. The expanded shale had a higher P sorption capacity and therefore showed a greater retention of P when compared to masonry sand. The Forbes et al. (2004) study suggested that soil amendments can greatly encourage the P retention by raising the hydraulic conductivity and increasing P sorption capacity of the substrate.

Ann, et al. (2000) studied the effectiveness of various chemical amendments on rendering soluble soil P immobile in wetland sediments that were flooded. Aluminum sulfate, also referred to as alum (Al_2SO_4), and ferric chloride ($FeCl_3$) were among the six amendments considered. Results showed that 1-2 g kg^{-1} of $FeCl_3$ amendment was required to minimize P release to overlying floodwater whereas 12 g kg^{-1} was required when using Al_2SO_4. While $FeCl_3$ was found to more effectively immobilize soluble P, saturated environments create anaerobic conditions, which ultimately encourage the reduction of Fe (III) to Fe (II), thus releasing the bound P back into the water column.

If $FeCl_3$ is to be used as a chemical soil amendment for removing SRP from solution, an aerobic soil environment needs to be fostered. Aquatic macrophytes release oxygen from

their roots, which can influence biogeochemical processes within wetland sediments (Barko, et al., 1991; Sundaravadivel and Vigneswaran, 2001) (Figure 2.2). Reddy et al. (1989) suggests that some wetland plants can release enough oxygen into the root zone to support microbial activity, which would deter soils from turning anaerobic. As a result, in this research study, standard grade sand was coated with $FeCl_3$ before being mixed into wetland soil. The addition of large amounts of emergent macrophytes was used in attempt to induce aerobic conditions. Sand was chosen as the method of application of Fe (III) based on the suggestions provided by Forbes, et al. (2004) who stated that soil amendments can greatly increase the P retention with higher hydraulic conductivity. Sand has a typical hydraulic conductivity of ~10^{-4} m s^{-1} (Schultz and Ruppel, 2002) which is comparable to the hydraulic conductivities reported for sand by the Rosetta Lite on-line soil property database of 7.5 x 10^{-5} m s^{-1} (Schaap, et al., 2001). Theoretically, the addition of sand should only encourage additional hydraulic conductivity. Chapter 3 provides the method of application and Chapter 5 presents the results from the study.

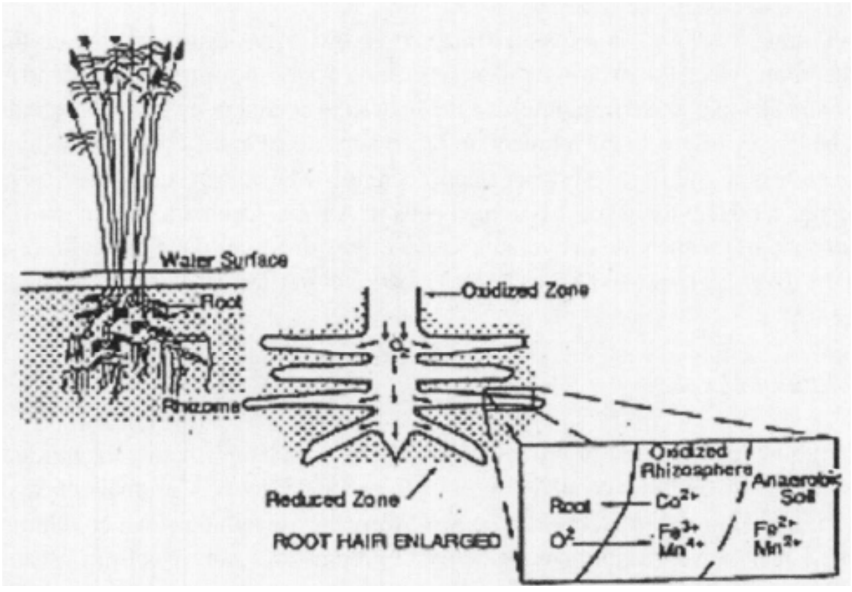

Figure 2.2. Rhizosphere oxygenation (Sundaravadivel and Vigneswaran, 2001).

(2) Aluminum Water Treatment Residuals

Potentially the most promising of soil amendments, water treatment residuals (WTRs), is a coagulation waste product from drinking water purification processes. These residuals are high in Al, Fe, Mg, and Ca, which are all elements known to attract P. Aluminum WTRs (Al WTR) result from the use of aluminum sulfate during coagulation and have been found to best remove the soluble form of P compared to ferric-sulfate (Elliott, et al., 2002). Using this byproduct is also desirable because of the ability to re-use the material as opposed to wasting this end-product in a landfill. Studies have shown WTRs to "dramatically reduce soluble P" through a soil profile as a result of their large P sorption capacities and are suggested as methods for immobilizing P in P-sensitive ecosystems (Elliott, et al., 2002; Makris, et al., 2004). These residuals, on their own, have in some instances exhibited P sorption capacities of 5000 mg kg^{-1} in their as-received form (O'Conner, et al., 2001).

2.6 Mesocosm Studies

Vertical and horizontal mesocosm studies have been previously used in soil research. Several column studies looking at pore water samples have shown trends in SRP retention using bioretention media (Hsieh, et al., 2007) as well as metals removal in wetland sediment (Xu and Jaffe, 2006). These bench-scale laboratory mesocosms allow the researcher to control external inputs while studying specific internal processes. The interaction between wetland sediment and sub-surface water flow is important to address when studying wetland water and chemical budgets (Min, et al., 2010). Preferential flow

pathways have been shown to affect solute transport processes (Noguchi, et al., 2001; Weiler and McDonnell, 2007), however, sampling and tracking of pore water solutes has not been well documented (Sade, et al., 2010). As such, horizontal laboratory mesocosms will be employed in this research and designed using previous mesocosm studies (Xu and Jaffe, 2006; Bassein, E., Jaffe, P.R., 2009; Forbes, et al., 2004) to ensure both vertical and horizontal flow pathways are understood for SRP fate and transport.

Chapter 3 Research Methodology

This chapter provides an explanation of chosen research methodology and steps for completing the research goal and objectives. The goal of this research was to understand the effects of vertical and horizontal flow components on soluble reactive phosphorus (SRP) fate and transport within a surface-flow constructed stormwater wetland (CSW) when two soil amendments were employed: aluminum water treatment residuals (Al WTR) and iron (III) coated sand. The objectives of this research were:

1. To observe and measure pathways of SRP fate and transport through a surface-flow constructed stormwater wetland (CSW) soil profile.
2. To quantify pore water SRP mass removal associated with two soil enhancement strategies (Al WTR and iron (III) coated sand).
3. To analyze physical and chemical characteristics of soil matrices that may relate to SRP mass removal seen in pore water analyses.
4. To verify horizontal sub-surface flow mechanisms through a 2-D numerical model (HYDRUS) and to demonstrate implications of vertical and longitudinal flow pathways in phases I and II.

3.1 Research Methods

A two-phased bench-scale laboratory mesocosm study was designed to complete all research objectives. Using a mesocosm approach allows for manipulation of individual environmental parameters (flow, vegetation, soil characteristics), while maintaining the overall system as close to in situ conditions as possible (precipitation, temperature, relative humidity) (Bassein, E., Jaffe, P.R., 2009). Internal factors in each mesocosm reflected the existing Villanova University CSW and are defined in section 3.2. Phase I addressed objective 1. Two bench-scale laboratory mesocosm studies were constructed in phase I to observe basic fate and transport pathways of SRP within the vertical and

horizontal flow profiles while simultaneously discerning any differences between a non-vegetated and vegetated system. Phase II was designed to complete objectives 2 and 3 and to inform results for objective 4. Similar to phase I, laboratory mesocosms were the chosen methodology in phase II where two soil amendment strategies were tested: Fe (III) coated sand and aluminum water treatment residuals (Al WTR). The Fe (III) coated sand was analyzed with and without plants to determine if oxygenation through root rhizospheres had any effect on inhibiting the development of reduced conditions. Reduced conditions may cause Fe (III) to gain an electron and become Fe (II). When this transformation occurs, SRP previously bound to Fe (III) will be released back into solution, thus potentially causing an export of SRP. The Al WTR amendments were tested at various mix ratios to determine if the quantity of Al WTR amendment had an effect on SRP removal. Mesocosm construction, descriptions of experimental runs, pore water and soil sampling techniques, and methods of analysis are presented in this chapter for both phases.

3.2 Mesocosm Design and Construction

3.2.1 Phase I

Two horizontal flow-through laboratory mesocosms were constructed for phase I, one vegetated and one non-vegetated (used as the control). Both were placed in Villanova University's research greenhouse. Each experimental pseudo replicate (hereto referred to as a replicate) lasted for 24 hrs and eight replicates were completed in both the vegetated and non-vegetated mesocosms. Influent water was dosed with only SRP during these

replicates. A second study was completed over seven days; influent water dosed with SRP and chloride was pumped through each mesocosm over a four-day period to verify long-term pore water movement. Surface water was then removed while sub-surface flow remained during a three day study where pore water was monitored and analyzed for SRP leaching.

Each mesocosm was designed to exhibit both ground water and surface water interactions, much like Villanova's existing surface-flow CSW. Prior to running any dosed experiments, a surface-flow CSW environment was simulated by fully saturating the soil in each mesocosm with de-ionized water (D.I. water). Since the objective of phase I was to observe and measure the fate and transport of SRP through the soil column, D.I. water was chosen as the sub-surface flow to avoid additional introduction of SRP. The sub-surface water source was stored in a 113 L (30 gallon) barrel and was gravity fed during the course of each experimental replicate. Sub-surface flow was regulated at the outlet location using a 0.64 cm (1/4 in) brass ball valve at the inlet and outlet locations (Figure 3.1).

During each replicate, two inlet tanks were filled with 113 L of tap water, dosed to approximately 0.6 mg L^{-1} PO_4-P of SRP using a combination of sodium phosphate monobasic (Na_2HPO_4) and sodium phosphate dibasic (NaH_2PO_4), and pumped through the mesocosm using a Cole Parmer low-flow peristaltic pump (Masterflex®L/S® Variable Speed #EW-07553-75). A value of 0.6 mg L^{-1} PO_4-P was chosen as the dosing amount because this value represents the 50% exceedance probability point associated with storm event data collected from the previous Villanova CSW (Wadzuk, B. et al.,

2010). The dosing chemicals were added to each barrel at the beginning of an experimental replicate and influent concentrations were monitored along with surface (Q_{in}, $Q_{0cm\ Out}$) and sub-surface flow ($Q_{3\ and\ 8cm\ Out}$) (Figure 3.1).

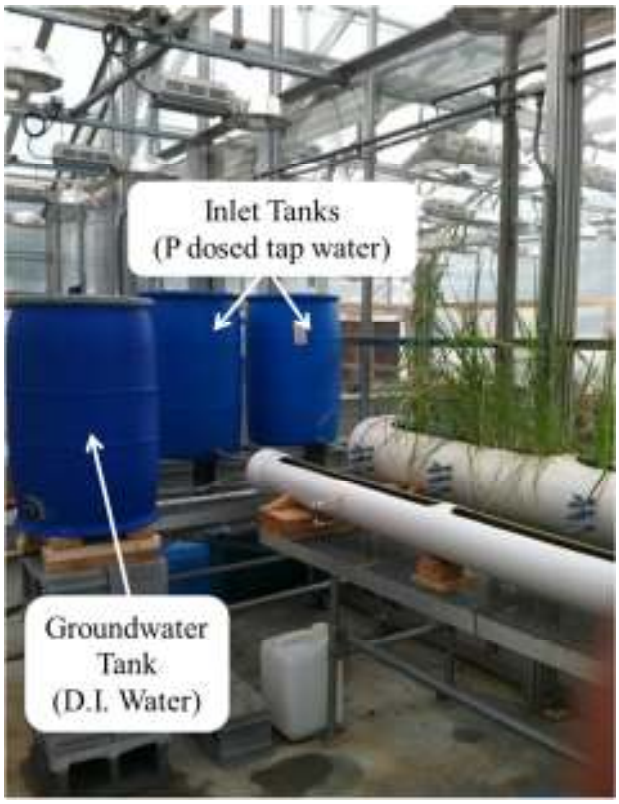

Figure 3.1. Experimental set-up in greenhouse during phase I. The barrel to the far left contains the D.I. water, while the two remaining barrels hold inlet water for each experimental run of 24 hrs.

Table 3.1. Summary of phase I flow values, SRP inlet concentrations, and mass inputs for non-vegetated and vegetated mesocosms. These values reflect the study consisting of eight-24 hour experimental runs in each mesocosm.

	Eight - 24 hr Runs	
	Non-Vegetated	Vegetated
Q_{in} (mL s^{-1})	2.60 ± 0.13 (n=16)	2.64 ± 0.09 (n=16)
$Q_{0cm\ Out}$ (mL s^{-1})	2.60 ± 0.06 (n=16)	2.35 ± 0.27 (n=16)
$Q_{3\&8cm\ Out}$ (mL s^{-1})	0.13 ± 0.01 (n=32)	0.20 ± 0.05 (n=32)
Inlet Conc. (mg L^{-1} PO_4-P)	0.53 ± 0.05 (n=32)	0.54 ± 0.04 (n=32)

Nutrient removal in wetlands is facilitated by shallow water depth (maximizing soil-water interactions), low velocities that provide additional sedimentation time, and high vegetated productivity (Mitsch, W. et al., 1995). The flow rate in both phase I and II was chosen for the practicality and capacity of the resources used. Xu, et al., (2004) conducted a vertical flow through column mesocosm study and measured the infiltration rate to be 0.004 mL s^{-1} in wetland sediments. Similarly, Liang, (2011) provided a flow rate of 0.006 mL s^{-1} in a vertical column study where WTR was employed in a sand mixture. These flow rates were less than those supplied to phase I mesocosms. Horizontal flow-through was found to be maintained through peristaltic pumps at rates of 0.18 – 0.2 mL s^{-1} (Bassein, E., Jaffe, P.R., 2009) and 0.32 mL s^{-1} (Zazo, et al., 2008) in two horizontal-flow wetland mesocosm studies, verifying the sub-surface pore water flow values used during this experiment similar to results seen in the literature.

Runs were not conducted simultaneously due to setup limitations. When mesocosms were not being used for testing, D.I. water continually saturated the soil and 3 and 8 cm outlet ports were opened to allow flow through.

A chloride tracer and P leaching analysis was completed for both the vegetated and non-vegetated mesocosms. Chloride and SRP dosing occurred over the first four days (ended at t=96 hrs) (Table 3.2). Samples were taken prior to dosing (t=0 hrs), during dosing (t=24, 48, 72, and 96 hrs), and three additional days post dosing while only sub-surface DI water flow was present (t=120, 144, 168 hrs).

Table 3.2. Summary of phase I flow values, and SRP/ chloride inlet concentrations for non-vegetated and vegetated mesocosms. These values reflect the seven day study dosed surface water was existed over the first 4 days and then ceased. Pore water samples were collected for the duration of the experimental run.

	7 Day Run (4 day dosing)	
	Non-Vegetated	Vegetated
Q_{in} (mL s^{-1})	2.64 ± 0.11 (n=7)	2.62 ± 0.12 (n=7)
$Q_{0cm\ Out}$ (mL s^{-1})	2.60 ± 0.30 (n=7)	2.60 ± 0.08 (n=7)
$Q_{3\&8cm\ Out}$ (mL s^{-1})	0.15 ± 0.10 (n=7)	0.21 ± 0.06 (n=7)
Inlet Conc. (mg L^{-1} PO_4-P)	0.52 ± 0.11 (n=14)	0.55 ± 0.03 (n=10)
Inlet Conc. (mg L^{-1} Cl^-)	138 ± 12 (n=10)	145 ± 14 (n=10)

Non-Vegetated Mesocosm Construction The non-vegetated mesocosm was constructed with a 15.2 cm (6 in) schedule 40 PVC pipe, 3.05 m (10 ft) in length (Figure 3.2). Sampling ports for pore water samples are located at 0, 3, and 8 cm soil depth and at horizontal locations 0.6 m and 2.4 m from the inlet (Figure 3.2). The vertical depths associated with the pore water samples were chosen based on recommendations from Vadas, et al. (2006) who stated that environmental pore water sampling can be completed at depths shallower (0-10 cm) than typical of agronomic soil depths (0–20 cm). Soil obtained from Villanova's existing CSW filled the non-vegetated mesocosm to a depth of 10 cm (4 in). The soil was added to each mesocosm without any compaction and could be described qualitatively as loosely packed. The top portion of the PVC pipe was removed to allow for surface water observation.

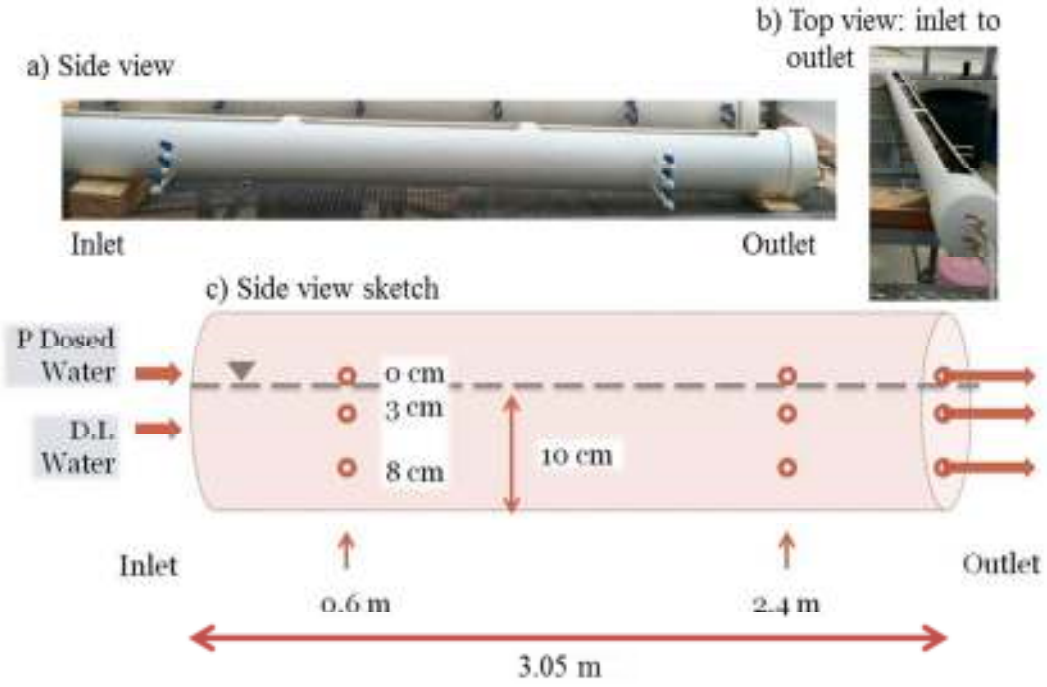

Figure 3.2. Photographs (a, b) and technical sketch (c) of non-vegetated, 15.2 cm mesocosm. The open circles are the sampling ports, located 0.6 m and 2.4 m from the inlet, the heavy arrows indicate the direction of flow.

All ports along the longitudinal profile were made from 0.3 cm polyethylene tubing. Tubing extended into the soil through the PVC wall and perforations were made in the section of tubing that was buried. Silicon sealant and aquarium glue created a water-proof seal at each port location. Longitudinal ports were connected to a two-way stopcock for easy sample extraction (Figure 3.3a) and inlet/outlet ports were connected to brass ball valves (Figure 3.3b). At the inlet, a 0.64 cm (1/4 in) brass valve connected tubing from a peristaltic pump to the inlet location at the soil surface (0 cm). Another inlet valve connected tubing to the sub-surface flow source at 3 cm depth. The outlet consisted of 0.64 cm (1/4 in) brass valves at depths of 0, 3, and 8 cm. Each PVC pipe was capped and

fixed on a 2% slope, which reflected the slope found in the flow channels of Villanova's existing CSW.

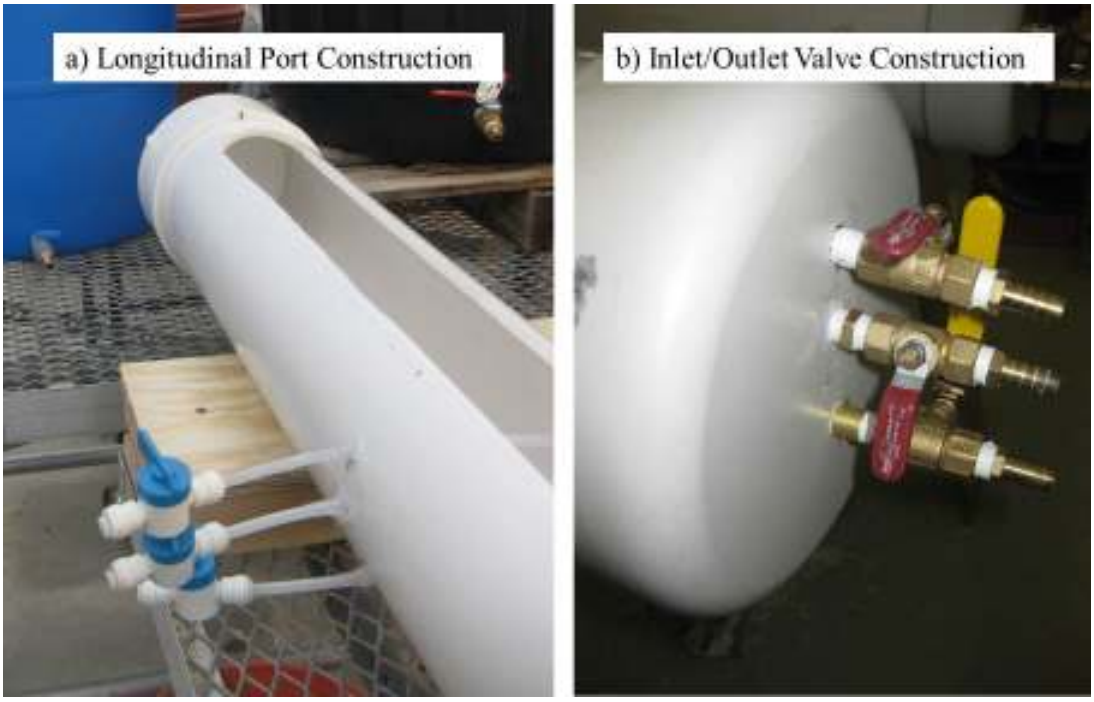

Figure 3.3. Typical port construction in phase I. Longitudinal ports were constructed using polyethylene tubing connected to two-way stopcocks (a) and inlet/outlet valves were constructed using 0.64 cm brass ball valves (b).

Vegetated Mesocosm Construction A larger, vegetated mesocosm was similarly constructed using a 25.4 cm (10 in) diameter PVC schedule 40 pipe, 3.05 m (10 ft) in length. Additional horizontal sampling locations, the soil column depth (15 cm), and the presence of vegetation differ from the non-vegetated mesocosm. The soil depth was chosen to accommodate the wetland plant species and sampling ports are located at horizontal distances of 0.18, 0.6, 1.2, 1.8, 2.4, and 2.9 m from the inlet and at 0, 3, and 8 cm depth within the vertical soil profile (Figure 3.4). All wetland plant species were

consistent with Villanova's CSW and randomly placed in 15 cm (6 in) of soil throughout the entire length of the mesocosm.

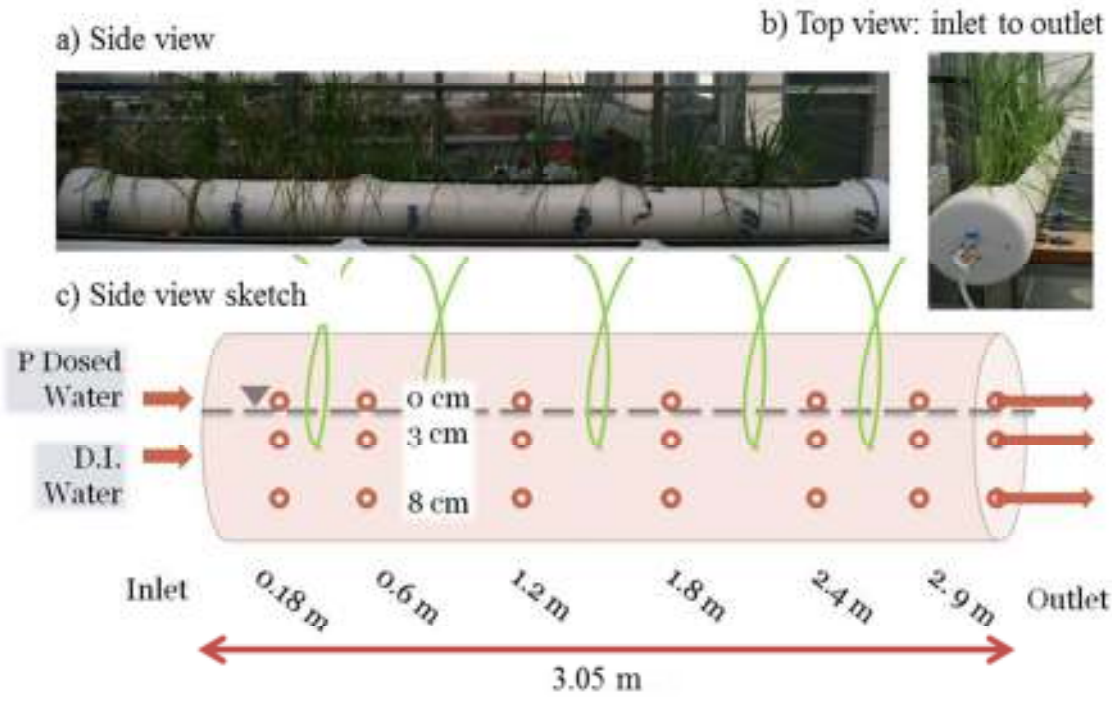

Figure 3.4. Photographs (a,b) and technical sketch (c) of vegetated, 25.4 cm diameter mesocosm. The open circles are the sampling ports, located 0.18, 0.6, 1.2, 1.8, 2.4, and 2.9 m from the inlet, the heavy arrows indicate the direction of flow.

Longitudinal pore water sampling ports for the vegetated mesocosm were constructed using 0.64 cm diameter schedule 80 PVC pipe (Figure 3.5). The ends of the ports were threaded to fit 0.64 cm diameter PVC ball valves. Inlet and outlet port construction remained consistent with the non-vegetated construction techniques (see Figure 3.3b).

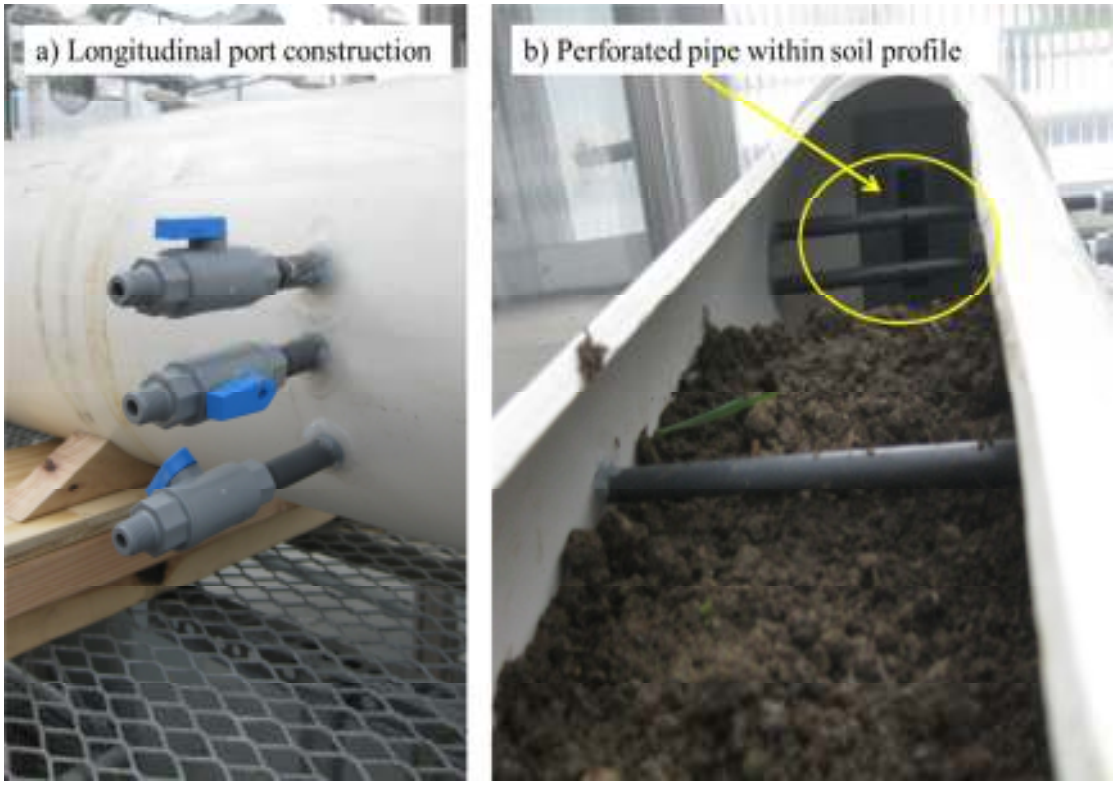

Figure 3.5. Typical port construction in phase I. Longitudinal ports were constructed using 0.64 cm diameter Sch. 80 PVC pipe connected to a threaded PVC ball valve (a) and perforated port construction is shown in (b).

3.2.2 Phase II

Horizontal flow-through laboratory mesocosms were constructed for use in phase II of this research. Mesocosms were set-up in Villanova's research greenhouse where temperature (22.8 ± 4.4 °C) and relative humidity (66.8 ± 14.1%) were monitored and collected using iButtons at an increment of 10 mins over the course of the study.

An experimental run in phase II is described as a separate soil treatment (this was not a pseudo replicate), of which there were eight. Only four experimental runs could be operated at one time because there were four mesocosm set-ups, reservoir tanks, and

peristaltic pumps. Each run was a minimum of 4 weeks. Table 3.3 shows the description and ID (which will be used from here onwards) of all experimental runs, their duration and dates ran. The Control mesocosm was made-up entirely of Villanova wetland soil and acted as the control for all mesocosm studies.

Table 3.3. Mesocosm identification, description of study, and length in weeks. Aluminum water treatment residuals (Al WTR) and iron (III) coated sand were chosen as the amendment strategies for the phase II study.

Mesocosm ID	Mesocosm Description	Duration (wks)
Control	Control mesocosm with no amendments added to typical wetland soil	12
FeP	5% by dry weight of Fe (III) coated sand added and thoroughly mixed into typical wetland soil; WITH PLANTS	12
Fe	5% by dry weight of Fe (III) coated sand added and thoroughly mixed into typical wetland soil; NO Plants	10
Al 2	2% by dry weight of Al WTR added and thoroughly mixed into typical wetland soil	4
Al 2D	Duplicate 2% by dry weight of Al WTR added and thoroughly mixed into typical wetland soil	4
Al 5	5% by dry weight of Al WTR added and thoroughly mixed into typical wetland soil	4
Al 5D	Duplicate 5% by dry weight of Al WTR added and thoroughly mixed into typical wetland soil	8
Al 8	8% by dry weight of Al WTR added and thoroughly mixed into typical wetland soil	4

Each mesocosm was constructed similarly to phase I with some differences. A 20 cm (8 in) diameter PVC schedule 40 pipe 3.05 m (10 ft) in length was used (Figure 3.6). Longitudinal pore water sampling ports were constructed using 0.64 cm (1/4 in) polyethylene tubing. This tubing was capped with a two-way stopcock valve for easy

sample extraction; similar to phase I non-vegetated mesocosm construction (Figure 3.3). Tubing extended into the soil through the PVC wall and perforations were made in the section of tubing that was buried. Silicon sealant and aquarium glue created a water proof seal at each port location. Longitudinal port locations were: 0.18, 0.6, 1.2, 1.8, 2.4, and 2.9 m from the inlet, at depths of 3 cm and 8 cm within the soil column. No 0 cm ports were constructed based on qualitative observations from phase I where the surface water at the 0 cm location could be easily extracted using a 10 mL luer-lok syringe. These surface water samples were taken directly from the top openings of the mesocosm as close to the water-soil interface as possible and at three points along the width of the mesocosm to reflect a composite sample. Surface water was generally less than 2 cm in depth.

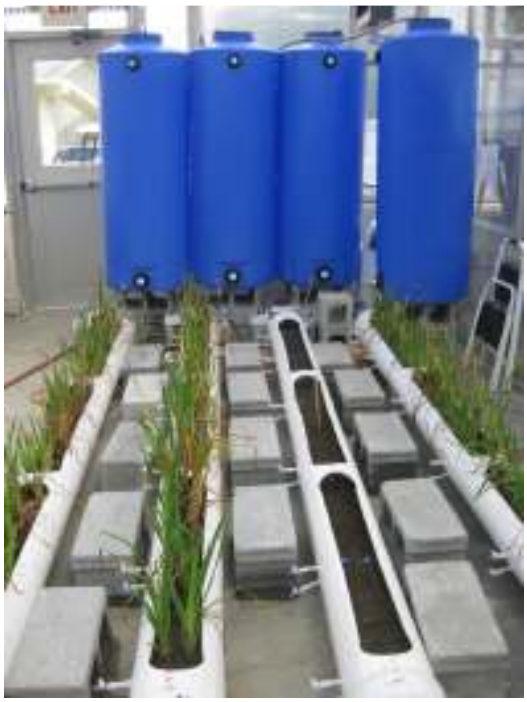

Figure 3.6. Phase II experimental set-up in Villanova's research greenhouse. Reservoir inlet tanks were 379 L in volume.

Fifteen centimeters of soil was added without compaction to each mesocosm and vegetation was placed in a randomly chosen pattern and then planted in the same order for each experimental run. Two plugs were placed in each row and a total of 30 rows were present. The plants [*Iris Versicolor* (Blueflag Iris) and *Sparganium Eurycarpum* (Giant Bur-Reed)] were obtained from Pinelands Nursery and Supply in Columbus, NJ (Figure 3.7). Plants were chosen based on their presence in Villanova's existing wetland. Two inch plugs were delivered prior to each experimental run to ensure plants between mesocosm runs were at comparable points in their growing cycles. Each mesocosm held 60 plants: 30 *Sparganium Eurycarpum* and 30 *Iris Versicolor*.

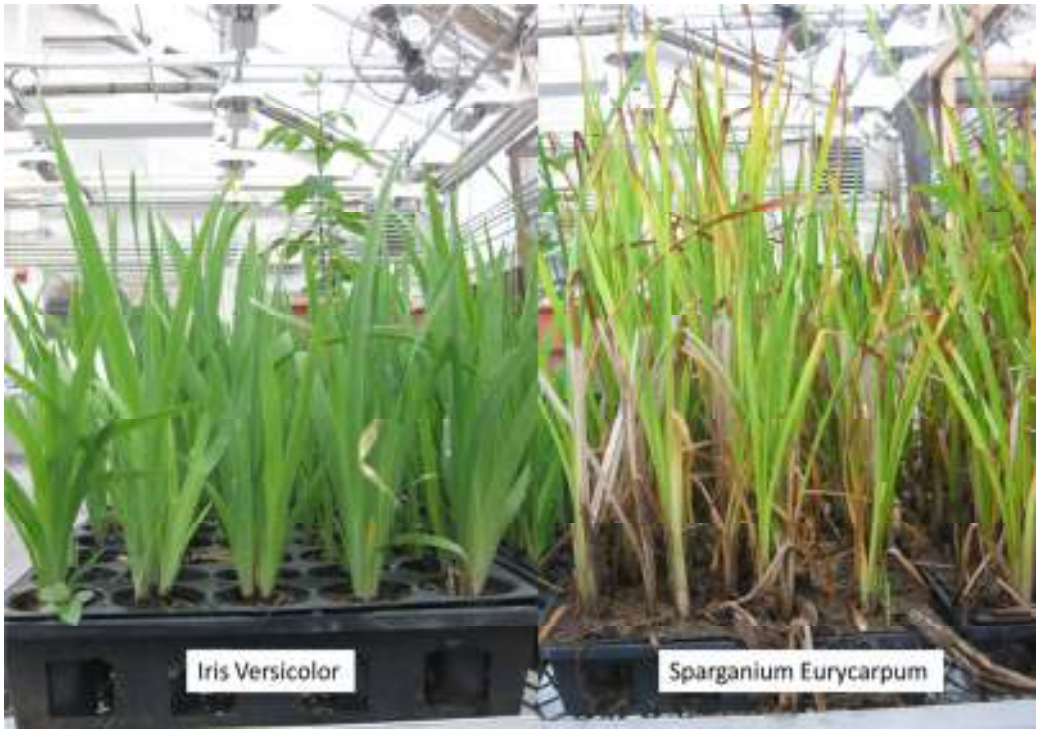

Figure 3.7. Phase II plants. *Iris Versicolor* (n = 30) and *Sparganium Eurycarpum* (n = 30) were added to each mesocosm in the same random pattern.

Tap water saturated the soil in each mesocosm for approximately five days prior to running any dosed water through them. Outlet valves were left open to allow for flow through the mesocosm during this initial saturation time. Flows were not monitored at this point. As stated previously, no separate sub-surface water was used during this phase due to the space constraints in the greenhouse and the availability of the DI water. However, influent water created both surface and sub-surface flow during each experimental run with sub-surface flow through created by opening the 3 and 8 cm outlet ports. Surface water infiltrated the saturated soil profile throughout the duration of the experimental run. An inlet valve was constructed using a 0.64 cm (1/4 in) brass ball valve and connected via Tygon tubing to a Masterflex®L/S® Variable Speed (Model #EW-07553-75) peristaltic pump at the inlet location of 0 cm (soil surface level). Each of the four mesocosms had a separate peristaltic pump and inlet water reservoir tank (379 L) to allow for simultaneous experimental runs (Figure 3.8). The outlet ports consisted of 0.64 cm (1/4 in) brass valves at depths of 0, 3, and 8 cm.

Figure 3.8. Peristaltic pump orientation for phase II experimental design. Four Masterflex®L/S® Variable Speed (Model #EW-07553-75) peristaltic pumps were used.

Influent water was dosed to approximately 0.6 mg L^{-1} PO_4 – P (using a combination of Na_2HPO_4 and NaH_2PO_4) and 150 – 200 mg L^{-1} chloride using NaCl (exact values are found in Chapter 5 under each mesocosm experimental run). Flow rates were measured at the inlet and outlet locations using a stop watch and a graduated cylinder. Three time trials were completed to verify each reading. Sub-surface flow through the soil was induced by opening the 3 and 8 cm valves at the outlet so that flow was approximately five times smaller than that of the surface water. This was completed in an attempt to provide a longer retention time for SRP removal to occur. Occasionally, flow was partially blocked at port locations as a result of soil particulates. When this was observed, valves were flushed with air or water until flow was restored. Table 3.4 provides a summary of flow rate data for phase II experimental runs.

Table 3.4. Average flow rates, standard deviations, and n values for each mesocosm over the entire duration of each experimental run.

Mesocosm ID	Avg Q_{In} (mL s^{-1})	n_{In}	Avg $Q_{Out\ 0\ cm}$ (mL s^{-1})	Avg $Q_{Out\ 3\ \&\ 8\ cm}$ (mL s^{-1})	n_{Out}
Control	1.46 ± 0.04	96	1.20 ± 0.12	0.24 ± 0.02	54
FeP	1.43 ± 0.15	72	1.23 ± 0.04	0.25 ± 0.01	67
Fe	1.44 ± 0.06	74	1.18 ± 0.12	0.23 ± 0.04	50
Al 2	1.45 ± 0.01	36	1.17 ± 0.09	0.22 ± 0.01	19
Al 2D	1.44 ± 0.05	60	1.02 ± 0.10	0.26 ± 0.02	46
Al 5D	1.43 ± 0.02	101	1.22 ± 0.09	0.22 ± 0.04	72
Al 8	1.54 ± 0.13	45	1.23 ± 0.07	0.22 ± 0.01	43
Avg	1.46		1.18	0.23	

Soil Treatments in Phase II

Iron (III) coated sand Aluminum water treatment residuals (Al WTR) were the two amendment strategies studied in phase II. Both amendments were added on a dry mass basis in their existing conditions (residuals were added in the form they were received). Buckets of wetland soil and amendments were prepared, 19 L (5 gallons) at a time, to get a well-mixed sample before the soil was placed in the appropriate mesocosm. The original wetland soil each amendment was mixed with a moisture content of 0.36 ± 0.02 (n=9) (Mass moisture/Total mass soil). Soil clods were observed in all mesocosm mixes as a result of the moist conditions.

Fe (III) Coated Sand Iron (III) coated sand was made in Villanova's soils laboratory using a method described in (Brooks, et al., 1996) where ferric chloride was used to coat Quikrete commercial grade fine sand (meets ASTM C33 specifications) (Figure 3.9). Sand was initially soaked in 1 N HNO_3 for 24 hrs then rinsed with DI water. Ferric chloride ($FeCl_3$) was dissolved in DI water and adjusted to a pH of 7.5 using 10 N NaOH. Suspension was aged overnight. Sand was gently mixed into the ferric chloride suspension and agitated four times throughout the day and again aged overnight. The clear solution was siphoned off the sand mixture and replaced with an equal volume of 0.1 mM of NaCl. This process was completed for three more days. On the last day, once the clear phase was siphoned off the sand, the iron phase was left behind and mixed into the sand. The sand was then dried at room temperature using forced air convection and mixing daily to prevent wicking (Figure 3.9a). There was an orange tint to the iron coated sand, which can be visually seen in Figure 3.9b, but showed similar physical

characteristics as the original commercial grade fine sand. When the iron coated sand was added to the wetland soil, a more homogenous mix was observed due to the small sand size and the ability of sand to stick to all surfaces of soil.

Figure 3.9. Phase II iron (III) coated sand soil mixture. a) drying of iron (III) coated sand; b) coloration difference of sand before and after the addition of iron (III); c) mixing 5% iron (III) coated sand by dry mass into typical wetland soil; d) final mixture; e) individually mixed buckets.

Two mesocosms were filled using a mixture of 5% by dry weight of iron (III) coated sand with typical wetland soil. One mesocosm had plants (FeP) and the other did not (Fe) for the purpose of discerning the role of vegetation in soil aeration and SRP retention. Soil aeration slows the reduction of Fe (III) to Fe (II) and prevents the release of soil-bound SRP. The Fe mesocosm served as the control for FeP. Quantification of reduced

conditions was completed through the use a ferrozine assay (described in section 3.3 Phase II Pore Water Analyses). Each week, the control and iron mesocosms were assessed for reduced conditions (values are reported in Chapter 5).

Al WTR Aluminum WTR were obtained from Pickering Creek West Water Treatment Plant in Phoenixville, PA (owned by Aqua America, Inc.) and stored at 4°C until use. Preparation of each mesocosm was completed in the same manner, with the Al WTR added to the soil on a dry mass basis and in as-received condition (post-filter press). The as-received condition of the Al WTR was clumpy, had the texture similar to clay, and had a moisture content of 0.73 ± 0 (n=3) and hydraulic conductivity measured to be 7.8 ± 4.5 x 10^{-6} cm s^{-1} (n=5) (Komlos, et al., In Review). Residuals were broken apart by hand into small clumps (typically less than 1 cm in diameter), sprinkled into wetland soil obtained from Villanova's CSW, and mixed thoroughly. This method was chosen to reflect a realistic field-application procedure. If this amendment is to be added to wetland soil in future field applications, is unlikely, at this point in time, that construction crew members would add these residuals any way other than as-received (unless the residuals are provided in a different form).

Three Al WTR amendment mix percentages were chosen to be: 2, 5, and 8% (dry mass basis). Duplicates of the 2 and 5% Al WTR mix were also completed. The Al 5D mesocosm was run for 8 weeks to see if removal percentages remained consistent, or if P export would be observed over a longer period of study. The first run using a 5% Al WTR mixture was found to be an outlier and is presented on its own in Chapter 5.

Table 3.5 summarizes mass of amendments in each soil matrix along with the actual mass of Al and Fe (kg) added to each mesocosm. Normalizing the data was not possible when comparing amounts of Al and Fe added from a mg kg^{-1} perspective.

Table 3.5. The mass of wetland soil and respective amendments were known for each bucket prior to being placed in each mesocosm. Total mass of Al and Fe (III) added (kg) via amendments was calculated using the dry mass.

	Total Mass Soil Matrix (kg)*	Amendment Mass (kg)*	Amendment Dry Mass (kg)	Total Al added (kg Al)**	Total Fe (III) added (kg Fe)**
Control	83.0	-	-	-	-
FeP	82.5	3.5	3.2	-	0.004
Fe	85.5	3.5	3.1	-	0.004
Al 2	82.4	4.4	1.2	0.12	-
Al 2D	87.8	4.8	1.2	0.13	-
Al 5D	88.6	10.6	2.8	0.29	-
Al 8	84.2	17.2	4.5	0.46	-

*Mass is shown in field moisture

**Fe (III) coated sand = 1260 mg kg^{-1} and Al WTR = 104,000 mg kg^{-1}

3.3 Pore Water Analysis

Approximately 30 mL of pore water sample at each sampling location was extracted and stored in a polyethylene bottle at 4°C until tested. Initial samples were collected prior to each experimental run when no dosed water had been sent through the system yet, but soil had been fully saturated with tap water. These samples will be referred to as t=0 hrs for the duration of this report. Samples were taken again at t=24 hrs in both phases and weekly for the duration of each phase II run. Samples were filtered prior to analysis through 0.45µm cellulose acetate membrane syringe filters and analyzed on a HACH DR/4000 Spectrophotometer using method 8048 for SRP (detection limit 0.01 mg L^{-1}

PO_4-P). Pore water samples were tested for chloride using a Systea Scientific EasyChem discrete analyzer within 28 days.

Total mass SRP removed (Equation 3.1) and percent removal of SRP [($Mass_{removed}$/$Mass_{input}$) x 100%] was determined. The outlet concentrations were taken from the 2.9 m location as opposed to the 3 m location, as erosion was noticed at the outlet (3 m location) allowing surface water to permeate the groundwater interface and artificially elevating the outlet concentrations at the 3 and 8 cm depths. Flow rates at each inlet and outlet location were measured regularly and used in Equations 3.2 and 3.3.

$$Mass_{removed} = Mass_{input} - Mass_{output} \quad 3.1$$

$$Mass_{input} = [(CQ)_{input}]\, t_i \quad 3.2$$

$$Mass_{output} = \sum_{t_0 - t_i} [(CQ)_{0cm} + (CQ)_{3cm} + (CQ)_{8cm}]\, t_i \quad 3.3$$

Where: t_i = duration of experimental run, Q = flow rate at port location (mL s^{-1}), C = concentration at port location (mg L^{-1})

Phase I Pore and surface water samples were collected by opening valves located on all ports and allowing pore water to drip out. Approximately 30 mL of pore water sample at each sampling location was extracted and stored in a polyethylene bottle at 4°C until tested for PO_4 – P within three days of extraction. During the seven-day experimental run, surface and pore water samples were collected and analyzed for both PO_4 – P and chloride within three and 28 days of extraction, respectively.

Phase II Pore and surface water samples were collected using a luer-lok syringe for the surface water samples and by opening valves located on all ports and allowing pore water

to drip out. Approximately 30 mL of pore water sample at each sampling location was extracted and stored in a polyethylene bottle at 4°C until tested for PO_4 - P and chloride within three and 28 days of extraction, respectively. In phase II, samples were extracted once a week for the duration of each experimental run (refer to Table 3.3 in section 3.2). A chloride tracer was employed in the influent water simultaneously by adding NaCl to synthesize concentrations between 150 and 200 mg L^{-1} (for phase II only). The chloride tracer showed the movement of surface water through the soil medium over the duration of each experimental run in phase II.

Reduced conditions were verified by quantifying the Fe (II) in solution using a modified ferrozine assay method of (Stookey, 1970). Ferrozine reacts with iron (II) in solution creating a magenta color that can then be analyzed on a spectrophotometer at a wavelength of 562 nm. Three solutions are needed for this analysis: 0.5 N HCl, 6.25 N hydroxylamine, and a ferrozine solution. A ferrozine solution was made by adding 1 g ferrozine and 11.92 g of hepes buffer to 1 L of deionized water. The solution was adjusted to a pH of 7 using 10 N NaOH. Five mL of ferrozine solution was pre-measured in capped glass containers and stored at 4°C until analysis. Iron (II) Standards were synthesized using ferrous ammonium sulfate (F.W. 392.1 g mol^{-1}) at concentrations of 0, 0.01, 0.05, 0.1, 0.5, 1, 2, 5 mM as Fe (II). Approximately 1 mL of pore water was extracted from each port within the soil layer (3 and 8 cm) by placing a 3 mL luer-lok syringe on the end of each stopcock, extracting the sample, and preserving it directly into 1 mL of 1 N HCl until analysis (1 N HCl was measured into capped glass containers prior to extractions). Samples were analyzed within 2 hours of extraction. For analysis, 0.1 mL

of preserved sample was added to the previously prepared 5 mL of ferrozine solution. A HACH DR/4000 Spectrophotometer was used to analyze samples within 30 minutes in a 1 cm cuvette at 562 nm for Fe (II). Total iron could be measured by adding 3 mL of 0.5 N HCl to the 1 mL extracted sample/1 mL 1 N HCl mixture to make a total volume of 5 mL. Then 0.2 mL of 6.25 N hydroxylamine was added to the 5 mL solution. After one hour, 0.1 mL of the hydroxylamine solution was added to 5 mL of ferrozine solution and analyzed at 562 nm. Results are discussed in Chapter 5.

3.4 Soil Analyses

Physical and chemical soil characteristics were determined before and after experimental runs were completed using the techniques described herein. Composite soil samples were taken at t=0 hrs (prior to running dosed water through the mesocosms) at inlet and outlet locations by taking a soil core in phase I and by removing a grab sample from the respective buckets of soil before they were placed in the mesocosm in phase II. Initial samples were analyzed for physical and chemical parameters. Soil cores were taken at the end of all experimental runs in phase I and at various times in each mesocosm during phase II. The method of removal and preparation of each sample is described in each section. Analyses were conducted for phases I and II unless specified otherwise.

3.4.1 Chemical Characteristics of Soil Matrices

(1) Phosphorus Sorption Isotherms

Phosphorus sorption isotherms were performed to determine the maximum amount of PO_4 - P the soil can retain. The saturation point is typically found using batch-experiments where soils are subjected to solutions containing various amounts of PO_4 - P (see description for each phase), shaken at 100 rpm for 24 hr (on a reciprocal shaker), and the filtrate is analyzed for SRP (SERA-IEG, 2009; Nair, et al., 1984).

Phase I Batch sorption experiments were performed on the initial soil of both vegetated and non-vegetated mesocosms to determine the PO_4 - P sorption maximum of each. Nair, et al. (1984) was used as the basis for the adsorption study. NaH_2PO_4 was used to create 0, 0.5, 1.5, 5, 10, 25, and 50 mg L^{-1} PO_4 - P solutions with a 0.01 M KCl background electrolyte. A 1:25 media:solution ratio (1.0 g air dried soil/25 mL solution) was employed using 50 mL centrifuge tubes (n=2) and placed on a reciprocal shaker (Cole-Parmer Orbital Shaker, a 51300-SERIES) for 24 hrs at a speed of 100 rpm. A second sample set was left on the shaker for an additional 24 hrs (total of 48 hrs) to verify the soil had reached its equilibrium concentration (n=1). These results are shown in Chapter 4.

Phase II Batch sorption experiments were performed on the initial soil of all mesocosms in phase II. The method provided by Nair, et al. (1984) was used as the basis of this adsorption study. NaH_2PO_4 was used to create 2.5, 5, 10, 15, and 25 mg L^{-1} PO_4 - P solutions with a 0.01 M KCl background electrolyte solution. Each solution's pH was

adjusted to 7.0 (± 0.5) using 1 M NaOH (Komlos and Traver, 2012). A 1:25 media:solution ratio (1.8 g air dried soil/45 mL solution) was employed using 50 mL centrifuge tubes leaving approximately 10% headspace (n = 2). Samples were rotated on a reciprocal shaker (Cole-Parmer Orbital Shaker, a 51300-SERIES) for 24 hrs at a rate of 100 rpm. A second set of 10 mg L^{-1} PO_4 – P samples were left on the shaker for an additional 24 hrs (t = 48 hrs total) to verify the soil had reached its equilibrium concentration. Final pH was spot measured to be 7.25 ± 0.28 (n=16).

Both Phases After shaking, the soil suspension was left to settle for an hour after which the supernatant was filtered using a 0.45 μm cellulose acetate membrane filter. The filtrate was analyzed for SRP using an inductively coupled plasma mass spectrophotometer (ICP). A linearized Langmuir adsorption equation was fit to the isotherm data and was used to predict the maximum amount of PO_4 - P that could be sorbed to the soil (equation 3.4).

$$\frac{C}{S} = \frac{1}{kS_{max}} + \frac{C}{S_{max}} \qquad 3.4$$

where: $S = S' + S_o$, the total amount of P retained (mg kg^{-1}), S' = P retained by the solid phase (mg kg^{-1}), S_o = P originally sorbed on the solid phase (previously adsorbed P) (mg kg^{-1}), C = concentration of P after 24 hr equilibrium (mg L^{-1}), S_{max} = P sorption maximum (mg kg^{-1}), and k = a constant related to the bonding energy (L mg^{-1} P)

The isotherm analysis was used to provide the PO_4 - P sorption capacity of the soil at the average inlet concentration for each experimental run. Determination of S_o was found using the oxalate extraction procedure described in the following section.

(2) Oxalate Extractable P, Fe, and Al

The amount of P sorbed to soil can be found by various extraction solutions. The oxalate extraction has been used widely for measuring short-range-order minerals in soils such as Al and Fe (del Campillo and Torrent, 1992), which are main P sorbents in noncalcareous soils (McKeague and Day, 1966; Schoumans, 2000) and exhibits a strong correlation between oxalate-extractable phosphorus, aluminum, and iron (P_{ox}, Al_{ox}, and Fe_{ox}) (SERA-IEG, 2009; Beek, 1978; Schwertmann, 1964; Richardson, 1985; Reddy and D'Angelo, 1994). Standards were prepared in an ammonium oxalic acid matrix for P, Fe, and Al using KH_2PO_4 for the P standards, and 1000 mg L^{-1} Al and Fe stock standards. The standard series contained 0, 1.25, 5, 12.5, and 25.0 mg L^{-1} of PO_4-P and 0, 2.5, 10, 25, 50, 100, and 125 mg L^{-1} of Fe and Al.

Phase I In the phase I analysis, initial sample soil cores [2.54 cm diameter, 10 cm deep (non-vegetated) and 15 cm deep (vegetated)] were taken from the inlet and outlet locations of the vegetated and non-vegetated mesocosms prior to any dosed experimental runs. Upon completion of all 24 hr runs, a soil core was taken at both the inlet and outlet regions of each mesocosm. Mesocosms were left to air dry with no influent flow for approximately 4 days to more easily extract the core from slightly saturated soil. Each soil core was 6.9 ± 0.7 cm (n = 4) in length for the non-vegetated and 10.3 ± 0.2 cm (n = 4) for the vegetated mesocosm (Table 3.6). Sample cores had variable lengths because soil was still moist and easily compacted with the soil coring tool, so each core was separated into three representative vertical sections denoting each vertical sampling port locations, and analyzed using the oxalate extraction method.

Table 3.6. Characteristic depths of soil plugs from non-vegetated and vegetated mesocosms, pre and post experimental runs in phase I.

Non-Vegetated (cm)	Vegetated (cm)
0 - 1.3	0 - 2.5
1.3 - 3.8	2.5 - 5.1
3.8 - 6.9 ± 0.7	5.1 - 10.3 ± 0.2

A modified method of McKeague and Day (1966, 1993) called for a soil:extraction solution ratio of 1:40 (0.5 g:20 mL). An extraction solution of 0.275 M ammonium oxalate (0.175 M ammonium oxalate and 0.1 M oxalic acid and adjusted to a pH of 3.0 ± 0.1 with 1 M HCl) was chosen based on recommendations from Wolf and Baker (1990) who suggest using 0.275 M acid ammonium oxalate solution to eliminate possible interferences associated with oxalate's affinity towards complexing with molybdate. Samples were shaken in the dark for 4 hrs (to minimize the reducing action of oxalic acid on Fe^{3+} ions), centrifuged for 20 mins at 2000 rpm, and filtered through a 0.45 μm cellulose acetate membrane filter. Phosphorus samples were analyzed using a HACH DR/4000 spectrophotometer method (#8048), while an ICP-AES determined amounts of Al and Fe.

Phase II The Schwertmann (1964) method was used to determine the oxalate extractable fractions of Al, Fe, and P from soil samples taken from all mesocosms (Table 3.7). A 2.54 cm (1 in) diameter push soil coring tool was used to remove soil from the central region of inlet, middle, and outlet locations (depth = 15 cm). Extraction and preparation of samples post-dosing is presented in Figure 3.10.

Table 3.7. Oxalate Extraction Samples (Comp=Composite, I=Inlet, M=Middle, O=Outlet).

	Time & Location				
Mesocosm ID	0 Wk	4 Wks	8 Wks	10 Wks	12 Wks
Control	Comp	I, M, O	-	-	I, M, O
FeP	I, O	-	-	-	I, M, O
Fe	I, O	-	-	I, M, O	-
Al 2	I, O	I, M, O	-	-	-
Al 2D	I, O	I, M, O	-	-	-
Al 5	I, O	I, M, O	-	-	-
Al 5D	I, M, O	I, M, O	I, M, O	-	-
Al 8	I, O	I, M, O	-	-	-

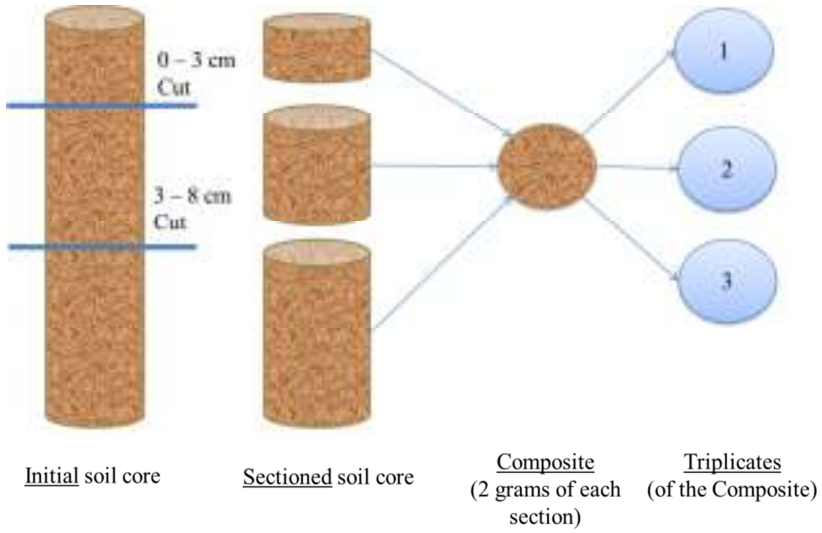

Figure 3.10. Soil core extraction method. Triplicate samples were taken from a composite sample of 2.54 cm diameter soil core.

An extraction solution (pH = 3.0 ± 0.1) was made using ammonium oxalate monohydrate and oxalic acid dihydrate. A 1:20 media:solution ratio (1.25 g/25 mL) was executed in 50 mL centrifuge tubes. Samples were rotated at 180 rpm on a reciprocating shaker for 2 hrs in the dark (to minimize the reducing action of oxalic acid on Fe^{3+} ions). Ten mL of

supernatant were filtered through a 0.45 μm cellulose acetate membrane filter and diluted (1:5) with 40 mL of 0.01 M HCl to make a 50 mL sample. Concentrations of P, Al, and Fe were analyzed on an ICP within 1 week.

Determination of the oxalate extractable forms of P, Fe, and Al was found using equations 3.5 – 3.7.

$$P_{ox} = \frac{5a(0.025\ L)}{m\ (30.97\ g\ mol^{-1})} \quad 3.5$$

$$Fe_{ox} = \frac{5a(0.025\ L)}{m\ (55.85\ g\ mol^{-1})} \quad 3.6$$

$$Al_{ox} = \frac{5a(0.025\ L)}{m\ (26.98\ g\ mol^{-1})} \quad 3.7$$

where: P_{ox}, Fe_{ox}, Al_{ox} = P, Fe, Al content of the dried soil sample (mmol kg^{-1}), a = P, Fe, Al concentration in soil extraction solution (mg L^{-1}), b = P, Fe, Al concentration in blank extraction solution (mg L^{-1}), m = mass dry soil (g)

The 0.025 L is the diluted sample volume (1:5 dilution) is in the numerator and the molecular weight of P, Fe and Al, respectively, is in the denominator.

(3) Determination of pH

The pH of the CSW soil (obtained from Villanova's CSW and used in both the vegetated and non-vegetated mesocosms) was completed using two reagents: water (phase I only) and $CaCl_2$ (both phases) (Table 3.8). Soil pH is typically measured in a soil - water slurry, however, it can also be found in a soil - 0.01 M $CaCl_2$ slurry. According to Graham (1959), the presence of soluble salts may affect the pH of a solution; therefore, the excess

salt introduced into solution through the use of $CaCl_2$ will cover the effects of existing soluble salts. An electronic pH meter (HACH HQ40d multi-parameter meter) determined the pH of the soil potentiometrically.

Table 3.8. Results from soil pH study in phase II. No large differences were observed between studies.

	H_2O (n=2)	$CaCl_2$ (n=2)
NonVegetated	7.3 ± 0.1	7.2 ± 0.0
Vegetated	7.4 ± 0.1	7.3 ± 0.0
Control	-	7.7 ± 0.0
FeP	-	7.6 ± 0.2
Fe	-	7.5 ± 0.1
Al 2	-	7.6 ± 0.0
Al 2D	-	7.6 ± 0.1
Al 5D	-	7.5 ± 0.0
Al 8	-	7.6 ± 0.1

(4) Organic Matter: Phase II Only

Organic matter was obtained through loss-on-ignition (LOI) by oven drying approximately 4 g of soil [3.77 ± 0.24 g (n = 20)] then igniting the oven dried soil [2.76 ± 0.23 g (n = 20)] in a 550°C muffle oven for 20 mins. The final mass of all samples was 2.53 ± 0.22 g (n = 20). The procedure was taken from Selected Physical and Chemical Standard Methods for Students: Method 2540 E (Clesceri, et al., 1990). Equation 3.8 provides the percent organic matter (% OM) by LOI. Duplicates were analyzed for each mesocosm sample.

$$\%\ \text{OM by LOI} = \frac{(\text{Mass dry soil + crucible}) - (\text{Mass ash + crucible})}{(\text{Mass dry soil+crucible}) - (\text{Mass of crucible})}(100) \qquad 3.8$$

3.4.2 Physical Characteristics of Soil Matrices

(1) Grain Size Distribution

Physical characteristics of each soil sample were determined through a sieve analysis for coarser, larger-sized particles, and a hydrometer analysis for finer particles using a modified ASTM D 422 Standard Test Method for Particle-Size Analysis of Soils (Reddy and D'Angelo, 1994). Due to limited sample, a hydrometer analysis was performed prior to the sieve. Ten grams of soil was obtained to determine water content of each sample, and then about 100 g of soil was taken and placed in a milkshake container with 5 g of Calgon as a dispersion agent. Tap water was added to create a slurry mixture which was then poured into a 1000 mL cylinder and shaken. A 152 H hydrometer was used to record readings at 1, 2, 4, 8, 15, 30, 60 minutes, 2, 4, and 24 hours. Temperature values were also recorded.

(2) Moisture Content

Moisture content analyses were completed often and are reported in Chapters 4 and 5. Gravimetric water contents were determined using ASTM Method D2216 by drying in a 104°C oven for 24 hrs. Moisture content (w) is calculated using equation 3.9:

$$w = \frac{M_{Moisture}}{M_{Total}}(100) \qquad 3.9$$

where: $M_{moisture}$ = mass of moist soil and tin - mass of dry soil and tin (g), M_{Total} = mass of moist soil (g)

(3) Porosity: Phase II Only

The ASTM D7063 porosity (η) was calculated using equation 3.10 for each mesocosm using the weight of soil placed in each mesocosm, moisture content, and volume of soil:

$$\eta = \frac{V_{voids}}{V_{Total}} = \frac{(1-\gamma_d)}{(G_s \gamma_w)} \qquad 3.10$$

Where: $\gamma_d = \frac{\gamma_t}{(1+w)}$ = dry unit weight ; w=moisture content; $\gamma_t = \frac{\text{Weight of Soil}}{\text{Volume of Soil}}$; G_s=2.65; γ_w = unit weight of water

The porosity provides an estimation of initial pore space in each mesocosm mix but does not necessarily reflect the ability of the water to move through the soil once saturated. When the Al WTR residuals were added in their clumpy as-received conditions, they formed their own clods in addition to the soil clods found in the native wetland soil. As a result, the effective porosity of the soil mixed with Al WTR's was greater than calculated for the control and mesocosms amended with iron coated sand (Table 3.9).

Table 3.9. Summary of mass of soil matrix mixture, mass of amendment added (kg), and resulting effective porosity. As mass of amendment increases, so does the effective porosity.

	Total Mass (kg)	Mass Amendment (kg)	Porosity η (%)
Control	83.0	-	64
FeP	82.5	3.5	65
Fe	85.5	3.5	65
Al 2	82.4	4.4	66
Al 2D	87.8	4.8	67
Al 5D	88.6	10.6	70
Al 8	84.2	17.2	71

*Note: Mass is shown in field moisture

(4) Saturated Hydraulic Conductivity: Phase II Only

Constant head hydraulic conductivity (k) was measured using ASTM Method D2434-68: Standard Test Method for Permeability of Granular Soils (Constant Head). A rigid-wall compaction-mold permeameter was used (r=3.80 cm, A=45.4 cm^2) and three different heads were analyzed (27.5, 53.5, and 62.5 cm). Approximately 200 g of initial soil from each mesocosm was used and loosely-packed in the permeameter to be consistent with experimental conditions. The sample was left to become fully saturated for a minimum of 2 hrs, and flow measurements were recorded after the sample had reached saturation equilibrium. The value of k, was found using equation 3.11:

$$k = \frac{QL}{hA} \qquad 3.11$$

where: k = saturated hydraulic conductivity (cm s^{-1}), Q = volume per time (mL s^{-1}), A = area of permeameter (cm^2), h = head (cm), L = length of soil sample (cm)

3.5 Statistical Analyses

Descriptive statistics were completed for each mesocosm study where appropriate. Two-sample t-tests and ANOVA (Analysis of Variance) analyses were conducted using Prism Graph Pad 6.0 with a p=0.05. Results are documented in Chapters 4 and 5, where analyses were deemed necessary.

Chapter 4 Phase I Analysis Examining Fate and Transport of SRP

This chapter reports the findings from phase I pore water sampling and soil analyses where the objective was:

1. To observe and measure pathways of soluble reactive phosphorus (SRP) fate and transport through a surface-flow constructed stormwater wetland (CSW) soil profile.

Phase I consisted of two mesocosm studies: non-vegetated and vegetated. Eight, 24 hr, experimental (pseudo) replicates were conducted within each mesocosm where pore water samples were extracted and analytically analyzed for SRP. Additionally, a four-day chloride tracer study showed pathways of SRP transport within each mesocosm followed by a three day SRP desorption analysis. Flow measurements were taken at the inlet (0 cm port) and the outlet ports at 0, 3, and 8 cm (soil) depths (Table 4.1). Both surface and sub-surface flow were provided in the phase I study. De-ionized water was gravity-fed at the inlet at a depth of 3 cm within the soil column to provide sub-surface flow during each experimental replicate. Each mesocosm had similar inflow (2.6 ± 0.04 mL s^{-1}) and likewise similar outflow at the 0 cm (2.3 ± 0.06 mL s^{-1}) and 3 and 8 cm ports (0.17 ± 0.04 mL s^{-1}). Pore water analyses are presented in section 4.1.

Table 4.1. Average flow rates of non-vegetated and vegetated mesocosms. Sample size is 16 for all data sets. Inlet and outlet flow values are shown for eight, 24-hr, experimental runs.

Mesocosm ID	Avg Q_{In} (mL s^{-1})	Avg $Q_{Out\ 0\ cm}$ (mL s^{-1})	Avg $Q_{Out\ 3\ \&\ 8\ cm}$ (mL s^{-1})
Non Vegetated	2.6 ± 0.04	2.3 ± 0.06	0.14 ± 0.03
Vegetated	2.6 ± 0.06	2.4 ± 0.08	0.19 ± 0.02
Avg	2.6	2.3	0.17
Std Dev	0.04	0.06	0.04

Soil cores were extracted prior to running dosed water through each mesocosm and after all eight experimental replicates were completed. Chemical and physical soil analyses are presented in section 4.2 and a summary of phase I results and discussion is found in section 4.3. Raw data is presented in Appendix A.

4.1 Pore Water Analysis Results and Discussion

Non-Vegetated Mesocosm Pore Water Analysis In the non-vegetated mesocosm, no plants and only 10 cm of wetland soil were present. Influent characteristics amongst all eight, 24-hr, experimental replicates were comparable (Table 4.2). Influent water had an average concentration of 0.53 ± 0.03 mg L^{-1} PO_4-P (n=8). Mass SRP in, out, and removed were calculated using methods described in Chapter 3. The flow rates were used to calculate the volume of water entering and exiting the mesocosm over 24 hrs.

Table 4.2. Influent concentrations of SRP in non-vegetated mesocosm. Mass SRP input, output, and subsequent removal are shown for each experimental replicate (24-hr test), of which there were eight. Sample size was four for all test influent concentrations. Total mass SRP input was 470 mg PO_4-P.

	Influent SRP (mg L^{-1})		Mass SRP	% SRP
	Avg	Stdev	Removed (mg)	Removed
Test 1	0.57	0.09	32	23%
Test 2	0.56	0.04	38	28%
Test 3	0.57	0.04	114	86%
Test 4	0.54	0.04	62	52%
Test 5	0.51	0.03	68	60%
Test 6	0.47	0.05	61	58%
Test 7	0.52	0.02	48	41%
Test 8	0.52	0.01	47	40%
Average	0.53		59	48%
Std Dev	0.03		26	20%

Replicates 1 – 8 were analyzed for SRP at ports 0 cm (a), 3 cm (b), and 8 cm (c) (Figure 4.1). The chloride tracer study was conducted after all eight, 24-hr, experimental replicates were completed and was used to demonstrate how the water moved through the soil of the non-vegetated mesocosm. When the normalized chloride C/C_o value is close to 1, the water had infiltrated at that depth and horizontal distance over the course of the 24-hr period. At port 0 cm, the influent water had generally reached both horizontal locations (C/C_o>0.75; Figure 4.1a). At port 3 cm (Figure 4.1b) the influent water did not fully reach either horizontal location. The 8 cm location (Figure 4.1c), showed only about half of the influent water (C/C_o=0.5) reached this port. This suggests that the vertical and horizontal hydraulic conductivity prevented equilibrium from occurring within the 24-hr timeframe. SRP removal is shown when the chloride concentrations were greater than the SRP data point. This was not the case at any port location except the 8 cm, 0.6 m location from the inlet (although this point was very close to the SRP data) (Figure 4.1).

Pore water concentrations were summarized by time, vertical, and horizontal parameters. These data sets were then used to complete two-sample t-tests to determine whether there were significant differences ($p < 0.05$) between combinations of time and space. There were significant differences between the t=0 hr [0.18 ± 0.19 mg L^{-1} PO_4-P (n=18)] and t=24 hr SRP concentrations [0.73 ± 0.19 mg L^{-1} PO_4-P (n=18)] when all values were analyzed, verifying that SRP had infiltrated the soil column. Additionally, there was a significant difference between the mass SRP in (123 ± 12 mg PO_4-P) and out (64 ± 29 mg PO_4-P) over all eight, 24-hr experimental replicates (two-sample t-test, $p<0.05$, R^2=0.75) (Table 4.3), indicating removal had, in fact, occurred; regardless of what the

chloride study had noted. Discrepancies could have resulted from having only conducted one chloride tracer study post-simulations.

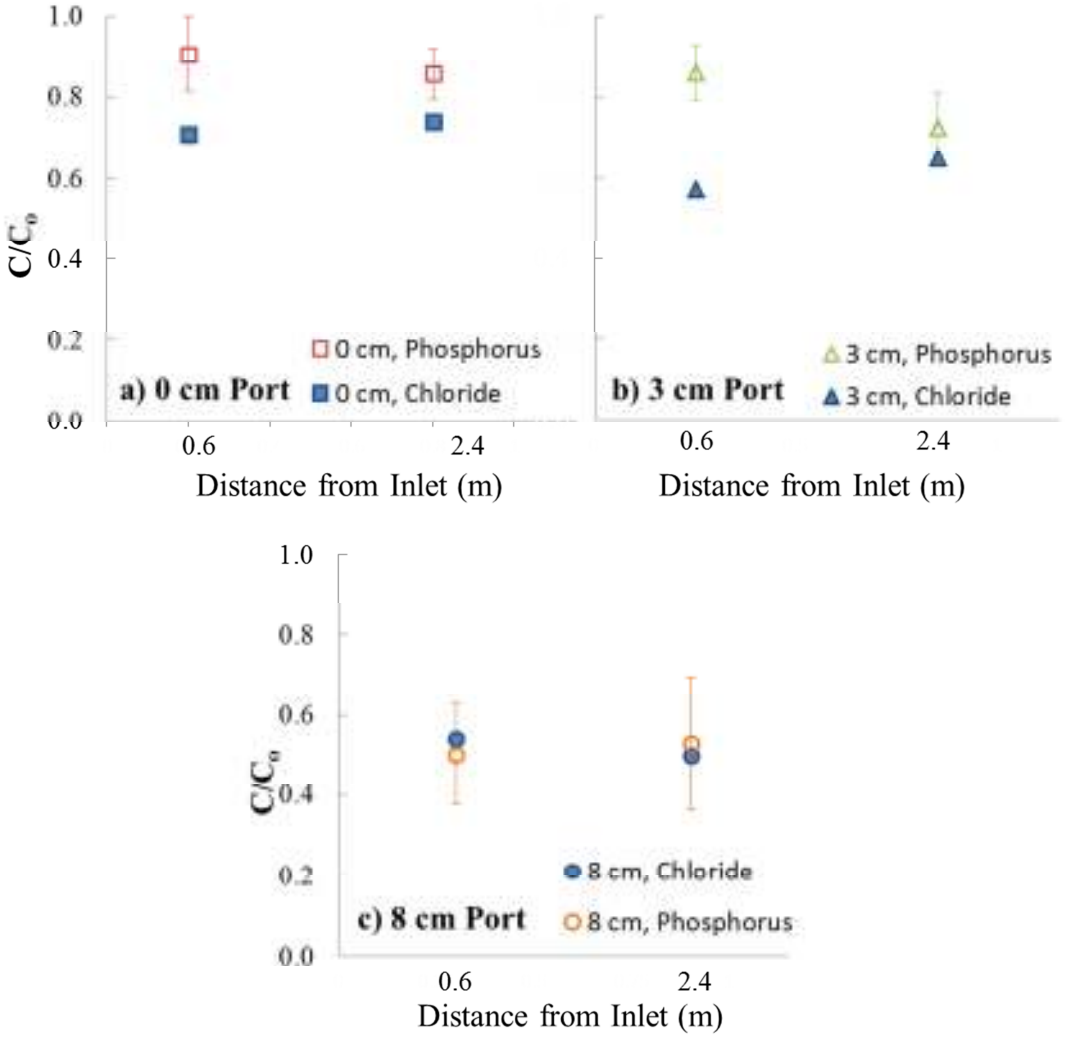

Figure 4.1. Phosphorus (open symbols) and chloride (closed symbols) concentrations from the non-vegetated mesocosm pore water results at port 0 cm (a), 3 cm (b), and 8 cm (c). Values are an average of eight 24-hr experimental runs (± std).

Table 4.3. Mass SRP input and output values for all eight 24-hr experimental runs in the non-vegetated mesocosm.

	Mass SRP In (mg)	Mass SRP Out (mg)
Test 1	141	109
Test 2	134	96
Test 3	133	18
Test 4	121	58
Test 5	115	46
Test 6	105	44
Test 7	117	69
Test 8	117	69
Average	123	64
Std Dev	12	29

A one-way ANOVA analysis was completed on the 0, 3, and 8 cm ports at the 24 hr point to determine whether there was a significant difference in removal over each depth. The resulting analysis showed there was a significant difference between values at each location ($p<0.05$, $R^2=0.69$), while the largest difference occurred between the 0 and 8 cm locations (mean difference = 0.39). This result was consistent with the results shown from the chloride tracer where only limited amounts of influent water were able to reach a depth of 8 cm, which may have resulted from the sub-surface DI water input. Consequently, the ANOVA analysis indicates that more SRP removal occurred within the first 3 cm than between 3 and 8 cm within the soil column.

Mass removal values from the pore water analysis are represented graphically in Figure 4.2. Replicates one and two showed lower mass and percent SRP removal than replicates four through eight. Replicate three had the highest mass SRP removed. It is unclear why removal values during the first three replicates were variable, although the mass SRP

input was the highest in those three (Table 4.3). Mass removal values of replicates four through eight demonstrate a downward trend, suggesting that soil was becoming more P saturated. Results are further discussed in section 4.2.

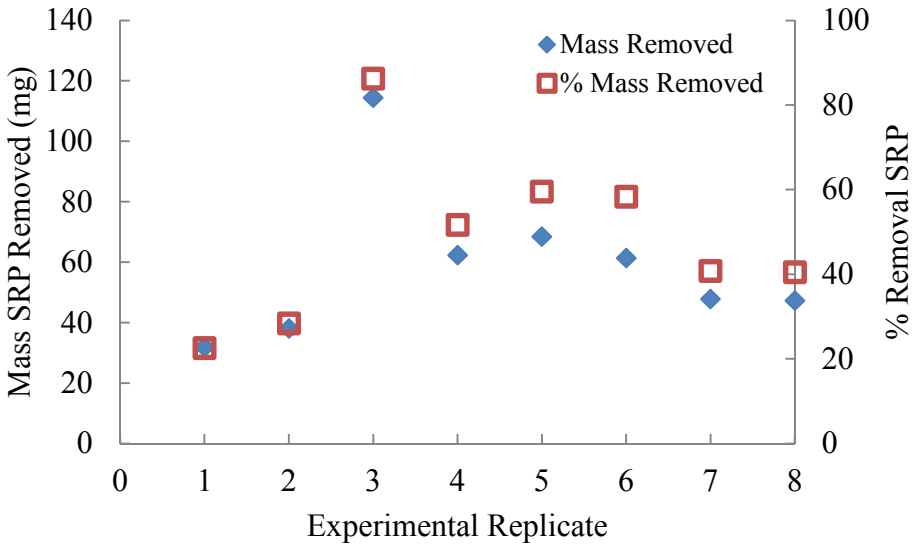

Figure 4.2. Mass SRP removed and percent SRP removal values of all eight, 24-hr, experimental replicates. Replicates 1-3 showed variable removal, while replicates 4-8 demonstrated a more consistent removal trend.

A seven day study was conducted after all eight 24-hr experimental replicates had been completed. Four days of SRP (0.54 ± 0.05 mg $L^{-1}PO_4$-P) and chloride dosed (190 ± 22 mg $L^{-1}Cl^-$) influent water were pumped through the non-vegetated mesocosm at a rate of 2.6 ± 0.3mL s^{-1}. Pore water samples were taken daily. After the fourth day, the surface water was removed and the sub-surface flow of DI water remained for an additional three days. Pore water samples were taken daily for three days post-dosing to observe whether desorption of SRP occurred. The purpose of the seven day study was: (1) to employ a chloride tracer so sub-surface water transport could be determined and (2) to observe desorption of SRP after surface flow had ceased at t=96 hrs (represented by the vertical

line in Figure 4.3). Results confirm that minimal SRP desorption within the soil layer occurs as a result of sub-surface pore water movement.

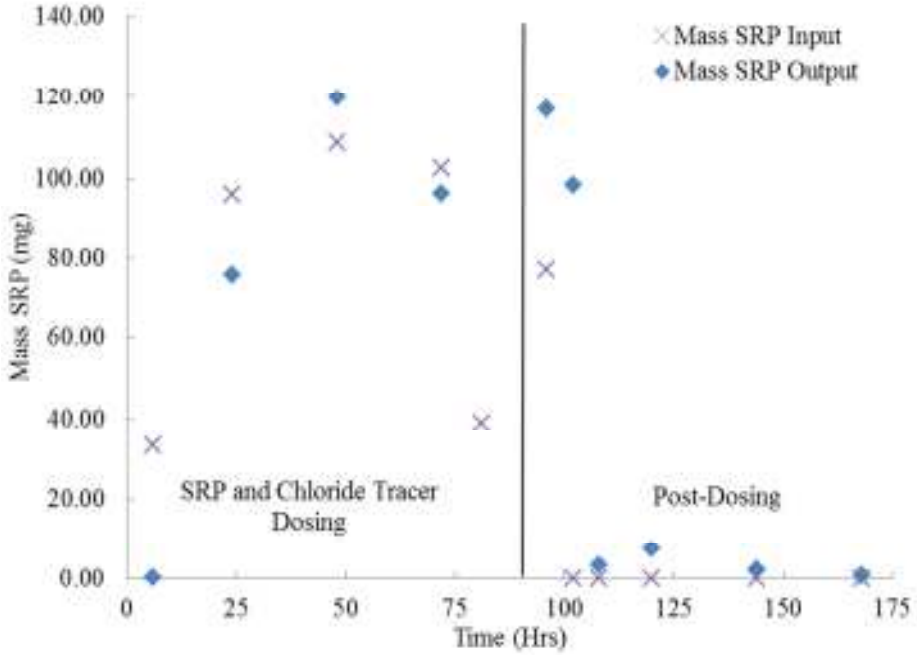

Figure 4.3. Results of the seven day analysis where four days of SRP and chloride dosed water was followed by three days of no surface flow. Results show minimal desorption through the soil layer post-dosing.

Vegetated Mesocosm Pore Water Analysis Wetland plants were placed in 15 cm of typical wetland soil in the vegetated mesocosm. Influent characteristics amongst all eight, 24-hr, experimental replicates were comparable (Table 4.4). Influent water had an average concentration of 0.54 ± 0.04 mg L^{-1} PO_4-P (n=8). Mass SRP in, out, and removed were calculated using methods described in Chapter 3.

Table 4.4. Mass SRP summary of eight, 24 hr experimental replicates in phase I vegetated mesocosm. Average percent removal was 40 ± 8% (n=8).

	Influent SRP (mg L^{-1})		Mass SRP	% SRP
	Avg	Stdev	Removed (mg)	Removed
Test 1	0.59	0.02	73	54%
Test 2	0.58	0.03	61	45%
Test 3	0.57	0.03	40	31%
Test 4	0.55	0.05	53	44%
Test 5	0.51	0.02	36	32%
Test 6	0.54	0.02	43	36%
Test 7	0.51	0.04	47	41%
Test 8	0.48	0.02	36	34%
Average	0.54		49	40%
Std Dev	0.04		13	8%

Replicates 1 – 8 were analyzed for SRP for the vegetated study at the 0, 3, and 8 cm depths with average values ± std reported (Figure 4.4). Figure 4.4a shows the 0 cm port data over the length of the mesocosm. Normalized chloride C/C_o values began at 0.86, decreased to 0.69 at the 1.8 m location and then increased again to 0.79; however, the trend generally decreased over the length of the mesocosm. This shows the water fully saturating the first half of the mesocosm. Surface water seemingly enters the soil as it moves from inlet to outlet as demonstrated in Figure 4.5. The thickness of the arrows in the figure represents the perceived water movement according to the chloride tracer analysis.

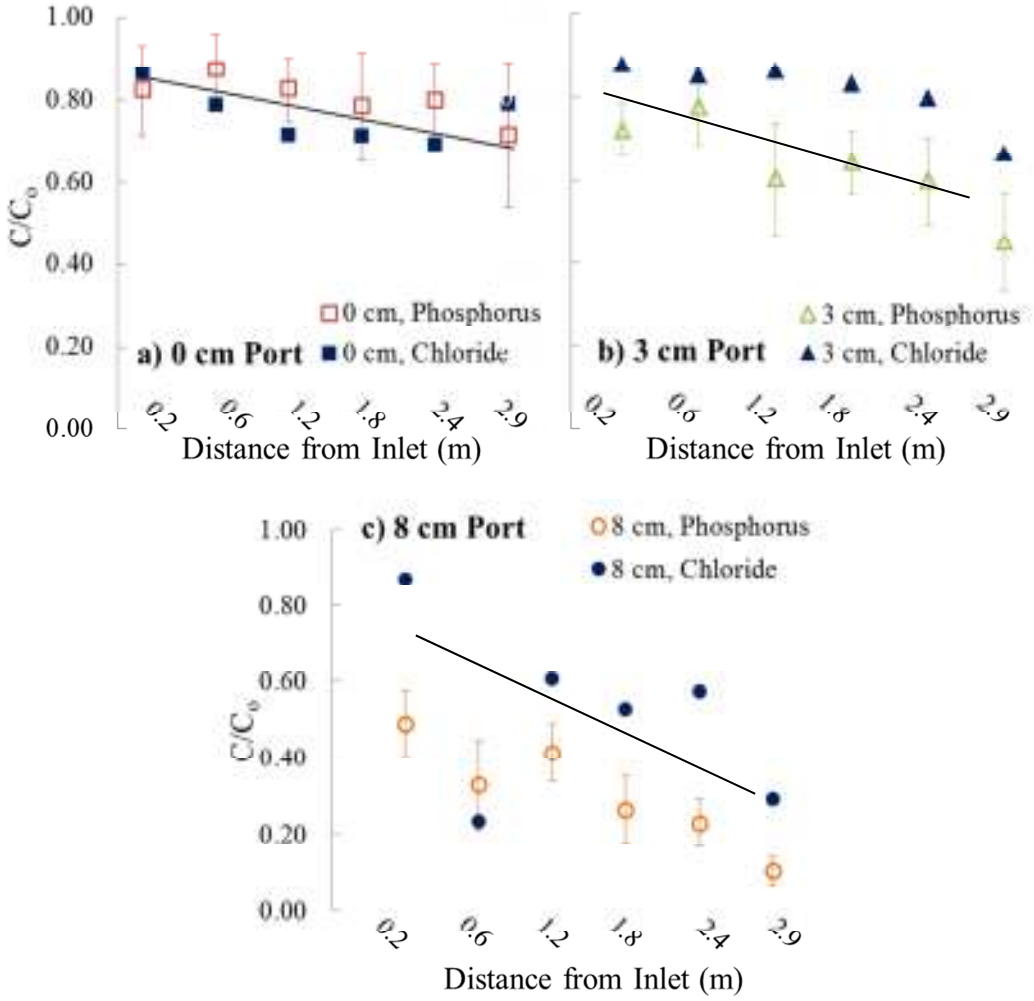

Figure 4.4. Phosphorus and chloride concentrations from the vegetated mesocosm pore water results at port 0 cm (a), 3 cm (b), and 8 cm (c). Values are an average of eight 24-hr replicates (± std). Trendlines are for chloride data.

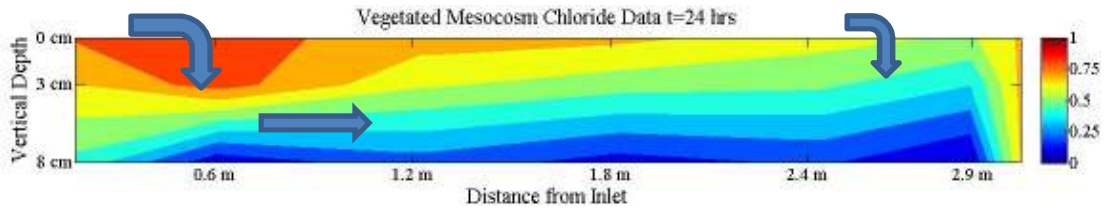

Figure 4.5. Contour plot of chloride C/C_o values from the vegetated mesocosm at t=24 hrs in phase I. Thickness of arrows represent the amount of infiltration associated with the inlet and outlet regions. Influent water seemingly infiltrates the soil from inlet to outlet. After a 24 hr period, the influent water in this mesocosm did not fully saturate the soil media.

At port 3 cm (Figure 4.4b), the chloride values were above the phosphorus values, symbolizing that the influent water had reached the 3 cm locations; however, the trend seen for 0 cm was mimicked at this depth as well. This further supports the idea that surface water had infiltrated the sub-surface flow at the inlet region first and then slowly infiltrated the soil medium as water moved towards the outlet. Additionally, the chloride values were shown to be above the SRP values, signifying SRP removal had occurred in this region. The 8 cm location (Figure 4.4c) showed similar trends to both the 0 and 3 cm ports, although (relative) concentrations were much lower (chloride had only fully reached the 0.2 m location). In all other locations C/C_o values were less than 0.6; suggesting that the vertical and horizontal hydraulic conductivity did not allow for full infiltration to occur within the 24-hr timeframe.

Two-sample t-tests determined significant differences ($p<0.05$) between various combinations of time and space. There was a significant difference between the SRP concentrations at t = 0 hrs [0.26 ± 0.35 mg L^{-1} PO_4-P (n=143)] and t = 24 hrs [0.58 ± 0.25 mg L^{-1} PO_4-P (n=161)] at all ports and all experimental replicates ($p<0.05$, $R^2=0.25$) verifying SRP removal. Additionally, there was a significant difference between the mass SRP inputs and outputs of all replicates (Table 4.5), representing the removal of SRP ($p<0.05$, $R^2=0.89$). A one-way ANOVA analysis was completed on the 0 cm [0.80 ± 0.12 mg L^{-1} PO_4-P (n=53)], 3cm [0.63 ± 0.14 mg L^{-1} PO_4-P (n=53)], and 8 cm ports [0.30 ± 0.15 mg L^{-1} PO_4-P (n=53)] at the 24 hr point of all replicates to determine whether there was a significant difference in removal over each depth. The resulting analysis showed there was a significant difference between values at each location ($p<0.05$,

R^2=0.69), while the largest difference in means occurred between the 0 and 8 cm locations (mean difference=0.50). This verifies that less removal of SRP occurred at the 8 cm depth, most likely as a result of the influent having not reached this location. Values from the pore water analysis are represented graphically in Figure 4.6. Mass removal values demonstrate a downward trend throughout all eight experimental replicates.

Table 4.5. Mass SRP input and output values for all eight 24-hr replicates in the vegetated mesocosm study.

	Mass SRP In (mg)	Mass SRP Out (mg)
Test 1	134	61
Test 2	134	73
Test 3	128	88
Test 4	119	67
Test 5	113	77
Test 6	119	76
Test 7	115	68
Test 8	105	70
Average	121	72
Std Dev	10	8

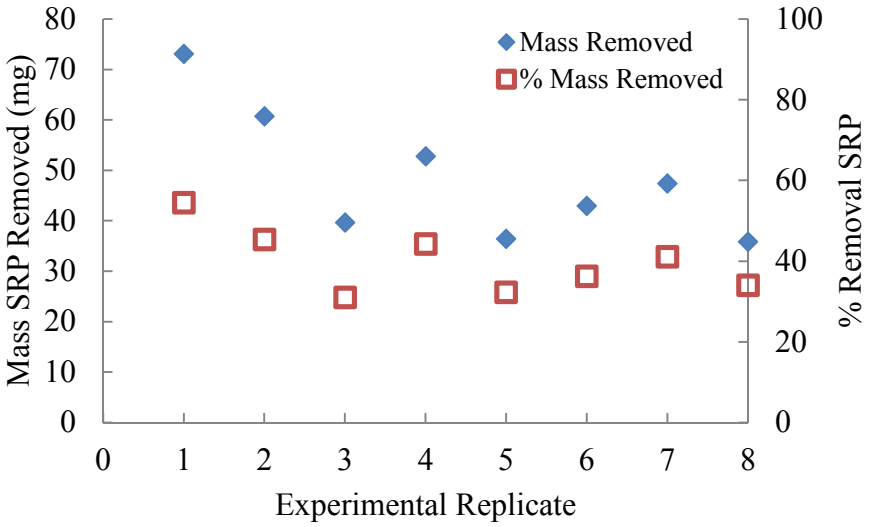

Figure 4.6. Trend of SRP retention over the eight 24-hr replicates in the vegetated mesocosm. A downward trend was observed as additional replicates were completed.

A seven day study was conducted after all eight 24-hr experimental runs had been completed. Four days of SRP (0.55 ± 0.01 mg $L^{-1}PO_4$-P) and chloride dosed (143 ± 17 mg $L^{-1}Cl^-$) influent water were pumped through the non-vegetated mesocosm at a rate of 2.6 ± 0.3mL s^{-1}) (Figure 4.7). Pore water samples were taken daily. After the fourth day, the surface water was removed and the sub-surface flow of DI water remained for an additional three days. Pore water samples were taken daily three days post-dosing to observe whether desorption of SRP had occurred. Figure 4.7 shows that 12 hrs after dosing was ceased, SRP mass output was negligible. Desorption of SRP within the sub-surface soil media was not observed.

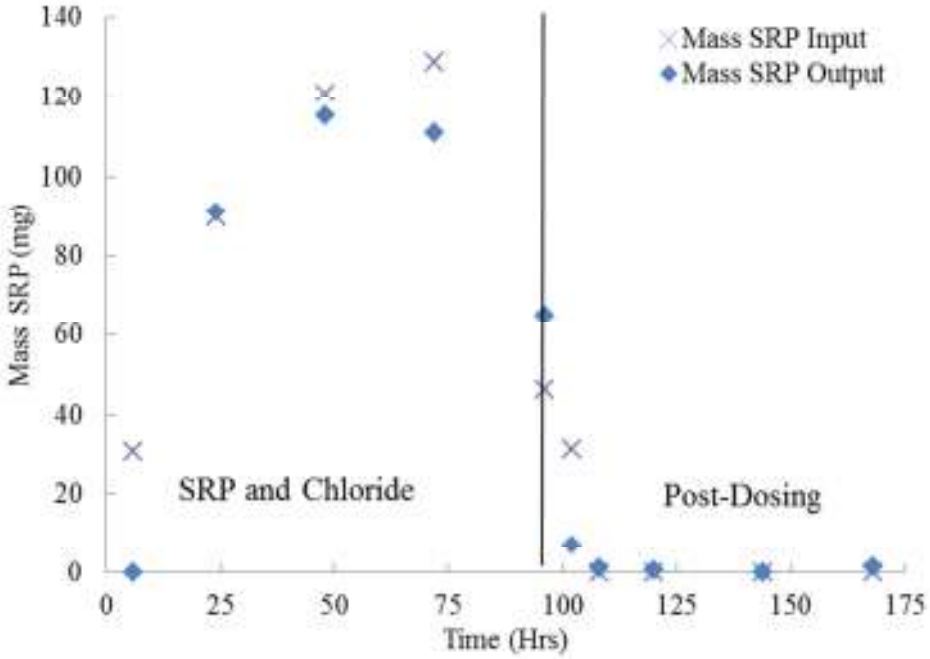

Figure 4.7. Results from P leaching analysis in the vegetated mesocosm. Dosing ceased at t=96 hrs, at which point, the mass SRP output nearly stopped, signifying no desorption of SRP had occurred.

4.2 Soil Chemical Analysis Results and Discussion

Phosphorus sorption isotherms, soil extractions using the oxalate method, and pH analyses were completed on each mesocosm soil to determine: (1) the P sorption capacity of soil placed in both nonvegetated and vegetated mesocosms (using P sorption isotherms); (2) amounts of P, Fe, and Al (mg kg^{-1}) within each mesocosm (oxalate extraction) at specified time points; and (3) the initial pH of the matrix soil.

(1) P Sorption Isotherms

Phosphorus sorption isotherms provide the amount of P the soil can retain given a specific aqueous P concentration. Initial soil samples were taken from each mesocosm prior to running dosed water through the soil medium. Results for the soil placed in both the nonvegetated and vegetated mesocosms showed a P sorption capacity of 330 ± 20 mg kg^{-1} (n=2) for an influent concentration of 0.52 mg L^{-1} PO_4-P. Average P sorption values from t=48 hr samples [0.20 ± 0.18 mg g^{-1} (n=6)] were not significantly different than values obtained in sets run for t=24 hrs [0.20 ± 0.17 mg g^{-1} (n=12)] (p=0.99), verifying equilibrium was reached after 24 hrs.

(2) Oxalate Analysis

An oxalate extraction was completed on the initial soil samples taken from each mesocosm prior to any P dosed simulations (Table 4.6). Results between the nonvegetated and vegetated mesocosms were similar for P, Fe, and Al.

Table 4.6. Results from oxalate extraction in phase I. Values from both the nonvegetated and vegetated mesocosms were reasonably similar for all constituents. No major differences were observed prior to P dosing.

	P_{ox} (mg kg^{-1})			Fe_{ox} (mg kg^{-1})			Al_{ox} (mg kg^{-1})		
	Avg	Std Dev	n	Avg	Std Dev	n	Avg	Std Dev	n
NonVeg	230	100	4	4100	1860	6	1280	580	6
Veg	250	100	6	4390	1840	6	1270	530	6

*All Values are from initial soil samples prior to dosed water analysis.

After all dosing experiments were complete; a second soil core was taken from the inlet and outlet locations of each mesocosm. Results from the oxalate extraction are shown in Table 4.7. When the final P_{ox} results were compared to initial values, there was no significant difference in the nonvegetated ($p=0.25$, $R^2=0.16$) or vegetated ($p=0.64$, $R^2=0.03$) mesocosm concentrations, indicating there was no mass SRP removal within each mesocosm. However, large standard deviations and heterogeneous soil samples, may have contributed to the variations within the mass balance.

Table 4.7. Summary of oxalate extractions after all eight, 24 hr dosing experiments were completed. No significant differences were found between the initial P, Fe, and Al concentrations in Table 4.1 and the final concentrations documented here.

	P_{ox} (mg kg^{-1})			Fe_{ox} (mg kg^{-1})			Al_{ox} (mg kg^{-1})		
	Avg	Std Dev	n	Avg	Std Dev	n	Avg	Std Dev	n
NonVeg	245	95	6	4150	1660	6	1240	470	6
Veg	240	93	6	4430	1800	6	1310	570	6

*All Values are from initial soil samples AFTER dosed water analysis.

(3) pH Determination

Determining the pH of the soil was completed using both water and $CaCl_2$ as reagents, showing a higher pH for the water slurry than the $CaCl_2$ slurry. The wetland soil used in

this study was found to be slightly above neutral, and was consistent with the pH found in the surface water present in the existing wetland (7.30). Results showed an average pH of 7.35 ± 0.08 (n=4) in H_20 and 7.20 ± 0.02 (n=4) in $CaCl_2$.

4.3 Summary

The phase I objective was to observe and measure SRP pathways through a surface-flow CSW soil profile. A nonvegetated and vegetated mesocosm were employed in this phase. Pore water samples were taken at various vertical and horizontal heights throughout the soil profile and analyzed for SRP and in some instances chloride. Values from the eight, 24 hr simulations within the nonvegetated mesocosm showed decreasing concentrations at each vertical depth (0, 3, and 8 cm) as well as along the lateral flow profile (0.6 and 2.4 m). However, chloride tracer results demonstrated that surface water did not fully saturate the soil column at all depths and horizontal locations over the course of the 24-hr simulation. This suggests that the vertical and horizontal hydraulic conductivity prevented equilibrium from occurring within the 24-hr timeframe. A two-sample t-test was used to determine that there was a significant difference between the SRP concentrations at t=0 hrs and t=24 hrs for all eight mesocosm studies. It was also verified that there was a significant difference between the mass SRP going into the mesocosm (123 ± 12 mg PO_4-P) and out (64 ± 29 mg PO_4-P) over all eight, 24-hr experimental runs in the non-vegetated mesocosm (two-sample t-test, $p<0.05$, $R^2=0.75$). This confirmed that there was, in fact SRP removed within the soil column.

The chloride tracer study from the vegetated mesocosm showed that influent water had generally reached the 0 and 3 cm port locations over the full horizontal length of the study; although less infiltration occurred as the water moved from the inlet to the outlet. At the 8 cm depth, the chloride tracer did not fully infiltrate at all horizontal locations; however, more surface water reached the 8 cm depth at the inlet region than it did the middle or outlet regions of the soil. The 8 cm port follows a similar trend seen in the 0 and 3 cm ports where surface water infiltration occurred at the inlet first and then moved towards the outlet. Additionally, a one-way ANOVA analysis was completed on the 0 cm [0.80 ± 0.12 mg L^{-1} PO_4-P (n=53)], 3cm [0.63 ± 0.14 mg L^{-1} PO_4-P (n=53)], and 8 cm ports [0.30 ± 0.15 mg L^{-1} PO_4-P (n=53)] at the 24 hr mark of all tests to determine whether there was a significant difference in removal over each depth. The resulting analysis showed there was a significant difference between SRP concentrations at each location ($p<0.05$, $R^2=0.69$), while the largest difference occurred between the 0 and 8 cm locations (mean difference=0.50). This indicates that less removal of SRP occurred between the 3 and 8 cm depths, which was likely a result of the influent having not reached this location.

There was no significant difference between the mass removal between values between the vegetated mesocosms 390 mg P (49 ± 13 mg P wk^{-1}) and nonvegetated 470 mg P (59 ± 26 mg P wk^{-1}) mesocosms ($p=0.34$, $R^2=0.09$). This suggests that the addition of emergent plants did not directly contribute to the removal of SRP within pore water. Results from phase I showed there were both horizontal and vertical flow characteristics

that ultimately affected SRP advection through the soil profile. Surface water infiltration into the depths of the soil also can play a role in the removal possibilities for SRP.

Chapter 5 Phase II Results and Discussion of Soil Amendment Experimental Runs

This chapter reports the findings from phase II where there were two objectives:

1. To quantify pore water soluble reactive phosphorus (SRP) mass removal associated with two soil enhancement strategies (Al WTR and iron (III) coated sand).
2. To analyze physical and chemical characteristics of soil matrices that may relate to SRP mass removal seen in pore water analyses.

Phase II consisted of soil amendments mixed into wetland soil taken directly from Villanova University's constructed stormwater wetland (CSW) (as detailed in section 3.2.2). Pore water samples were extracted from each mesocosm and analytically analyzed for SRP and a chloride tracer. Flow measurements at all inlet and outlet locations were measured routinely and used to determine mass removals. Physical and chemical parameters were found for each soil amendment mixture and results were used to explain and verify trends shown in the pore water extraction study. The preliminary soil chemical analyses are presented in section 5.1 followed by the pore water experiment results for each mesocosm in section 5.2. Soil analyses are presented in section 5.3. There was one mesocosm (Al 5: 5% Aluminum WTR by dry mass) that behaved differently than the others and is analyzed separately in section 5.4. Raw data is found in Appendix B.

5.1 Preliminary Soil Chemical Analysis Results

The P sorption isotherm provides the amount of P a certain soil can retain in equilibrium using a specified aqueous P concentration. The higher this value, the more potential a soil matrix has for P removal. A representative graphic of P sorption isotherm data is shown in Figure 5.1 for the control mesocosm soil (data from all mesocosms are found in

Appendix B). Experimental data (closed blue diamonds) was fit to the Langmuir isotherm model where the maximum sorption capacity and P sorption capacity at the average influent SRP concentration could be determined. Average inlet concentrations for the control mesocosm was 0.53 ± 0.07 mg L^{-1} (n=41), therefore the P sorption capacity (S_{max}) of this soil at the average inlet SRP concentration was 390 mg kg^{-1}. This process was completed for each mesocosm soil mixture and is summarized in Table 5.1.

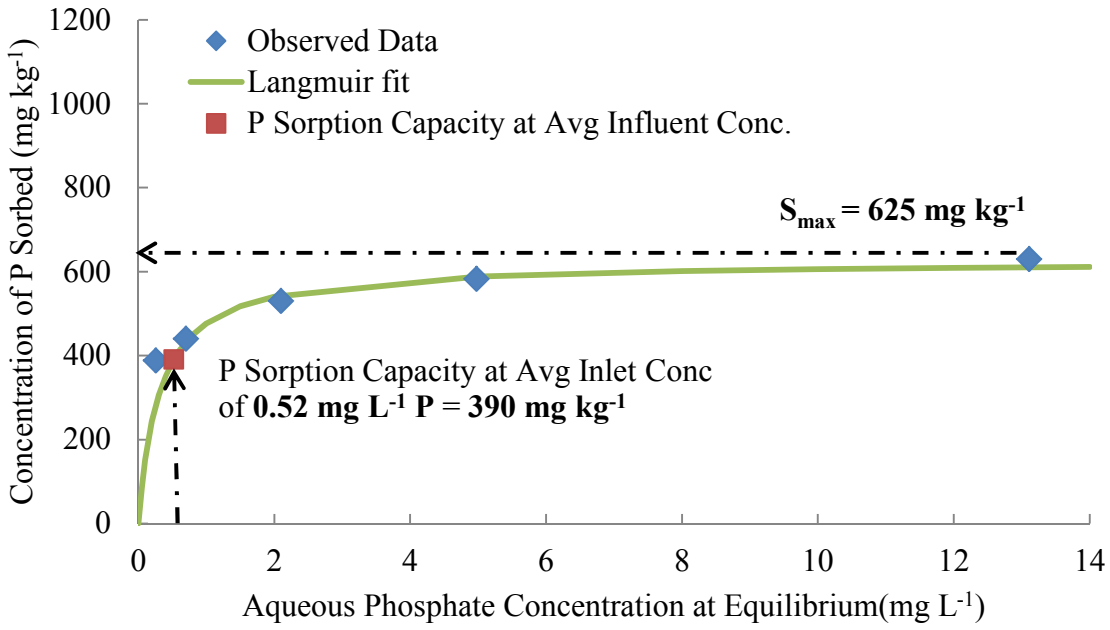

Figure 5.1. P sorption isotherm for control mesocosm soil (blue closed diamonds) fit to a Langmuir isotherm (green solid line). S_{max} = 625 mg kg^{-1} = maximum P soil can retain. P sorption capacity of soil at average inlet SRP concentration of 0.52 mg L^{-1} was 390 mg kg^{-1} (red square).

The P sorption capacities of each soil mix at the average influent concentration showed that the P sorption capacity of the control mesocosm (390 mg kg^{-1}) was within the range of both the FeP and Fe mesocosms (380 mg kg^{-1}). The P sorption capacity indicates that the amount of Fe (III) added to the soil (4 mg) via Fe (III) coated sand, did not provide

additional P sorption capacity. Additional chemical characteristics of each soil matrix are discussed in section 5.3.

The P sorption capacity increases as more residuals are added to the original wetland soil (Table 5.1). Both the Al 2 and Al 2D mesocosms showed the same P sorption capacities given the same average inlet concentrations (590 mg kg^{-1}). The Al 5D and Al 8 mesocosm soil matrices provided greater P sorption capacities of 750 and 900 mg kg^{-1}, respectively, suggesting mesocosms amended with Al WTR will provide the greatest SRP removal based on its chemical availability, while the control, FeP, and Fe mesocosms will perform the same with respect to SRP removal.

Table 5.1. Average inlet concentrations of SRP, P sorption capacity at average inlet concentrations, and mass removal values are reported for all mesocosms after four weeks.

Mesocosm	Avg Inlet SRP Conc. (mg L^{-1})	P Sorption Capacity at Avg Inlet P Conc. (mg kg^{-1})
Control	0.53 ± 0.03 (n=25)	390
FeP	0.51 ± 0.04 (n=27)	380
Fe	0.52 ± 0.03 (n=29)	380
Al 2	0.51 ± 0.08 (n=17)	590
Al 2D	0.51 ± 0.05 (n=23)	590
Al 5D	0.44 ± 0.04 (n=15)	750
Al 8	0.46 ± 0.02 (n=14)	900

Note: C_o solutions of 2.5, 5, 10, 15, and 25 mg P L^{-1} were used containing 0.01 M KCL as a background electrolyte and at pH 7.0 ± 0.5. A media to solution ratio of 1:25 was used.

5.2 Pore Water Analysis Results and Discussion

Each experimental run was at least four weeks in duration (refer to Table 3.3). Four of the mesocosms ran for extended periods of time: control, FeP, Fe, and Al 5D. The reasoning behind the length of these studies is discussed in each section. The organization of this section consists of a summation of all data followed by in-depth analyses on each individual mesocosm study.

A chloride tracer, employed in all mesocosms, verified that inlet water reached all port locations by week one (figures are reported in Appendix B). There was only dosed surface influent and no separate input of sub-surface water during phase II; however, horizontal sub-surface flow was created by opening the 3 and 8 cm port locations at the outlet. Surface flow was measured at inlet and outlet 0 cm locations. Flow was measured regularly using a graduated cylinder and stopwatch and averaged over the duration of each experimental run (Table 5.2).

Table 5.2. Average flow rates of all mesocosms. Sample sizes are shown for each mesocosm for both inlet and outlet flows over the duration of each experimental run.

Mesocosm ID	Avg Q_{In} ($mL\ s^{-1}$)	n_{In}	Avg $Q_{Out\ 0\ cm}$ ($mL\ s^{-1}$)	Avg $Q_{Out\ 3\ \&\ 8\ cm}$ ($mL\ s^{-1}$)	n_{Out}
Control	1.46 ± 0.04	96	1.20 ± 0.12	0.24 ± 0.02	54
FeP	1.43 ± 0.15	72	1.23 ± 0.04	0.25 ± 0.01	67
Fe	1.44 ± 0.06	74	1.18 ± 0.12	0.23 ± 0.04	50
Al 2	1.45 ± 0.01	36	1.17 ± 0.09	0.22 ± 0.01	19
Al 2D	1.44 ± 0.05	60	1.02 ± 0.10	0.26 ± 0.02	46
Al 5D	1.43 ± 0.02	101	1.22 ± 0.09	0.22 ± 0.04	72
Al 8	1.54 ± 0.13	45	1.23 ± 0.07	0.22 ± 0.01	43
Avg	1.46		1.18	0.23	

Each mesocosm had very similar inflow (1.46 ± 0.04 mL s^{-1}) and likewise similar outflow at the 0 cm (1.18 ± 0.07 mL s^{-1}) and 3 and 8 cm ports (0.23 ± 0.02 mL s^{-1}). All mesocosms showed comparable flow trends. Figure 5.2 represents the typical flow trend for all mesocosms (see Appendix B for all others). The initial value (t=24 hrs) for $Q_{Out\ 0cm}$ in Figure 5.2 is lower than the subsequent values because it was taken prior to having reached a steady state. The second data point represents the average values over the course of the first week once the system has reached equilibrium and that flow remains relatively constant for the duration of the study. Sub-surface flow (measured by combining the 3 and 8 cm ports) was regularly around five times lower than the surface flow ($Q_{Out\ 0\ cm}$). Table 5.3 summarizes influent concentrations of SRP and chloride, mass SRP input, and flow rates for all mesocosms over the durations noted.

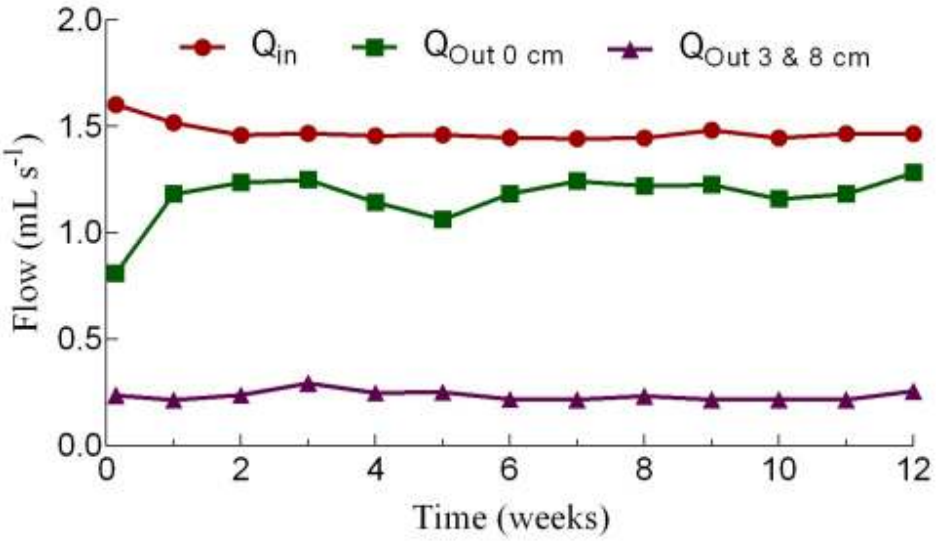

Figure 5.2. A typical flow regime for all wetland mesocosm studies. This particular set of data is the Control. Q_{in}, (red circles) is greater than both outlet flow values, while $Q_{Out\ 3and8\ cm}$ (purple triangles) is much lower (approximately five times lower) than $Q_{Out\ 0\ cm}$ (green squares).

Table 5.3. Influent concentrations of SRP and chloride, mass of SRP input per week and as a total, and influent flow rates are shown for each mesocosm reported at four weeks unless noted otherwise.

Mesocosm	Influent SRP ($mg\ L^{-1}$)	Influent Cl^- ($mg\ L^{-1}$)	Mass SRP In ($mg\ wk^{-1}$)	Mass SRP In (mg)	Flow Rate $mL\ s^{-1}$
Control	0.53 ± 0.03 (n=25)	170 ± 23 (n=19)	462 ± 10 (n=4)	1850	1.50 ± 0.06 (n=37)
Control[a]	0.53 ± 0.07 (n=41)	172 ± 22 (n=26)	456 ± 77 (n=8)	3670	1.46 ± 0.04 (n=96)
Control[b]	0.53 ± 0.07 (n=48)	173 ± 22 (n=30)	444 ± 57 (n=10)	4440	1.46 ± 0.04 (n=96)
Control[c]	0.52 ± 0.07 (n=55)	173 ± 21 (n=35)	443 ± 51 (n=12)	5310	1.46 ± 0.04 (n=96)
FeP	0.51 ± 0.04 (n=27)	172 ± 24 (n=23)	436 ± 27 (n=4)	1740	1.46 ± 0.05 (n=43)
FeP[c]	0.52 ± 0.06 (n=54)	174 ± 25 (n=39)	454 ± 44 (n=12)	5450	1.43 ± 0.15 (n=72)
Fe	0.52 ± 0.03 (n=29)	170 ± 27 (n=21)	445 ± 20 (n=4)	1780	1.46 ± 0.09 (n=43)
Fe[b]	0.54 ± 0.06 (n=51)	172 ± 28 (n=37)	468 ± 37 (n=10)	4680	1.44 ± 0.06 (n=74)
Al 2	0.51 ± 0.08 (n=17)	188 ± 29 (n=20)	440 ± 43 (n=4)	1760	1.45 ± 0.01 (n=36)
Al 2D	0.51 ± 0.05 (n=23)	118 ± 14 (n=29)	428 ± 17 (n=4)	1710	1.44 ± 0.05 (n=60)
Al 5D	0.44 ± 0.04 (n=15)	140 ± 22 (n=16)	367 ± 46 (n=4)	1470	1.44 ± 0.02 (n=37)
Al 5D[a]	0.47 ± 0.06 (n=37)	129 ± 20 (n=40)	391 ± 44 (n=8)	3125	1.44 ± 0.02 (n=101)
Al 8	0.46 ± 0.02 (n=14)	131 ± 9 (n=21)	425 ± 15 (n=4)	1700	1.54 ± 0.13 (n=45)

*Note: All values are reported at t = 4 weeks except: ; [a](t=8 wks); [b](t=10 wks); [c](t=12wks)

SRP removal trends are presented graphically in Figure 5.3 over the first four weeks to compare each treatment used. Mass SRP removed and percent SRP removed are shown for each mesocosm on a weekly basis. Trendlines are shown for the percent SRP removal values. All but the FeP mesocosm showed a downward trend of SRP removal over the four-week timeframe. The Fe and control mesocosm showed comparable trends. All mesocosms amended with Al WTR showed equivalent trends where the first week produced the highest removal of SRP, followed by relatively comparable values for the three weeks after. The control, FeP, and Fe mesocosms demonstrated more SRP removal than any of the Al WTR mesocosms over the four week duration.

Four mesocosms were run for durations longer than four weeks. Results from the control, FeP, Fe, and Al 5D mesocosms are shown in Figure 5.4 with three trendlines; one for

weeks one through four (dashed grey line); one for post-four weeks (dotted grey line); and one for the entire duration (solid black line), to demonstrate that post-four weeks, mesocosms seemingly approached a steady-state where the change in percent removal from week to week was relatively small. These trends are discussed again and in greater detail in each section.

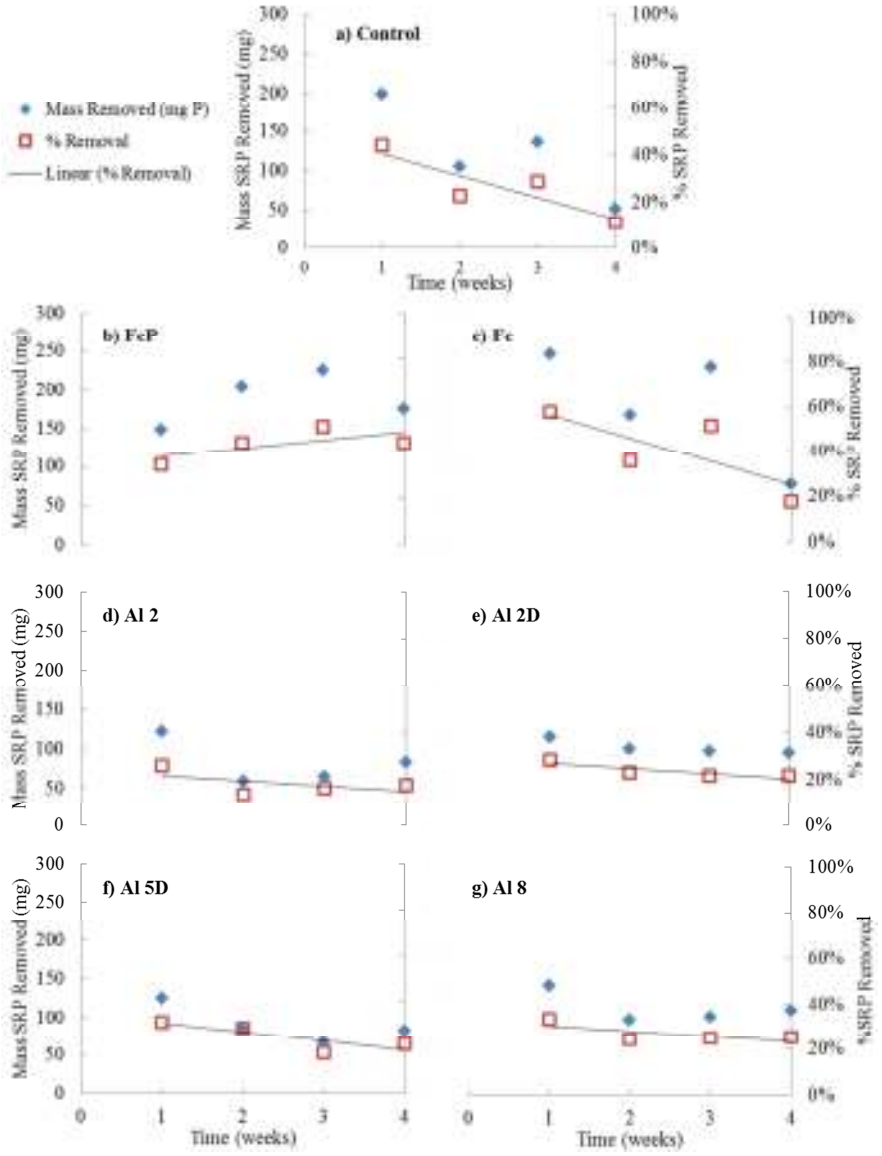

Figure 5.3. Mass SRP (mg P, blue diamonds) and percent removal (red squares) values shown each week over a 4 week duration. Trendlines were created for percent SRP removal values. All but the FeP mesocosm showed a negative slope as time progressed.

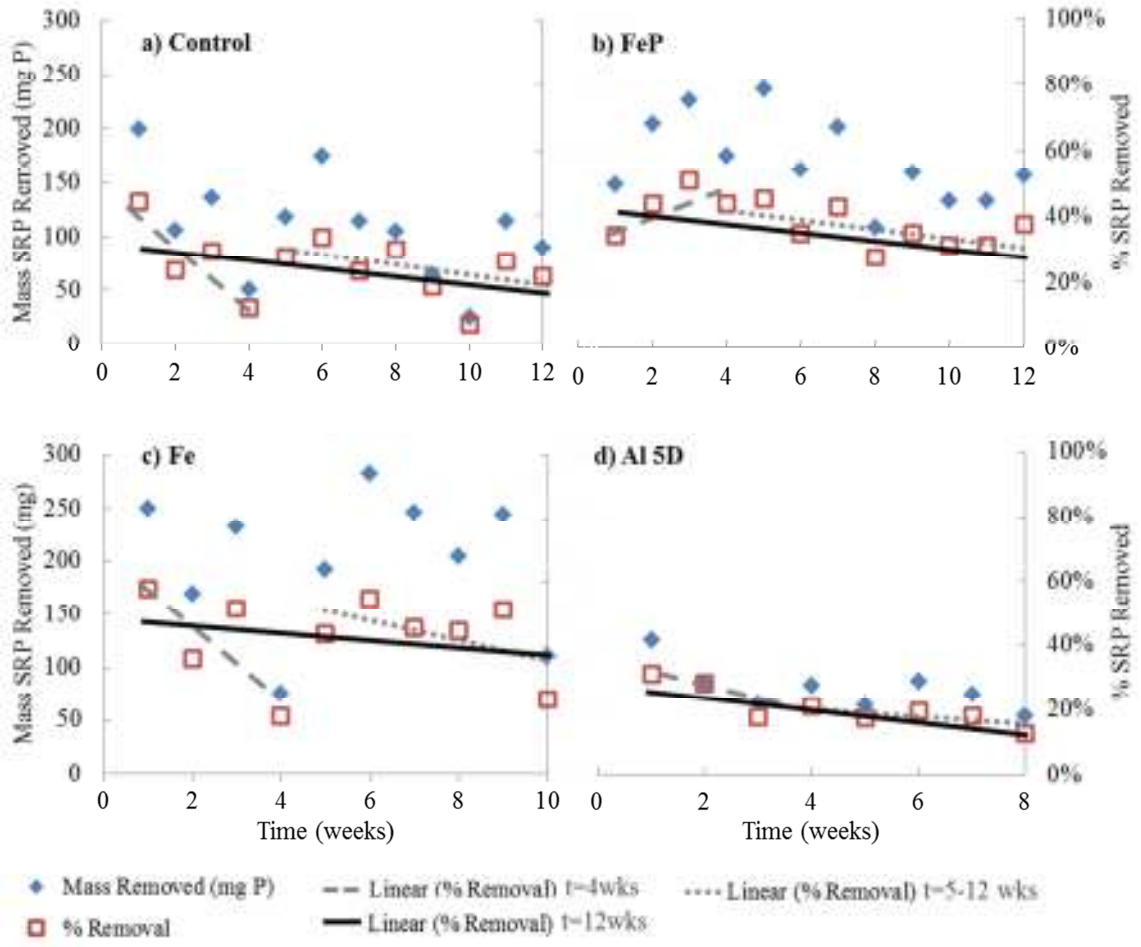

Figure 5.4. Mass SRP (mg P, blue diamonds) and percent removal (red squares) values shown each week over the duration of each extended study. Trendlines represent percent SRP removal values.

Results from Figures 5.3 and 5.4 are summarized in Table 5.4. Mass SRP removed per kg of soil were related to the percent SRP removals seen in the pore water analysis. A rate of mass SRP removal was also calculated for easy comparison amongst mesocosms. Over four weeks, the FeP mesocosm showed the highest removal of SRP with 9 mg kg^{-1} and 43% SRP removed, while all Al WTR mixes removed less SRP than the control (5.9 mg kg^{-1}), although only marginally.

Table 5.4. Summary table for all mesocosms reported at 4 weeks. Mass of SRP removed per kg of soil show the iron (III) amended soil to remove 9 mg kg^{-1} SRP, while all but Al 8 removed less SRP than the control mesocosm. Percent removal of SRP in pore water was quantified and correlated to mass SRP removal values.

Mesocosm	Mass SRP Removed (mg)	Mass SRP removed per kg Soil (mg kg^{-1})	Rate of Mass SRP Removal (mg $kg^{-1}wk^{-1}$)	% SRP Removed
Control	490	5.9	1.5	26%
Control[a]	1000	12.0	1.5	27%
Control[b]	1100	13.3	1.3	24%
Control[c]	1290	15.5	1.3	24%
FeP	750	9.0	2.3	43%
FeP[b]	1760	21.2	2.1	38%
FeP[c]	2060	24.8	2.1	38%
Fe	730	8.5	2.1	41%
Fe[b]	2010	23.4	2.3	43%
Al 2	350	4.5	1.1	20%
Al 2D	410	4.9	1.2	24%
Al 5D	360	4.0	1.0	24%
Al 5D[a]	630	7.1	0.9	20%
Al 8	460	5.5	1.4	27%

*Note: All values are reported at t = 4 weeks except: [a](t=8wks); [b](t=10 wks); [c](t=12 wks)

Fe (II) was measured in the pore water of the control, FeP, and Fe mesocosms each week for ten weeks (Figure 5.5) as a method for the detection of reduced conditions. At week eight, the average Fe (II) production in the Fe mesocosm drastically increased from a value of 5.4 to 13.8 mM Fe (II), while the values in the control and FeP remained below 2 and 5 mM Fe (II), respectively. Higher Fe (II) concentrations reflect the presence of reduced conditions. These results are further documented in the control, FeP, and Fe sections.

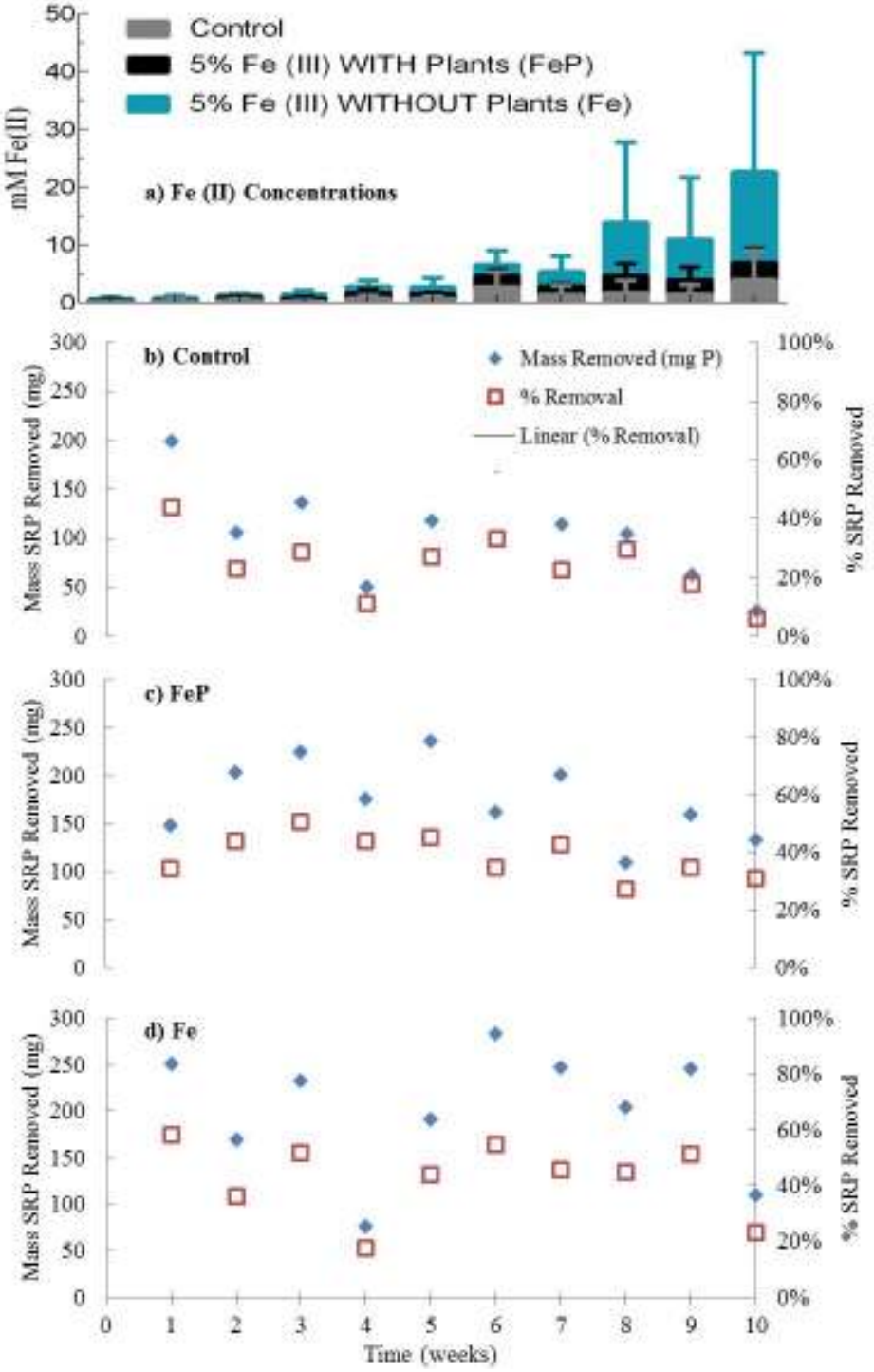

Figure 5.5. (a) Average Fe (II) concentrations including both 3 and 8 cm samples are shown with standard deviations and (b,c,d) mass SRP removed (blue diamonds) and percent SRP removed values (open red squares) shown over a 10 week period. Results indicate reduced conditions were present in all mesocosms at week 10; however, the Fe mesocosm showed highest levels of Fe (II) suggesting a more reduced condition.

Control: Soil Obtained from Villanova's Wetland

Results will be presented and discussed for each mesocosm individually. In the control mesocosm, no soil amendments were employed. Influent characteristics were comparable throughout the 12 week study (Table 5.5).

Table 5.5. Summary table for control mesocosm. Influent SRP and chloride values, mass of SRP input per week and total, and flow rates for respective time-frames are shown. No noticeable differences were observed between these values in the four and we week durations.

Mesocosm	Influent SRP ($mg\ L^{-1}$)	Influent Cl^- ($mg\ L^{-1}$)	Mass SRP In ($mg\ wk^{-1}$)	Mass SRP In (mg)	Flow Rate $mL\ s^{-1}$
Control	0.53 ± 0.03 (n=25)	170 ± 23 (n=19)	462 ± 10 (n=4)	1850	1.50 ± 0.06 (n=37)
Control[a]	0.53 ± 0.07 (n=41)	172 ± 22 (n=26)	456 ± 77 (n=8)	3670	1.46 ± 0.04 (n=96)
Control[b]	0.53 ± 0.07 (n=48)	173 ± 22 (n=30)	444 ± 57 (n=10)	4440	1.46 ± 0.04 (n=96)
Control[c]	0.52 ± 0.07 (n=55)	173 ± 21 (n=35)	443 ± 51 (n=12)	5310	1.46 ± 0.04 (n=96)

*Note: All values are reported at t = 4 weeks except: ; [a](t=8 wks); [b](t=10 wks); [c](t=12wks)

The control mesocosm was used as the comparison for all experimental runs. Values were taken at the four, eight, 10, and 12 week points. At t=4 weeks, the control mesocosm removed 5.9 mg kg^{-1} of SRP (Table 5.6). The same rate of removal was observed in the first eight weeks (1.5 mg kg^{-1} wk^{-1}), but a reduced rate in the last four weeks (0.88 mg kg^{-1} wk^{-1}) resulted in a removal rate of 1.3 mg kg^{-1} wk^{-1} over the 12 week duration (calculated using the mg SRP removed and mass soil matrix from Table 3.5). The decreasing trend in the last four weeks was reflected in the change in percent SRP removal (from 27% to 24%).

Table 5.6. Results of control pore water analysis. The decrease in mass of SRP removed from solution per kg of soil over a twelve week study, related with the decrease in percent of SRP removed.

Mesocosm	Mass SRP Removed (mg)	Mass SRP removed per kg Soil (mg kg^{-1})	% SRP Removed	Rate of Mass SRP Removal (mg $kg^{-1}wk^{-1}$)
Control	490	5.9	26%	1.5
Control[a]	1000	12.0	27%	1.5
Control[b]	1100	13.3	24%	1.3
Control[c]	1290	15.5	24%	1.3

*Note: All values are reported at t = 4 weeks except: [a](t=8wks); [b](t=10 wks); [c](t=12 wks)

There was a large drop in percent SRP removed over the first four weeks of the study (slope = -0.09 percent removal wk^{-1}) (Figure 5.4a). However, when the entire twelve week period was analyzed (Figure 5.4b) removal values rebounded at week five and then decreased at a constant slope of -0.02 percent removal wk^{-1}, which was consistent with what was observed over the entire duration (-0.02 percent removal wk^{-1}). The decreasing rate of SRP removal over time suggests this mesocosm was becoming P saturated. Desorption of SRP from the soil column was not observed (no negative mass SRP removed values). While week 10 dropped to 25 mg SRP removal, weeks 11 and 12 subsequently removed 110 and 90 mg SRP, respectively.

Fe (II) concentrations were measured in the control pore water. The concentrations for 3 and 8 cm pore water sampling ports were collected and averaged into one data point each week. Iron reduction appeared to have occurred throughout the duration of the study (Figure 5.6). As time progressed, the amount of Fe (II) found in solution increased [1.7 (week 8), 3.98 mM Fe (II) (week 10)], as compared to values taken prior to the

experimental run [(t=0 hrs) 0.13 mM Fe (II)] denoting the presence of reduced conditions. While reduced conditions were present, SRP desorption was not generally observed and removal still ensued suggesting the soil had not reached its maximum capacity for SRP. Soil analyses are reported in section 5.2.

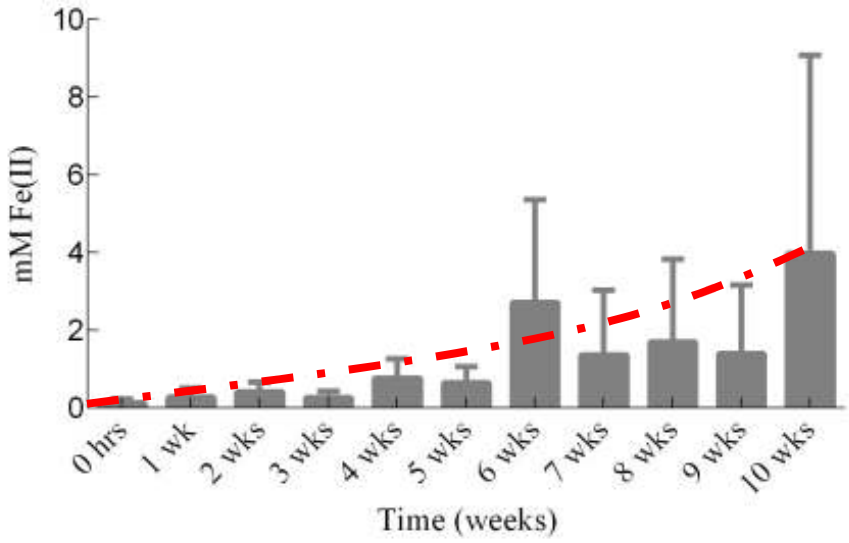

Figure 5.6. Ferrozine assay results for Control mesocosm over 10 weeks. Average Fe (II) concentrations including both 3 and 8 cm samples are shown with standard deviations. Fe (II) values began increasing at t = 4 weeks and continued to gradually increase through the duration of the study (with red dashed trendline).

FeP: Iron Coated Sand 5% Soil Mix with Plants

The FeP mesocosm included 5% iron (III) coated sand on a dry mass basis and 95% soil consistent with that of the control. Table 5.7 shows a summary of influent SRP and chloride concentrations, mass of SRP input both per week and over four/twelve weeks, and respective flow rates for both the control and FeP mesocosms. Values between the four and 12 week studies were comparable.

Table 5.7. Summary table for of influent SRP and chloride values, mass of SRP input, and flow rates for respective time-frames of the control and FeP mesocosms are shown. No noticeable differences were observed between these values in the four and 12 week durations.

Mesocosm	Influent SRP ($mg\ L^{-1}$)	Influent Cl^- ($mg\ L^{-1}$)	Mass SRP In ($mg\ wk^{-1}$)	Mass SRP In (mg)	Flow Rate $mL\ s^{-1}$
Control	0.53 ± 0.03 (n=25)	170 ± 23 (n=19)	462 ± 10 (n=4)	1850	1.50 ± 0.06 (n=37)
Control[a]	0.52 ± 0.07 (n=55)	173 ± 21 (n=35)	443 ± 51 (n=12)	5310	1.46 ± 0.04 (n=96)
FeP	0.51 ± 0.04 (n=27)	172 ± 24 (n=23)	436 ± 27 (n=4)	1740	1.46 ± 0.05 (n=43)
FeP[a]	0.52 ± 0.06 (n=54)	174 ± 25 (n=39)	454 ± 44 (n=12)	5450	1.43 ± 0.15 (n=72)

*Note: All values are reported at t = 4 weeks except: [a](t=12wks)

At t=4 weeks, the control mesocosm removed 5.9 mg P kg^{-1} (26% removal of SRP), while the FeP mesocosm removed 9 mg P kg^{-1} (43% removal) verifying that the addition of iron (III) increased SRP removal (Table 5.8). This same drop in mg P kg^{-1} soil wk^{-1} mass removal was observed in the control and FeP mesocosms between weeks four and twelve (0.2 mg P kg^{-1} soil wk^{-1}). Over a 12 week study, the control mesocosm removed 15.5 mg P kg^{-1} (24% removal of SRP), while the FeP mesocosm removed 24.8 mg P kg^{-1} (38% removal). As the percent removal values decreased for each mesocosm reflecting less mass SRP removal as time progressed, the FeP mesocosm still showed a relatively large percent removal of 38% after 12 weeks of analysis.

Table 5.8. Results of FeP pore water analysis. The decrease in mass of SRP removed from solution per kg of soil over a twelve week study, correlated with the decrease in percent of SRP removed.

Mesocosm	Mass SRP Removed (mg)	Mass SRP removed per kg Soil ($mg\ kg^{-1}$)	Rate of Mass SRP Removal ($mg\ kg^{-1} wk^{-1}$)	% SRP Removed
Control	490	5.9	1.5	26%
Control[a]	1290	15.5	1.3	24%
FeP	750	9.0	2.3	43%
FeP[a]	2060	24.8	2.1	38%

*Note: All values are reported at t = 4 weeks except: [a](t=12 wks)

The FeP mesocosm had a positive percent removal slope (0.04 percent removal wk^{-1}) over the first 4 weeks of the study (most likely as a result of experimental variation) (Figure 5.4b). While the first three weeks showed increasing SRP removal, the four week mark decreased suggesting a change in trend post four weeks, which was verified after continuing the study for 12 weeks (Figure 5.4b). Over the 12 week analysis the mass SRP removal decreased over weeks five through 12 at a slope of -0.01 percent removal wk^{-1}. This slope was the similar to the one observed in the control mesocosm over the same duration (-0.02 percent removal wk^{-1}). Over the twelve week study, average removal percentages were higher for the FeP mesocosm (38 ± 7%) than the control (24 ± 10%), which was significantly different ($p<0.05$, $R^2=0.44$).

Fe (II) concentration in the FeP mesocosm study reflected the trend seen in the control mesocosm (Figure 5.7). Fe (II) concentrations were elevated in the FeP mesocosm each week. The addition of Fe (III) through the iron amended sand, may have contributed to the increase in reduced conditions as compared to the control. Having more Fe (III) within the soil would provide additional opportunities for reduction to occur. At week four, the Fe (II) concentrations for FeP began to increase compared to initial values [0.23 mM Fe (II) (week 0), 1.7 mM Fe (II) (week 4)], indicating reduced conditions had begun. The Fe (II) concentrations appeared to be increasing with time: weeks six through ten showed average values below 7 mM Fe (II). Mass P removal was above 100 mg P each week (170 ± 39 mg wk^{-1}) for the duration of the FeP study and no desorption of SRP was observed.

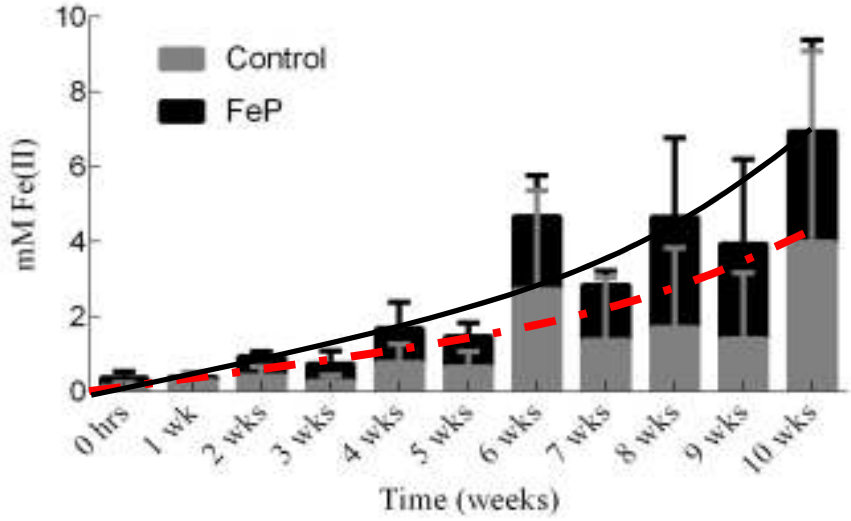

Figure 5.7. Ferrozine assay results for Control and FeP mesocosms over 10 weeks. Average Fe (II) values are shown with standard deviations. Fe (II) values for both the Control (red dashed trendline) and FeP mesocosms (solid black trendline) began increasing at t = 4 weeks and continued through the ten week study.

Fe: Iron Coated Sand 5% Soil Mix without Plants

Influent SRP and chloride concentrations, mass SRP inputs, and flow rates for the Fe mesocosm were consistent with results seen in both the control and FeP mesocosms (Table 5.9).

Table 5.9. Summary table of influent SRP and chloride values, mass of SRP input, and flow rates for respective time-frames are shown for the control, FeP, and Fe mesocosms. No noticeable differences were observed between these values over their respective experimental durations.

Mesocosm	Influent SRP ($mg\ L^{-1}$)	Influent Cl^- ($mg\ L^{-1}$)	Mass SRP In ($mg\ wk^{-1}$)	Mass SRP In (mg)	Flow Rate $mL\ s^{-1}$
Control	0.53 ± 0.03 (n=25)	170 ± 23 (n=19)	462 ± 10 (n=4)	1850	1.50 ± 0.06 (n=37)
Control[a]	0.53 ± 0.07 (n=48)	173 ± 22 (n=30)	444 ± 57 (n=10)	4440	1.46 ± 0.04 (n=96)
Control[b]	0.52 ± 0.07 (n=55)	173 ± 21 (n=35)	443 ± 51 (n=12)	5310	1.46 ± 0.04 (n=96)
FeP	0.51 ± 0.04 (n=27)	172 ± 24 (n=23)	436 ± 27 (n=4)	1740	1.46 ± 0.05 (n=43)
FeP[b]	0.52 ± 0.06 (n=54)	174 ± 25 (n=39)	454 ± 44 (n=12)	5450	1.43 ± 0.15 (n=72)
Fe	0.52 ± 0.03 (n=29)	170 ± 27 (n=21)	445 ± 20 (n=4)	1780	1.46 ± 0.09 (n=43)
Fe[a]	0.54 ± 0.06 (n=51)	172 ± 28 (n=37)	468 ± 37 (n=10)	4680	1.44 ± 0.06 (n=74)

*Note: All values are reported at t = 4 weeks except: [a](t=10 wks); [b](t=12 wks)

The Fe mesocosm shows a gradual increase in Fe (II) past week four, followed by a drastic increase at week eight [14 mM Fe (II)] (Figure 5.8). While the Fe (II) concentrations increase over time in all mesocosms, results indicate that the most Fe (III) reduction occurred in the Fe mesocosm. Additionally, soil removed from the mesocosm at week 10 was darker in color, trending towards grey as opposed to brown, in the lower 10 cm of the mesocosm soil (Figure 5.9) which signifies reduced conditions were present. Soil from the FeP mesocosm was light brown in color (Figure 5.10), thus signifying that reduced conditions were not as pronounced. Concentrations for the control, FeP, and Fe mesocosms at week 10 were: 4.0 ± 5.1; 6.9 ± 2.5; and 22.6 ± 21 mM Fe (II) (n=14), respectively. The magnitude of the reduced conditions provides evidence that the addition of plants successfully slowed the reduction of Fe (III) to Fe (II) in the FeP mesocosm (with plants) when compared to the Fe mesocosm (without plants).

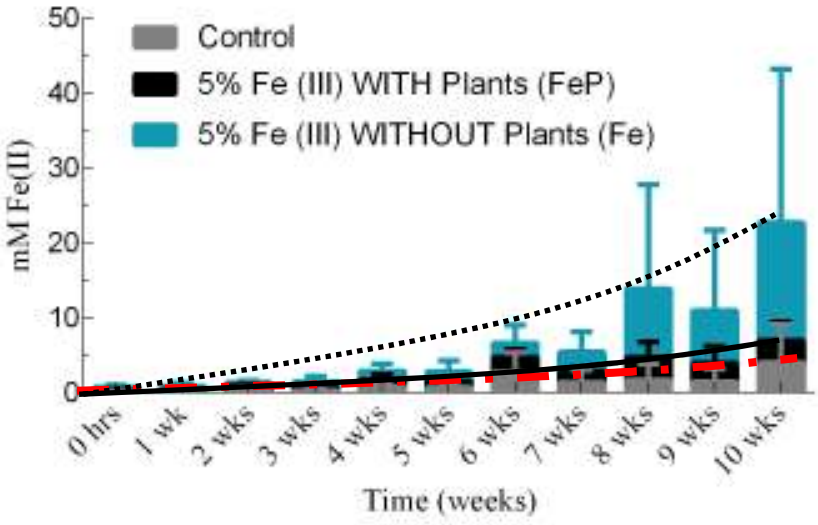

Figure 5.8. Fe (II) concentrations for control (red dashed trendline), FeP (solid black trendline), and Fe (dotted black trendline) mesocosms over 10 weeks. Average Fe (II) values are shown with standard deviations and trendlines.

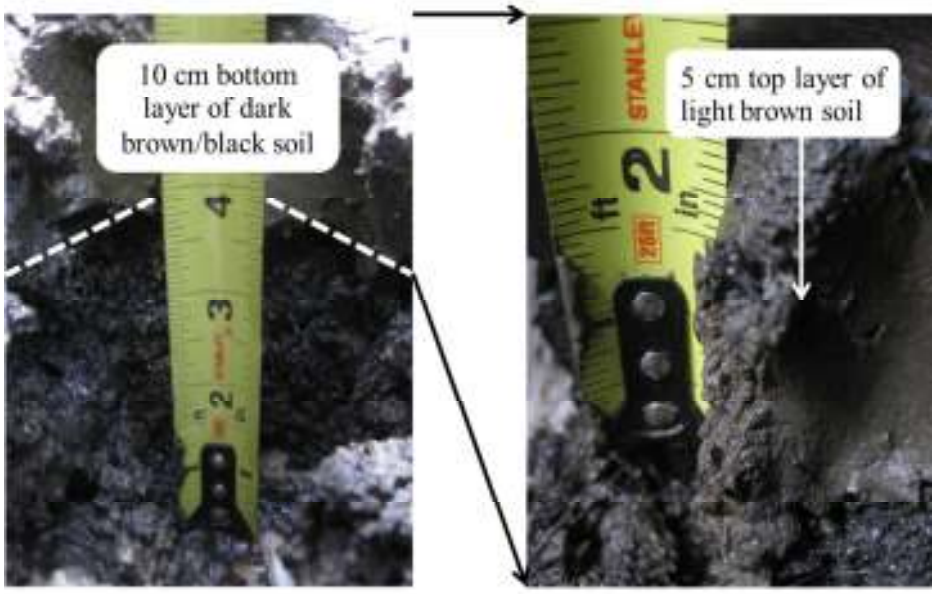

Figure 5.9. Photographs of Fe soil after a 10 week experimental run. The top 5 cm of soil was of a lighter brown color suggesting reduction had not occurred in this layer. The bottom 10 cm layer was observed to be dark grey; verifying quantitative results from the ferrozine assay that showed reduced conditions were present in the Fe mesocosm.

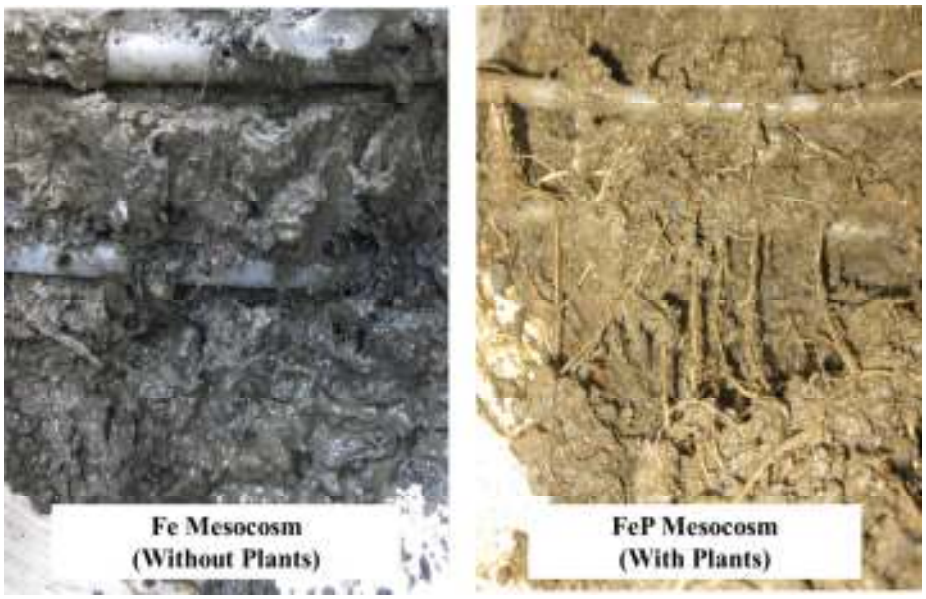

Figure 5.10. Comparison of soil between the Fe and FeP mesocosms. A darker grey soil was observed in the Fe mesocosm, where a lighter brown soil was observed in the FeP mesocosm during de-construction.

While the results showed the FeP and Fe mesocosm to have the similar removal capabilities over a four week period (9.0 and 8.5 mg kg^{-1}, respectively), over a ten week period the Fe mesocosm removed 23.4 mg kg^{-1} of SRP where the FeP and control mesocosms removed 21.2 and 13.3 mg kg^{-1}, respectively (Table 5.10). There was no significant difference between the Fe and FeP SRP mass removals ($p=0.31$, $R^2=0.07$), while there was a significant difference between the Fe, FeP, and control mesocosms over the ten week study ($p<0.05$, $R^2=0.36$), verifying that mass removal had occurred as a result of the addition of Fe (III) coated sand.

Table 5.10. Summary of pore water SRP removal in control, FeP, and Fe mesocosms over a four and 10 week duration. The Fe mesocosm showed the best mass SRP removal per kg soil (23.4 mg kg^{-1}) at the 10 week mark.

Mesocosm	Mass SRP Removed (mg)	Mass SRP removed per kg Soil (mg kg^{-1})	Rate of Mass SRP Removal (mg $kg^{-1}wk^{-1}$)	% SRP Removed
Control	490	5.9	1.5	26%
Control[a]	1100	13.3	1.3	24%
FeP	750	9.0	2.3	43%
FeP[a]	1760	21.2	2.1	38%
Fe	730	8.5	2.1	41%
Fe[a]	2010	23.4	2.3	43%

*Note: All values are reported at t = 4 weeks except: [a](t=10 wks)

When comparing the mesocosms amended with iron (III) over a ten week period, the FeP mesocosm showed the highest SRP removal at 23.4 mg kg^{-1} (Table 5.11). The FeP and control mesocosms were run for a total of 12 weeks. At the end of 12 weeks, the FeP mesocosm had removed a total of 24.8 mg kg^{-1} (38%), while the control removed 15.5 mg kg^{-1} SRP (24%).

Table 5.11. Summary table of iron (III) coated sand mesocosm study in comparison with the control. The Fe mesocosm exhibited the most removal (25 mg kg^{-1}) over a 10 week study, although the slope was most steep (-0.03) suggesting this mesocosm may not have had as great removal past ten weeks.

Mesocosm	Mass SRP Removed (mg)	Mass SRP removed per kg Soil (mg kg^{-1})	Rate of Mass SRP Removal (mg $kg^{-1}wk^{-1}$)	% SRP Removed
Control	490	5.9	1.5	26%
Control[a]	1100	13.3	1.3	24%
Control[b]	1290	15.5	1.3	24%
FeP	750	9.0	2.3	43%
FeP[a]	1760	21.2	2.1	38%
FeP[b]	2060	24.8	2.1	38%
Fe	730	8.5	2.1	41%
Fe[b]	2010	23.4	2.3	43%

*Note: All values are reported at t = 4 weeks except: [a](t=10wks); [b](t=12 wks)

Al 2 and Al 2 Duplicate: Aluminum WTR 2% Soil Mix

Two mesocosms with 2% Al WTR were employed. The duplicate study (Al 2D) was conducted to demonstrate repeatability of results from the Al 2 mesocosm. Soil in the Al 2 and Al 2D (duplicate) was amended with 2% by dry mass Al WTR mixed into 98% typical wetland soil. These mesocosms will be discussed simultaneously to demonstrate similarities. Influent concentrations, mass SRP inputs, and flow rates are reasonably consistent between the control and Al 2 mesocosms over the four week duration (Table 5.12). The chloride influent concentrations in the Al 2D were lower than both the Al 2 and control mesocosms, most likely as a result of changes in background chloride concentrations within the tap water. Additionally, the SRP mass input was slightly higher

in the control mesocosm than the Al 2 and Al 2D, however, there was no significant differences between mass SRP inputs ($p>0.05$, $R^2=0.35$).

Table 5.12. Influent SRP and chloride values, mass SRP input, and influent flow rates are presented for the control, Al 2, and Al 2D mesocosm over a four week period of study.

Mesocosm	Influent SRP ($mg\ L^{-1}$)	Influent Cl^- ($mg\ L^{-1}$)	Mass SRP In ($mg\ wk^{-1}$)	Mass SRP In (mg)	Flow Rate $mL\ s^{-1}$
Control	0.53 ± 0.03 (n=25)	170 ± 23 (n=19)	462 ± 10 (n=4)	1850	1.50 ± 0.06 (n=37)
Al 2	0.51 ± 0.08 (n=17)	188 ± 29 (n=20)	440 ± 43 (n=4)	1760	1.45 ± 0.01 (n=36)
Al 2D	0.51 ± 0.05 (n=23)	118 ± 14 (n=29)	428 ± 17 (n=4)	1710	1.44 ± 0.05 (n=60)

*Note: All values are reported at t = 4 weeks

While very little amendment was added, the large SRP sorption potential of these residuals was expected to remove large amounts of SRP and because the soil mix was made using 98% soil similar to the control, the Al 2 and Al 2D were expected to remove at a minimum as much SRP as the control; this outcome was not observed (Table 5.13). The Al 2 mesocosm reported a removal of 4.5 $mg\ kg^{-1}$ of SRP and the Al 2D removed 4.9 $mg\ kg^{-1}$ compared to 5.9 $mg\ kg^{-1}$ found in the control, while the percent of mass removed over the four week study for Al 2 was only 20% as compared to the 26% seen in the control. The values for the Al 2D mesocosm proved higher than the Al 2 study (4.9 $mg\ kg^{-1}$ versus 4.5 $mg\ kg^{-1}$ SRP removed) (Table 5.13), and both showed results lower than the control (5.9 $mg\ kg^{-1}$). Additionally, the mass removal rates per week were below that of the control (1.5 $mg\ kg^{-1}\ wk^{-1}$).

Table 5.13. Summary of mass SRP removal in the control, Al 2, and Al 2D mesocosms over a four week study. The control mesocosm showed the highest removal of SRP per kg of soil (5.9 mg kg^{-1}), which was unexpected based on the P sorption capacity of the Al WTR.

Mesocosm	Mass SRP Removed (mg)	Mass SRP removed per kg Soil (mg kg^{-1})	Rate of Mass SRP Removal (mg $kg^{-1}wk^{-1}$)	% SRP Removed
Control	490	5.9	1.5	26%
Al 2	350	4.5	1.1	20%
Al 2D	410	4.9	1.2	24%

*Note: All values are reported at t = 4 weeks

Results for both the Al 2 and Al 2D mesocosms (Figure 5.3d,e) demonstrated a larger SRP removal during week one than the following three weeks. While the results showed an increase in removal between weeks two and four for the Al 2 (14 to 18%) and a decrease in SRP removal for Al 2D (23 to 22%), both trendlines remained relatively mild (-0.02 percent removal wk^{-1}), indicating results post-four weeks would most likely have remained consistent with the previous three weeks. A two-sample t-test verified that there was no significant difference between the mass of SRP removed in the Al 2 and Al 2D mesocosms, which demonstrates that the analysis is repeatable ($p>0.05$, $R^2=0.67$). These results confirm that adding 2% Al WTR to the wetland soil, did not increase the removal of SRP compared to the control, therefore suggesting that the method of removal for SRP in a CSW using amendment strategies may not be entirely due to the P sorption capacity of the soil matrix.

Al 5D: Aluminum WTR 5% Soil Mix Duplicate

While the mesocosms with 2% residuals did not show an increase in removal of SRP compared to the control, it was possible the mix required more Al WTR for more

removal to be realized. A 5% soil mix was prepared and run for a total of eight weeks. The reason for the longer run was: (1) to confirm trends seen in both Al 2 and Al 2D mesocosms over a four week period where lower percent and mass SRP removal were measured as compared to the control, and (2) to determine whether the trend from the first four weeks had continued. Influent concentrations, mass SRP in, and flow rates over the referenced durations were comparable between all mesocosms (Table 5.14); there was a noticeable difference in the mass of SRP influent (mg kg^{-1}) for the Al 5D mesocosm over the first four weeks. There was 380 mg less SRP input into the Al 5D over four weeks than the control and 550 mg less SRP input into the Al 5D over the eight week comparison than the control. This resulted from a lower influent SRP concentration.

Table 5.14. Influent SRP and chloride values, mass SRP input, and influent flow rates are presented for the control, Al 2, Al 2D, and Al 5D mesocosm over a four week period and for the control and Al 5D over an eight week study.

Mesocosm	Influent SRP (mg L^{-1})	Influent Cl^- (mg L^{-1})	Mass SRP In (mg wk^{-1})	Mass SRP In (mg)	Flow Rate mL s^{-1}
Control	0.53 ± 0.03 (n=25)	170 ± 23 (n=19)	462 ± 10 (n=4)	1850	1.50 ± 0.06 (n=37)
Control[a]	0.53 ± 0.07 (n=41)	172 ± 22 (n=26)	456 ± 77 (n=8)	3670	1.46 ± 0.04 (n=96)
Al 2	0.51 ± 0.08 (n=17)	188 ± 29 (n=20)	440 ± 43 (n=4)	1760	1.45 ± 0.01 (n=36)
Al 2D	0.51 ± 0.05 (n=23)	118 ± 14 (n=29)	428 ± 17 (n=4)	1710	1.44 ± 0.05 (n=60)
Al 5D	0.44 ± 0.04 (n=15)	140 ± 22 (n=16)	367 ± 46 (n=4)	1470	1.44 ± 0.02 (n=37)
Al 5D[a]	0.47 ± 0.06 (n=37)	129 ± 20 (n=40)	391 ± 44 (n=8)	3125	1.44 ± 0.02 (n=101)

*Note: All values are reported at t = 4 weeks except: [a](t=8 wks)

The control mesocosm removed 5.9 mg kg^{-1} SRP over the four week duration, while the Al 5D removed only 4.0 mg kg^{-1} (Table 5.15). Over an eight week period, the control mesocosm removed 12 mg kg^{-1} SRP, while the Al 5D removed 7.1 mg kg^{-1}. Neither

analysis proved to be significantly different than the control over the same time frame ($p>0.05$, $R^2=0.67$ for 4 wks; $R^2=0.57$ for 8 wks).

Table 5.15. Summary of mass SRP removal in the control, Al 2, Al 2D, and Al 5D mesocosms over the durations noted. The control mesocosm showed a higher removal of SRP per kg of soil (5.9 and 12 mg kg^{-1}) over a four and eight week study, which was greater than all mesocosms amended with Al WTR.

Mesocosm	Mass SRP Removed (mg)	Mass SRP removed per kg Soil (mg kg^{-1})	Rate of Mass SRP Removal (mg $kg^{-1}wk^{-1}$)	% SRP Removed
Control	490	5.9	1.5	26%
Control[a]	1000	12.0	1.5	27%
Al 2	350	4.5	1.1	20%
Al 2D	410	4.9	1.2	24%
Al 5D	360	4.0	1.0	24%
Al 5D[a]	630	7.1	0.9	20%

*Note: All values are reported at t = 4 weeks except: [a](t=8wks)

SRP mass removal trends over an eight week period from the Al 5D mesocosm showed the same percent removal wk^{-1} as both the Al 2 and Al 2D mesocosms (-0.02 percent removal wk^{-1}) (Figures 5.3 and 5.4). The trend demonstrated by the Al 5D mesocosm over eight weeks can be applied to each of the other mesocosms with Al WTR. This presents the question: while mesocosms amended with Al WTR do not present larger mass removals than the control or iron (III) amended soils, will it ultimately remove more SRP over an extended period of time? This question is not within the scope of this analysis, but if this mesocosm demonstrated a removal rate of 0.9 mg $kg^{-1}wk^{-1}$ for another four weeks, the total mass SRP removed would be 960 mg, which is still less than the 1290 mg SRP removed in the control mesocosm over the 12 weeks.

Al 8: Aluminum WTR 8% Soil Mix

Given that the Al 2 and 5% mesocosms did not show a substantial increase in SRP removal, a mesocosm was made consisting of 8% Al WTR and 92% typical wetland soil by dry mass. The Al 8 mesocosm was run for four weeks. Influent concentrations were slightly lower than those measured in the control mesocosm study, resulting in less mass SRP input over the four week period of study (Table 5.16). All other factors were similar.

The Al 8 mesocosm exhibited a mass removal of 5.5 mg kg^{-1} of SRP, while the control showed a 5.9 mg kg^{-1} removal over a four week study (Table 5.17), but there was no significant difference between mass SRP removed in the Al 8 and the control ($p>0.05$, $R^2=0.02$). The Al 8 was the only mesocosm amended with Al WTR that demonstrated a larger percent removal than the control, although only by 1% (27 and 26%, respectively).

Table 5.16. Influent SRP and chloride values, mass SRP input, and influent flow rates are presented for the control, Al 2, Al 2D, Al 5D, and Al 8 mesocosm over a four week period and the control and Al 5D over an eight week study.

Mesocosm	Influent SRP (mg L^{-1})	Influent Cl^- (mg L^{-1})	Mass SRP In (mg wk^{-1})	Mass SRP In (mg)	Flow Rate mL s^{-1}
Control	0.53 ± 0.03 (n=25)	170 ± 23 (n=19)	462 ± 10 (n=4)	1850	1.50 ± 0.06 (n=37)
Control[a]	0.53 ± 0.07 (n=41)	172 ± 22 (n=26)	456 ± 77 (n=8)	3670	1.46 ± 0.04 (n=96)
Al 2	0.51 ± 0.08 (n=17)	188 ± 29 (n=20)	440 ± 43 (n=4)	1760	1.45 ± 0.01 (n=36)
Al 2D	0.51 ± 0.05 (n=23)	118 ± 14 (n=29)	428 ± 17 (n=4)	1710	1.44 ± 0.05 (n=60)
Al 5D	0.44 ± 0.04 (n=15)	140 ± 22 (n=16)	367 ± 46 (n=4)	1470	1.44 ± 0.02 (n=37)
Al 5D[a]	0.47 ± 0.06 (n=37)	129 ± 20 (n=40)	391 ± 44 (n=8)	3125	1.44 ± 0.02 (n=101)
Al 8	0.46 ± 0.02 (n=14)	131 ± 9 (n=21)	425 ± 15 (n=4)	1700	1.54 ± 0.13 (n=45)

*Note: All values are reported at t = 4 weeks except: [a](t=8 wks)

Table 5.17. Summary of mass SRP removal in the control, and all Al WTR mesocosms over the durations noted. The control mesocosm showed the highest removal of SRP per kg of soil (5.9 mg kg^{-1}) over the four week duration.

Mesocosm	Mass SRP Removed (mg)	Mass SRP removed per kg Soil (mg kg^{-1})	Rate of Mass SRP Removal (mg $kg^{-1}wk^{-1}$)	% SRP Removed
Control	490	5.9	1.5	26%
Control[a]	1000	12.0	1.5	27%
Al 2	350	4.5	1.1	20%
Al 2D	410	4.9	1.2	24%
Al 5D	360	4.0	1.0	24%
Al 5D[a]	630	7.1	0.9	20%
Al 8	460	5.5	1.4	27%

*Note: All values are reported at t = 4 weeks except: [a](t=8wks)

Summary and Discussion

The pore water analysis confirmed that the iron (III) amendment was most successful at removing SRP over a four week period (Table 5.18).

Table 5.18. Summary of phase II results for t=4weeks. The mesocosms amended with 5% iron (III) coated sand proved best at removing SRP per kg soil (9.1 and 8.5 mg kg^{-1}). Mesocosms amended with Al WTR proved to remove less SRP than the control over a four week period of study (< 5.9 mg kg^{-1}).

Mesocosm	Mass SRP Removed (mg)	Mass SRP removed per kg Soil (mg kg^{-1})	Rate of Mass SRP Removal (mg $kg^{-1}wk^{-1}$)	% SRP Removed
Control	490	5.9	1.5	26%
FeP	750	9.1	2.3	43%
Fe	730	8.5	2.1	41%
Al 2	350	4.2	1.1	20%
Al 2D	410	4.7	1.2	24%
Al 5D	360	4.1	1.0	24%
Al 8	460	5.5	1.4	27%

*Note: All values are reported at t = 4 weeks.

The results from all Al WTR studies support the statement that the addition of Al WTR to a CSW does not demonstrate a greater ability to remove SRP than typical wetland soil (Table 5.19). This could be a result of several possibilities: (1) the Al WTR used in this study did not have the SRP sorption capacity as presented in previous studies (see Chapter 2); (2) the hydraulic conductivity of the soil mixture after the residuals were added prevented the surface water to infiltrate into the soil column, the horizontal movement through the soil was also compromised; (3) the method by which the residual was added (as-received) resulted in a smaller surface area for sub-surface water to come in contact with; and (4) a combination of soil physics and sub-surface flow hydraulics resulted in less-favorable SRP removal conditions in soil amended with Al WTR.

Table 5.19. Summary of pore water analyses in control and Al WTR amended mesocosms.

Mesocosm	Mass SRP Removed (mg)	Mass SRP removed per kg Soil (mg kg^{-1})	Rate of Mass SRP Removal (mg $kg^{-1}wk^{-1}$)	% SRP Removed
Control	490	5.9	1.5	26%
Control[a]	1000	12.0	1.5	27%
Al 2	350	4.5	1.1	20%
Al 2D	410	4.9	1.2	24%
Al 5D	360	4.0	1.0	24%
Al 5D[a]	630	7.1	0.9	20%
Al 8	460	5.5	1.4	27%

*Note: All values are reported at t = 4 weeks except: [a](t=8wks)

The first possibility (1) will be addressed further in Section 5.3, which details chemical analyses that were completed on each soil mix to determine the P sorption capacity. Additionally, the amount of P, Fe, and Al present on soil samples prior to each

experimental run may provide insight into each soil mixture's ability to retain SRP. The second possibility (2) was addressed through the completion of constant head saturated hydraulic conductivity tests on each mix (results are shown in Section 5.3.2). The third possibility (3) is complimentary to the second (2). When the Al WTR was added to the soil, it was broken apart into small clumps by hand and mixed thoroughly. The resulting soil mixture was observed to be made up of small soil clods; unlike the iron (III) coated sand that stuck to all soil surfaces, the residuals seemingly did not and remained as independent clods. The method by which these residuals are added has only minimally been studied (Komlos, et al., In Review). The fourth (4) possibility is a combination of all three. Since the soils amended with Al WTR did not provided better removal than the control, it is hypothesized that soil physics and sub-surface water flow hydraulics prevented flow to access all soil so not all the soil and chemical potential was utilized.

5.3 Soil Analysis Results and Discussion

After water analyses were completed, the question remained: why did the iron amendments produce greater percent removal than the control, while all four Al WTR mesocosms produced smaller percent removal than both the iron (III) amendments and the control? To answer this question, an assessment of the physical and chemical characteristics of each soil mixture was completed and discussed herein.

Evidence from the water analysis showed an increase in SRP removal when soil was amended with Fe (III) coated sand and a decrease with Al WTR when compared to the control. Since the flow rates were similar in all experimental runs (Table 5.3), additional

physical and chemical characteristics of each soil mix needed to be determined. Phosphorus sorption capacities determined in Section 5.1 suggested the chemical characteristics of each soil amendment should have dictated the SRP mass removed. Had this been the case, the soils amended with Al WTR would have presented greater mass SRP removal than either the control or soils amended with iron (III) coated sand. This was not observed (Table 5.4), suggesting there were additional factors affecting SRP sorption within the soil layer. The chemical characteristics of each soil mixture were determined, followed by several physical characteristics.

5.3.1 Chemical Analysis

Phosphorus sorption isotherms and soil extractions using the oxalate method were completed on each soil mixture to determine: (1) which soil matrix had the highest P sorption capacity based on its chemical characteristics (P sorption isotherms); (2) amounts of P, Fe, and Al (mg kg^{-1}) initially within each soil mix (oxalate extraction) and at specified time points post-dosing; and (3) whether the amounts of Fe and Al added to each soil correlated to the SRP removal seen in each experimental run (mg SRP per kg added amendment).

(1) P Sorption Isotherms

Section 5.1 discussed results from the P sorption isotherm analysis. Results confirmed that the P sorption potential of the soils amended with Al WTR was greater than that of either the control or Fe (III) amended soils (Table 5.1), which suggests that the Al WTR amended soils would provide additional SRP mass removal benefits; however, this was

not observed (Table 5.20). In soils amended with the Al WTR none of the mass SRP removals were significantly different than the control ($p=0.43$, $R^2=0.21$). These results illustrate that the addition of residuals does not result in additional mass SRP removal (Figure 5.11). Additionally, the P sorption capacity of the control, FeP, and Fe mesocosms were generally within the same range and there was no significant difference between the control mesocosm and of the mass SRP removal of any amended mesocosms over a four week study ($p>0.05$). However, over the entire duration of each experimental run, there was a significant difference between the mass SRP removed within the soils amended with Fe (III) coated sand and the control ($p<0.05$; Table 5.10). This suggests that the added removal of SRP as a result of the addition of Fe (III) coated sand may have been because of its physical characteristics (since it did not provide additional chemical P sorption capabilities).

Table 5.20. Average inlet concentrations of SRP, P sorption capacity at average inlet concentrations, and mass removal values are reported for all mesocosms after four weeks.

Mesocosm	Avg Inlet SRP Conc. (mg L^{-1})	P Sorption at Avg Inlet Conc. (mg kg^{-1})	Mass SRP Removed (mg)	Mass SRP removed per kg Soil (mg kg^{-1})
Control	0.53 ± 0.03 (n=25)	390	490	5.9
FeP	0.51 ± 0.04 (n=27)	380	750	9.1
Fe	0.52 ± 0.03 (n=29)	380	730	8.5
Al 2	0.51 ± 0.08 (n=17)	590	350	4.2
Al 2D	0.51 ± 0.05 (n=23)	590	410	4.7
Al 5D	0.44 ± 0.04 (n=15)	750	360	4.1
Al 8	0.46 ± 0.02 (n=14)	900	460	5.5

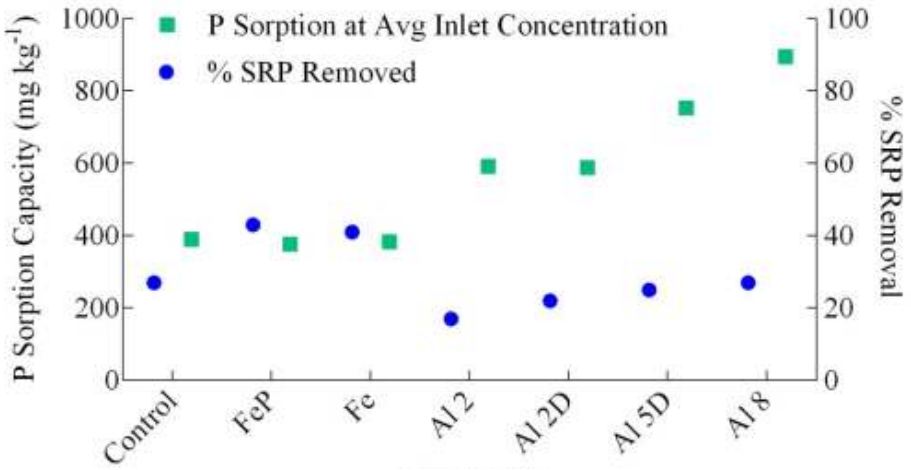

Figure 5.11. P sorption capacity increased (green squares) as Al WTR is added, while percent removal of SRP decrease (blue circles). This indicates that percent removal of SRP was not primarily dictated by the chemical characteristics of the soil.

(2) Oxalate Analysis

The amounts of P, Fe, and Al on each soil matrix were determined using the oxalate soil extraction methods provided in Chapter 3. This analysis was conducted on the initial soil mixture, herein referred to as t=0 hrs, and on final soil samples taken at the end of each experimental run. Table 5.21 provides the results from the oxalate extraction on all soil mixtures for initial soil samples (t=0 hrs).

Table 5.21. Oxalate extractable P, Fe, and Al from each mesocosm soil prior to dosed water analysis. Values shown in bold were considered different than the values obtained for the control mesocosm. Underlined values highlight the increase in Fe and Al in mesocosms amended with respective elements.

	P_{ox} (mg kg^{-1})			Fe_{ox} (mg kg^{-1})			Al_{ox} (mg kg^{-1})		
	Avg	Std Dev	N	Avg	Std Dev	N	Avg	Std Dev	N
Control	333	155	9	6843	1753	9	1135	306	9
FeP	307	134	11	**7221**	912	11	1172	171	11
Fe	334	135	11	**7582**	1049	11	1226	222	11
Al 2	**386**	105	11	**7812**	706	11	**3391**	559	11
Al 2D	**405**	125	11	**8750**	1361	11	**4880**	1913	11
Al 5D	**487**	185	11	**7427**	1018	11	**8184**	3398	11
Al 8	**532**	132	11	6813	673	11	**10003**	4343	11

*All Values are from initial soil samples prior to dosed water analysis.

Several observations could be made (Figure 5.12):

1. Phosphorus was present in all soil mixes prior to dosing. In mesocosms amended with Al WTR, as amounts of WTR increased, so did the amount of oxalate extractable P. Additionally, large standard deviations were found when conducting the oxalate extraction.
2. The addition of iron was verified in the FeP and Fe mesocosms; however, the Al 2, Al 2D, and Al 5D WTR mixes also contained similar concentrations of iron (although the form of iron is unknown as the oxalate extraction and subsequent analysis on an ICP measures total oxalate extractable iron).
3. Aluminum values in all Al mesocosms increased incrementally according to the percent of Al WTR added to the soil (Figure 5.12).

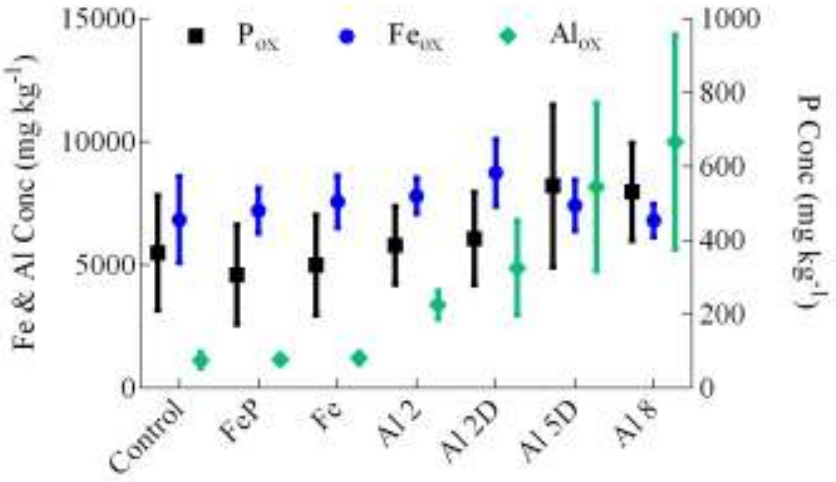

Figure 5.12. Oxalate extractable P, Fe, and Al in initial soil sample prior to dosed experimental runs. Increasing amounts of Al were found with the addition of Al WTR. Iron was found in all soil samples along with P.

While there was no significant difference in oxalate extractable P among mesocosms when compared to the control (see Table 5.21 using a one-way ANOVA, $p>0.05$),

observation 1 was most concerning because if more P was present in the soil initially, it may have already been at a near saturated state prior to the experimental run. Given the P amounts initially present on the soil and the P sorption capacities at the average inlet concentrations, Table 5.22 shows the potential P sorption capacity of each mesocosm (based on average P_{ox} values). The 'approximate remaining P sorption' capacity was determined by subtracting the average P_{ox} value from 'P sorption at average inlet concentration (mg kg^{-1}).' The remaining P capacity in all mesocosms was substantially greater than the mass removal shown from the water analysis indicating initial P amounts did not create a saturated state prior to the experimental run (provided the average P_{ox} value was used). The standard deviations of experimental data were a cause of concern when quantifying the 'Approximate Remaining P sorption capacity (mg kg^{-1}).' Had the upper bound of the P_{ox} data been used, the control, FeP, and Fe mesocosms would have reported full saturation, while all mesocosms amended with Al WTR would still have P removal capacities (the Al 2D reporting the lowest value).

Table 5.22. Results of the P sorption analysis and oxalate extraction are presented here. The approximate remaining P sorption capacity was determined by subtracting the average P_{ox} value from the P sorption capacity at the average inlet concentrations within each mesocosm. Results showed each mesocosm was not at a saturated state prior to the on-set of each experiment and more P sorption capacity remained in mesocosms amended with Al WTR.

	P Sorption at Avg	P_{ox} (mg kg^{-1})		Approx. Remaining P
Mesocosm	Inlet Conc. (mg kg^{-1})	Avg	Std Dev	Sorption (mg kg^{-1})
Control	390	333	155	57
FeP	376	307	134	69
Fe	383	334	135	49
Al 2	591	386	105	205
Al 2D	588	405	125	183
Al 5D	754	487	185	267
Al 8	895	532	132	363

*Note: All Mass P Removal and % Removal values are reported at t = 4

The large standard deviations observed within the oxalate extraction values from the initial soil samples was further compounded when values of P retained on the soil over each experimental run were calculated (Table 5.23). Results seen in Table 5.23 show the differences between the initial P_{ox} values and the P_{ox} values extracted from soil at the four week mark in each mesocosm. It is important to note that soil samples were not taken at t=4 weeks for the FeP and Fe mesocosms because it was difficult to obtain samples from the mesocosms when the soil was fully saturated. As a result, soil data for FeP and Fe was linearly scaled down to a four week estimate. Generally, soil was extracted approximately three days after the end of the experiment to allow for minimal drying to occur.

Table 5.23. Oxalate extraction for all mesocosms over a four week study. This data also indicates that wetland soil is not homogenous, which could account for such large deviations. More P was extracted from samples after four weeks than initially present.

	t=0 hrs: P_{ox} (mg kg^{-1})			t=4 wks: P_{ox} (mg kg^{-1})		
	Avg	Std Dev	n	Avg	Std Dev	n
Control	330	120	9	370	150	9
FeP	310	130	11	360*	140	9
Fe	330	130	11	390*	160	9
Al 2	390	100	11	530	110	9
Al 2D	410	120	11	480	120	9
Al 5D	490	180	11	840	170	9
Al 8	530	130	11	640	150	9

*Values are linearly interpolated between zero and 12 wks (FeP) or 10 wks (Fe)

Phosphorus concentrations extracted from the soils amended with Al WTR generally increased after the amendment was added at t=0 (~390-530 mg kg^{-1}), while after a four

week study, P_{ox} values fell within the range (~480-840 mg kg^{-1}). Large standard deviations were observed within each soil core (refer to Chapter 3 for soil extraction methodology) (Figure 5.13).

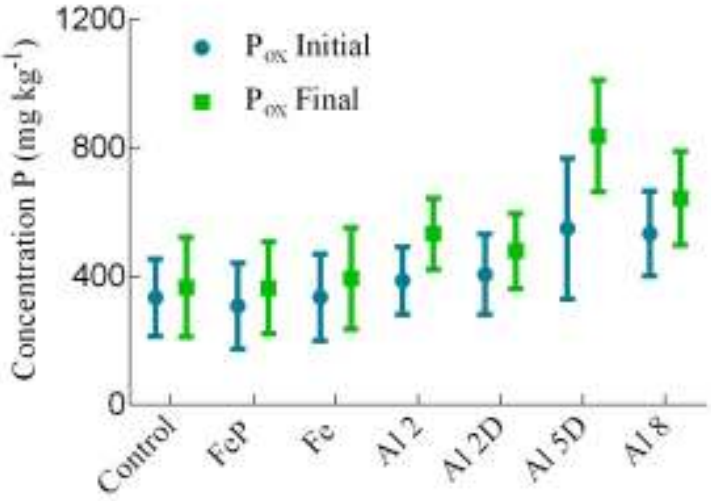

Figure 5.13. Oxalate extractable P. All final soil samples were taken at the 4 week mark unless otherwise noted. Initial P_{ox} values (blue circles) were well within the standard deviations of the final P_{ox} (green squares), making it difficult to accurately quantify mass of P retained within the soil column.

The large variations seen in the oxalate extraction demonstrate wetland soil is heterogeneous; making it difficult to accurately quantify the amount of P removed from each soil matrix. More samples would need to be extracted to obtain more reliable results. At this point, this is no longer possible.

Observation (2) refers to the amount of iron found in all mesocosms. While, it was shown that more iron was present in the FeP and Fe mesocosms in the form of iron (III), the same observation was made for all Al WTR mesocosms except the Al 8 when compared to the control. A one-way ANOVA analysis between all mesocosms and the control

showed there was no significant difference in amounts of iron ($p>0.05$) (see Table 5.21 for values).

Observation (3) says that the aluminum values in all mesocosms amended with Al WTR, increased incrementally according to the percent of Al WTR added. Given the large standard deviation of each data set, a one-way ANOVA analysis was performed to determine whether there was a significant difference in the amount of Al within each mesocosm. The amount of Al_{ox} within the Al 2 and Al 2D mesocosms was not significantly different ($p>0.05$) than that found in the control mesocosm. Additionally, there was no significant difference between the amount of Al_{ox} measured on the Al 5D soil and the Al 8 soil. While there was a significant difference in Al_{ox} between the mesocosms amended with 2% Al WTR and those amended with 5 and 8%, there was no significant difference between the mass SRP removals over the four week study, which further supports the argument that removal of SRP using the Al WTR is not solely a chemical process.

(3) Soil Amendment Addition

Each amendment was added by percent dry mass to wetland soil to create an amended soil mix. An oxalate extraction verified the amount of Fe (III) sorbed to the sand amendment was 1,260 ± 90 mg P kg^{-1} (n=2). The amount of Al present on the Al WTR was 104,000 mg kg^{-1} (Komlos, et al., In Review). A summary of Fe and Al mass amounts added to each mesocosm (in kg) are shown in Table 5.24. When compared to the amount of SRP removed as observed in the pore water analysis, the amount of mass SRP removed per kg of Al or Fe (III) added resulted in interesting results. In the soil amended

with iron (III), when normalized to the amount of Fe (III) added via amendment, mass of SRP removal was within the range of 185,000 - 190,000 mg P kg^{-1} Fe (III). When the same comparison was made for all mesocosms amended with Al, the mass SRP removed per kg of Al was less than 3200 mg P kg^{-1} Al. Additionally, mass of SRP removed per kg Al decreases as more Al is added via Al WTR (~3000 mg P kg^{-1} for 2% mix to 1000 mg P kg^{-1} Al for 8% mix). Neglecting the contribution of the wetland soil, these results indicate that the amount of Fe (III) added produced a larger removal of SRP than the addition of Al.

Table 5.24. Comparison between dry mass of amendments and resulting mass of SRP removed. Al 2 and Al 2D mesocosms showed the highest mass of SRP removed per kg of amendment added; however, the mass of SRP removed was still lower than that observed in the control, FeP, and Fe mesocosms, suggesting removal mechanisms of SRP do not necessarily correlate to the amount of amendment added.

	Dry Mass of Amendment (kg)	Al added to mesocosm (kg Al)	Fe (III) added to mesocosm(kg Fe)	Mass SRP Removed (mg)	Mass SRP removed per kg Al or Fe (III) (mg kg^{-1})
Control	-	-	-	490	-
FeP	3.2	-	0.004	750	190000
Fe	3.1	-	0.004	730	185000
Al 2	1.2	0.12	-	350	2900
Al 2D	1.2	0.13	-	410	3200
Al 5D	2.8	0.29	-	360	1300
Al 8	4.5	0.46	-	460	1000

*Note: Fe (III) coated sand = 1260 mg kg^{-1} and Al WTR = 104,000 mg kg^{-1}

The results of the analysis support the idea that more mass SRP is removed per kg of Fe (III) added. However, while this may be the case, this is not corroborated when considering the entire chemical composition of the soil. In two instances (Al 2 and Al 2D), the mesocosms amended with Al WTR showed that oxalate extractable iron was comparable or greater to what was seen in each Fe (III) mesocosm (~7500 mg kg^{-1}) (Table 5.21). Additionally, the oxalate extractable aluminum was less than the iron: 7810

mg kg^{-1} Fe and 3390 mg kg^{-1} Al for the Al 2 mesocosm and 8750 mg kg^{-1} Fe and 4880 mg kg^{-1} Al for the Al 2D mesocosm (Table 5.21). Since the Al 2 and Al 2D mesocosms did not show similar SRP removal to the mesocosms amended with iron (III) (Table 5.24), it can be presumed that either: (1) the iron (III) added via sand was more active than the iron in the WTR; (2) more pore water was able to come in contact with the iron (III) coated sand due to its ability to stick to existing soil particles (creating more opportunities for P sorption to occur); or (3) the addition of Al WTR reduced the hydraulic conductivity of the soil whereas the Fe (III) coated sand did not (preventing sub-surface flow from coming in contact with the Al WTR). These observations are further supported when considering that the P sorption capacities of the soil increased when Al WTR residuals were added, and the mass removed per kg of soil increased as residuals were added, but the mass removed per kg of amendment did not. This suggests that there are other mechanisms affecting, or even impairing, the removal of SRP through chemical sorption.

5.3.2 Physical Analysis

The chemical analysis suggested that the removal mechanisms of SRP in a CSW with soil amendments are not solely dependent on its chemical characteristics, but also its physical characteristics. As such, this section presents summaries of grain size distributions, soil classifications, and saturated hydraulic conductivity results.

(1) Grain Size Analysis and Bulk Density

Figure 5.14 grain size shows typical results from a sieve and hydrometer grain size analysis that was done on the control mesocosm soil (each soil mix can be found in Appendix B). A line drawn at 2 mm, 0.05 mm, and 0.002 mm delineate the gravel, sand, silt, and clay particles, respectively.

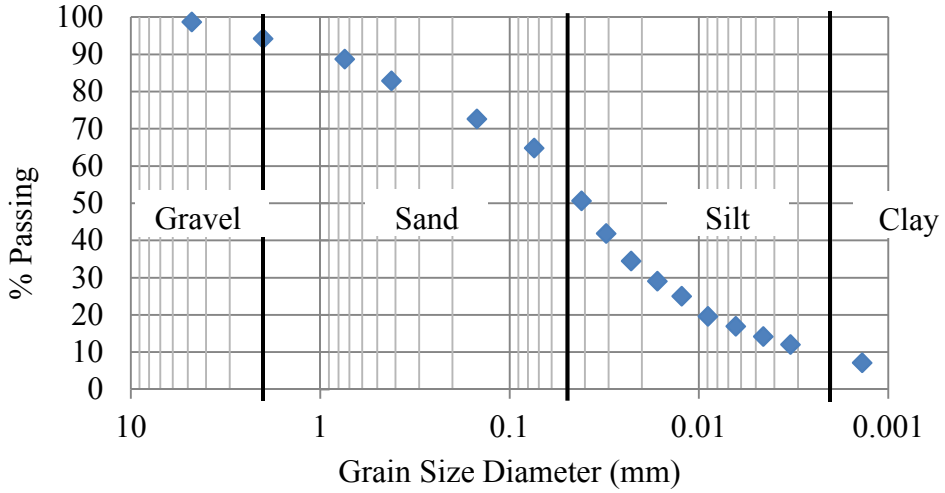

Figure 5.14. Typical grain size distribution of mesocosm soil. Vertical lines represent delineations between gravel, sand, silt, and clay particulates. This data is representative of the control mesocosm soil.

Soils were classified using the USDA soil classification triangle. Table 5.25 provides a summary of each grain distribution analysis, the USDA soil class, and the percent removal P from the water analysis. The FeP mesocosm, which had the most percent sand, was classified as Sandy Loam and also showed the highest removal at four weeks out of all mesocosm studies (43%). Campbell, et al. (2002) studied 14 natural and 12 constructed wetlands for soil characteristics and found natural wetland soils are generally clay loam textures high in silt content, whereas constructed wetland soil was of a sandy

clay loam texture, which was more closely related to soils obtained in this study from Villanova's CSW. Soil mixes having the highest percentage of sand (FeP and Fe) provided the most percent SRP removal, suggesting that physical characteristics and composition of amendment added play a role in SRP reduction. What was promising was the Al 2 and Al 8 soils had the same soil characteristics, yet the removal percentage for Al 2 was 20% and the Al 8 mix was 27%. This suggests that the chemical characteristics will preside if physical characteristics of the soil can be optimized.

Table 5.25. USDA classification of each soil mixture and percent removal values at t=4 weeks.

	Bulk Density ($g\ cm^{-3}$)	% Sand	% Silt	% Clay	USDA Class	% SRP Removed
Control	1.21	42%	48%	11%	Loam	26%
FeP	1.20	54%	37%	8%	Sandy Loam	43%
Fe	1.24	49%	43%	9%	Loam	41%
Al 2	1.15	45%	44%	11%	Loam	20%
Al 2D	1.19	48%	45%	7%	Loam	24%
Al 5D	1.22	36%	50%	14%	Loam/Silty loam	24%
Al 8	1.27	45%	44%	11%	Loam	27%

(2) Porosity, Organic Matter by LOI, and Saturated Hydraulic Conductivity

The porosity and organic matter of the amended soils were all higher than that of the control except for the FeP mesocosm (Table 5.26). Porosity values were calculated as volume of voids/total volume. A typical range of porosity values for mineral to organic wetland soils is generally between 55 and 80% (Mitsch and Gosselink, 2000). Porosity values observed from the mesocosms study were slightly higher than expected, based on their USDA soil characteristics, however, literature values showed freshwater wetland

soil to have porosities of 63% (Harvey, et al., 1995) and 60% (Bassein, E., Jaffe, P.R., 2009).

Table 5.26. Porosity, organic matter, and percent SRP removal values for all mesocosm studies. As the Al WTR was added, porosity and organic matter content increased as a result. Each amendment was mixed with soil representative of that found in the Control mesocosm. Porosity values calculated as volume of voids/total volume.

	Porosity η (%)	% Organic Matter by LOI (n=2)	% SRP Removed
Control	64	7.8 ± 0.4	26%
FeP	65	7.7 ± 0.8	43%
Fe	65	8.8 ± 0.6	41%
Al 2	66	8.6 ± 0.6	20%
Al 2D	67	8.0 ± 0.6	24%
Al 5D	70	8.8 ± 0.1	24%
Al 8	71	8.6 ± 0.3	27%

An increasing trend in porosity was observed as the amount of Al WTR was added implying there were more voids through which the sub-surface water could move. It was hypothesized that the method of Al WTR addition (as-received in clumps) caused the residuals to act more like small pebbles than fine grains creating smaller surface areas with which sub-surface flow could come in contact. The residuals are only effective if the pore water is able to contact these particles within the soil layer. From elementary soil mechanics, it is well known that a larger particle has a smaller surface contact area than many smaller ones. Therefore, these residuals may need to be added in a different form if they are to show significant SRP removal in-situ (Komlos, et al., In Review). This would better explain the lower removal percentages of SRP within the mesocosms amended

with Al WTR. This data also supports the argument that SRP removal through amendment strategies is not solely dictated by the chemical characteristics of the soil.

Organic matter (OM) was measured by loss-on-ignition. No obvious trends were evident amongst mesocosm studies. Two comments should be made: (1) soil higher in organic matter, generally has higher porosity values and lower hydraulic conductivities (Mitsch and Gosselink, 2000) and (2) when more organic matter is present, P treatment effectiveness may be reduced (Bratieres, et al., 2008; Kang, et al., 2009).

From a hydraulic standpoint, previous studies have shown the residuals to have an extremely low hydraulic conductivity when on their own as referenced in section 3.4.2. Porosity values based on the unit volume of voids/total volume of soil indicated an increase in porosity as more Al WTR was added, suggesting the hydraulic conductivity would also be higher. However, the hydraulic conductivity of the Al WTR mixtures decreased (Table 5.27), suggesting that the physical characteristics of the Al WTR are altered as soil becomes more saturated. While the measured hydraulic conductivity values were within the higher end of typical values for fine sand (0.01-0.001 cm s^{-1}) and on the lower end for silty clay (0.001-0.00001 cm s^{-1}) (Das, 2010), a decreasing trend in K_{sat} data is upheld with increasing amounts of Al WTR.

Table 5.27. Saturated hydraulic conductivity values in m hr^{-1} (K_{sat}) for all mesocosms amended with Al WTR.

Sample Name	K_{sat} (cm s^{-1})
Al 2	0.003
Al 2D	0.002
Al 5D	0.002
Al 8	0.001

5.4 Aluminum WTR 5% Mix

As noted in the introduction to Chapter 5, there was another mesocosm with 5% Al WTR that was run prior to running Al 5D, which will be referred to as Al 5. The Al 5 mesocosm was the only mesocosm showing significant mass removal when compared to the control mesocosm over a four week period. The percent removal for this mesocosm over a four week period was found to be 69% (Table 5.28).

Table 5.28. Summary of mass SRP input, output, removed, and percent removal values for all mesocosms with the inclusion of Al 5. The Al 5 mesocosm presented different results than all other mesocosm experiments (69% mass removal).

Mesocosm	Mass SRP In (mg)	Mass SRP Out (mg)	Mass P Removed (mg)	% SRP Removed
Al 5	1854	570	1284	69%
Al 5D	1467	1108	359	24%

*Note: All values are reported at t = 4 weeks.

There was no clear difference between the amount of Al added through the amendment (Table 5.29), P sorption potential (Table 5.30), or oxalate extracted P, Fe, or Al (Table 5.31), further suggesting and supporting the argument that SRP removal within a CSW that is amended with Al WTR is dependent upon both physical and chemical soil characteristics. Additionally, the results from the physical analysis did not show any clear differences in physical characteristics between the Al 5 and Al 5D mesocosms, leaving the option that for reasons unknown, the physical, chemical, and hydraulic properties within the Al 5 mesocosm created an optimal environment for significant SRP removal.

Table 5.29 Summary of Al added via Al WTR for all mesocosms, specifically highlighting the similar values for both the Al 5 and Al 5D mesocosms with large differences in percent removal of SRP.

	Dry Mass of Amendment (kg)	Al added to mesocosm (kg Al)	Mass SRP Removed (mg)	Mass SRP removed per kg Amendment (mg kg^{-1})
Al 5	2.7	0.28	1284	476
Al 5D	2.8	0.29	360	130

*Note: Fe (III) coated sand = 1260 mg kg^{-1} and Al WTR = 104,000 mg kg^{-1}

Table 5.30. P sorption results showing all mesocosms, specifically the values for Al 5 and Al 5D, which had similar P sorption capacities (783 and 754 mg $kg._1$ respectively).

Mesocosm	Avg Inlet SRP Conc. (mg L^{-1})	P Sorption at Avg Inlet Conc. (mg kg^{-1})
Al 5	0.53 ± 0.03 (n=27)	780
Al 5D	0.44 ± 0.04 (n=15)	750

Table 5.31.Summary of mass SRP input, output, removed, and percent removal values for all mesocosms with the inclusion of Al 5. The Al 5 mesocosm presented different results than all other mesocosm experiments (69% mass removal).

Mesocosm	P_{ox} (mg kg^{-1})			Fe_{ox} (mg kg^{-1})			Al_{ox} (mg kg^{-1})		
Al 5	**469**	68	9	**8625**	888	9	**6969**	1325	9
Al 5D	**487**	185	11	**7427**	1018	11	**8184**	3398	11

5.5 Summary and Conclusions

Given that the control, FeP, and Fe soil mixes exhibited comparable P sorption capacities (~380 mg kg^{-1}), it was thought that SRP removal would be similar as well; this was not the case. Soils amended with Fe (III) exhibited additional SRP removal. Additionally, the initial P values within the soil mixes were not significantly different from the control;

therefore initial P sorption potentials were comparable. This indicates that removal was not solely based on the chemical characteristics of the soil. When physical characteristics were studied, two things were observed: (1) the FeP and Fe had a greater sand composition and porosity value than the control, which may have assisted with increasing the hydraulic properties of the soil (if only minimally); and (2) after sand was applied to the wetland soil, it stuck to the surfaces of the existing soil clods, which may have provided a homogenous distribution of the sand within the soil and additional opportunities for the pore water to come in contact with the amendment; providing more SRP removal.

Quantitative results from the Fe (II) production analysis and qualitative results from the mesocosm de-construction indicated that the Fe mesocosm had reached a more reduced condition than that of either the FeP or the control. While plants do not play a role in P reduction (as shown here and in Phase I), the addition of plants within the FeP mesocosm successfully mitigated the development of reduced conditions when compared to the Fe.

The method by which the residual was added (as-received clumps) may have resulted in a smaller surface area for which sub-surface water to come in contact as the residuals did not stick to the wetland soil, rather, they formed soil clods that may not have been well-mixed into the soil structure. This hypothesis is further supported by the variations seen in the P_{ox} data where large standard deviations were observed. However, this still does not verify the reason for the Al WTR amended soils to exhibit less SRP removal than the control. The hydraulic conductivity of the Al WTR has been documented as low (~10^{-6} cm s^{-1}); which, when added to the existing wetland soil, the residual decreased the

hydraulic conductivity from 0.003 cm s^{-1} in a 2% mix to 0.001 cm s^{-1} in an 8% mix. It is presumed that a combination of soil physics and sub-surface flow hydraulics resulted in less-favorable SRP removal conditions in soil amended with Al WTR.

Overall, the mesocosms amended with Fe (III) coated sand provided the largest mass of SRP removal amongst all added amendments. The pore water analysis for the mesocosms amended with Al WTR showed that that WTR provided less SRP removal than the control; although the initial P sorption capacities were greater in the amended soil than the control. This indicates a similar conclusion as the soil amended with Fe (III) coated sand: SRP removal using soil amendments is not solely dependent upon the amendment's chemical characteristics, but is also dependent upon its physical characteristics.

Chapter 6 Vertical and Horizontal Flow Mechanisms

This chapter serves as a method for completing the following objective:

1. To verify horizontal sub-surface flow mechanisms through a 2-D numerical model (HYDRUS) and to demonstrate implications of vertical and longitudinal flow pathways in phases I and II.

Results from phase II indicated that the addition of iron (III) coated sand provided additional soluble reactive phosphorus (SRP) removal although there was no additional P sorption capacity compared to the control. Conversely, the Al WTR did not remove additional SRP from influent although an increase in P sorption capacity was observed when compared to the control. These results suggest that the physical characteristics of each amendment may have affected the pore water hydraulics of the system, which in turn hindered the chemical ability of each soil mix to remove SRP.

Actual hydraulic conductivity values (K) were only measured for the soil with Al WTR (described in Chapter 3). Representative vertical hydraulic conductivities (K_{satv}) were found using an empirical catalog called Rosetta Lite (Schaap, et al., 2001) (Table 6.1) that provides soil parameters based on the textural classes of the USDA soil triangle.

Table 6.1. Physical soil characteristics, including projected and actual hydraulic conductivity values (K_{sat}). Hydraulic conductivities are not comparable, however, the trend where the Ksat decreases as added Al WTR increases.

	Bulk Density ($g\ cm^{-3}$)	% Sand	% Silt	% Clay	USDA Class	Rosetta Lite K_{satv} ($cm\ hr^{-1}$)	Actual Values K_{satv} ($cm\ hr^{-1}$)
Control	1.21	42%	48%	11%	Loam	2.58	
FeP	1.20	54%	37%	8%	Sandy Loam	3.73	
Fe	1.24	49%	43%	9%	Loam	2.66	
Al 2	1.15	45%	44%	11%	Loam	3.15	9.30
Al 2D	1.19	48%	45%	7%	Loam	3.54	8.70
Al 5D	1.22	36%	50%	14%	Loam/Silty loam	2.03	6.70
Al 8	1.27	45%	44%	11%	Loam	1.87	5.00

Results from the Rosetta Lite catalog and the actual values measured for the Al 2, Al 2D, Al 5D, and Al 8 soil mixes did not agree, but a similar decreasing trend was observed in both instances as more Al WTR was added. This trend suggests that the addition of the Al WTR inhibits the ability for water movement, which could help explain why less removal of SRP was shown in the pore water analysis even though the P sorption capacity was greater (if the surface water was unable to come in contact with the Al WTR, SRP removal would not be seen).

To better understand the hydraulic implications presented by the addition of each amendment, it was first important to understand the hydraulics of a wetland environment. Surface-flow constructed stormwater wetlands (CSWs) have horizontal flow at both the surface and sub-surface levels in addition to vertical infiltration. As a result, the ability for the pore water to move in either direction is dictated by the soil matrix itself. Freeze and Cherry (1979) state that when the hydraulic conductivity (K) is variable in both the vertical and horizontal components, the soil is said to be heterogeneous. Additionally, soil consisting of interlayered deposits of clay and sand (such as what can be found in wetlands), the soil is said to have layered heterogeneity, which results in higher horizontal hydraulic conductivity than vertical. A 2-D numerical modeling program, HYDRUS, was used to better comprehend the pore water movement through the soil layer.

The HYDRUS modeling program allows users to demonstrate pore water flow in either a vertical or horizontal system; it will not model both simultaneously. Since the mesocosms used in this research consist of both vertical and horizontal flow, the model described

herein will act solely as an indication of sub-surface pore water flow. A horizontal flow-through mesocosm was modeled assuming fully mixed conditions, uniform flow, and an isotropic soil profile. Only the control mesocosm matrix was modeled. The hydraulic conductivity through the soil was provided by the Rosetta Lite soil catalog. Parameters used within the model are found in Table 6.2. The water flow boundary conditions were taken as constant flux in the inlet and outlet locations where flow through was present.

Table 6.2. HYDRUS parameters.

HYDRUS Parameters	
Bulk Density (g cm^{-3})	1.21
Longitudinal Dispersivity (m)	0.05
Transient Dispersivity (m)	0.1
Hydraulic Conductivity (cm hr^{-1})	2.58
Initial Chloride Conc. (mg L^{-1})	65
Influent Chloride Conc. (mg L^{-1})	175
Initial Soil Water Content	0.36

Note: assumes uniform and isotropic conditions

The chemical transport of solutes in the HYDRUS Wetland module is represented by a sequential first-order decay chain as shown in Equation 6.1.

$$\frac{\partial \theta c_1}{\partial t} + \frac{\partial \rho s_1}{\partial t} + \frac{\partial a_v g_1}{\partial t} = \frac{\partial}{\partial x_i}\left(\theta D_{ij,1}^{w} \frac{\partial c_1}{\partial x_j}\right) + \frac{\partial}{\partial x_i}\left(a_v D_{ij,1}^{g} \frac{\partial g_1}{\partial x_j}\right) - \frac{\partial q_i c_1}{\partial x_i} - Sc_{r,1} - \\ -(\mu_{w,1} + \mu_{w,1}^{'})\theta c_1 - (\mu_{s,1} + \mu_{s,1}^{'})\rho s_1 - (\mu_{g,1} + \mu_{g,1}^{'}) a_v g_1 + \gamma_{w,1}\theta + \gamma_{s,1}\rho + \gamma_{g,1} a_v \quad (6.1)$$

Where c, s, and g are solute concentrations in the liquid [MK^{-3}], solid [MM^{-1}], and gaseous [ML^{-3}], phases respectively; q_i is the i-th component of the volumetric flux density [LT^{-1}], μ_w, μ_s, and μ_g are first-order rate constants for solutes in the liquid, solid, and gas phases [T^{-1}], respectively; μ_w', μ_s', and μ_g' are similar first-order rate constants providing connections between individual chain species, γ_w, γ_s, γ_g are zero-order rate constants for the liquid [$ML^{-3}T^{-1}$], solid [T^{-1}], and gas [$ML^{-3}T^{-1}$] phases respectively; ρ is the soil bulk density [ML^{-3}], a_v is the air content [L^3L^{-3}], D_{ij}^{w} is the dispersion coefficient tensor [L^2T^{-1}] for the liquid phase, and D_{ij}^{g} is the diffusion coefficient tensor [L^2T^{-1}] for the gas phase (Simunek and van Genuchten, 1995).

Over a period of 24 hrs, Figure 6.1 shows the results of the chloride tracer movement through the pore water (initial value of 65 mg L^{-1} Cl^-) when K_{satv}=2.58 cm hr^{-1}. It is important to note that the K_{sat} values from Rosetta Lite catalog represent the vertical saturated hydraulic conductivity and not the horizontal. Since this model is meant to be an ideal scenario, isotropic conditions were assumed. Accordingly, the results may not be entirely representative of in-situ data, but this does provide an indication of the typical horizontal pore water movement over a 24 hr period. Figure 6.1 reveals that the chloride tracer would not fully travel through the soil media when only horizontal flow-through is present over the 24 hr timeframe.

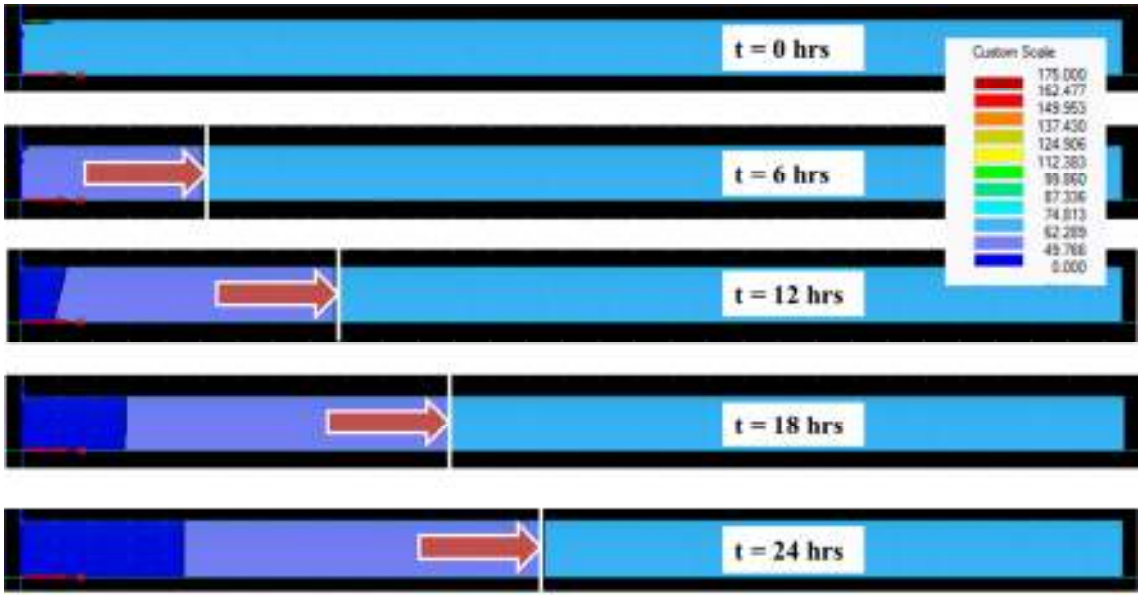

Figure 6.1. Modeling snapshots from HYDRUS 2-D numerical model. Results using a horizontal flow wetland module, show the chloride tracer (red arrows) did not reach the outlet after a 24 hr simulation. This confirms the idea that horizontal flow hydraulics may be a limiting factor in SRP advection and pore water movement. Initial chloride tracer was 65 mg L^{-1}. Custom scale for chloride tracer has units of mg L^{-1}.

The results presented by the HYDRUS modeling program demonstrated an ideal scenario where only horizontal sub-surface flow was present; however, this is not the case in a surface-flow constructed stormwater wetland. As stated previously, a wetland is not generally considered an isotropic environment. Petru, et al. (2013) determined the saturated hydraulic conductivity in both the vertical (K_{satv}) and lateral (K_{satl}) directions of several soil cores taken from two wetlands in Virginia. For the top portion of an undisturbed core, the K_{satv} value was 4.2 ± 7.6 cm hr^{-1} which is approximately three times slower than the K_{satl} (12.5 ± 13.6 cm hr^{-1}). Values reported by Min, et al. (2010) found vertical drawdown-based K_{satv} values ranging from 3.8 cm hr^{-1} to 88.8 cm hr^{-1} with an average of 27.5 cm hr^{-1}. In both studies, the approximations for K_{sat} values have large standard deviations and a wide range of values, which demonstrates the heterogeneity of wetland soil and proves the need for additional studies on soil hydraulic conductivity.

While horizontal pore water movement was seen using the HYDRUS model, it does not show the effects of vertical infiltration as a result of surface flow. Actual pore water data was used to determine contour plots of SRP and chloride data within each mesocosm. These plots were used to show interactions between both horizontal and vertical sub-surface flow. Figure 6.2 represents the data from the control mesocosm. Plots were created for t=0 hrs (a), 24 hrs (b), one (c) and two weeks (d) for both chloride (top graph) and SRP (bottom graph) concentrations. The chloride tracer contour plots in Figure 6.2 show the surface water had generally infiltrated the soil column, although this data shows a region between 1.6 m and 3 m where water had not infiltrated fully (black dotted ellipse). Chloride data from the 0 hr, 1 and 2 wk time steps looked as though they

followed a similar flow pattern where surface water infiltrated the beginning region of the mesocosm (<1.6 m) and then saturated the top portion of the mesocosm (>1.6m) which is represented by the red dashed boxes (Figure 6.2).

Concentrations for the SRP analysis are seen below the chloride contour plots for each time point. As time progressed and the surface water infiltrated the soil column, SRP removal seemingly took place within the top 3 cm of soil and within the first and last 0.6 m within the control mesocosm (as noted by the contour plots showing a dark blue color in the areas opposite of the one described). The dark blue color in Figure 6.2 is consistent with the concentration found in the initial tap water suggesting either the surface water did not infiltrate to that depth (which was the case in the region below 3 cm and between 1.6 m and 3 m), or SRP removal occurred before water had reached said depth.

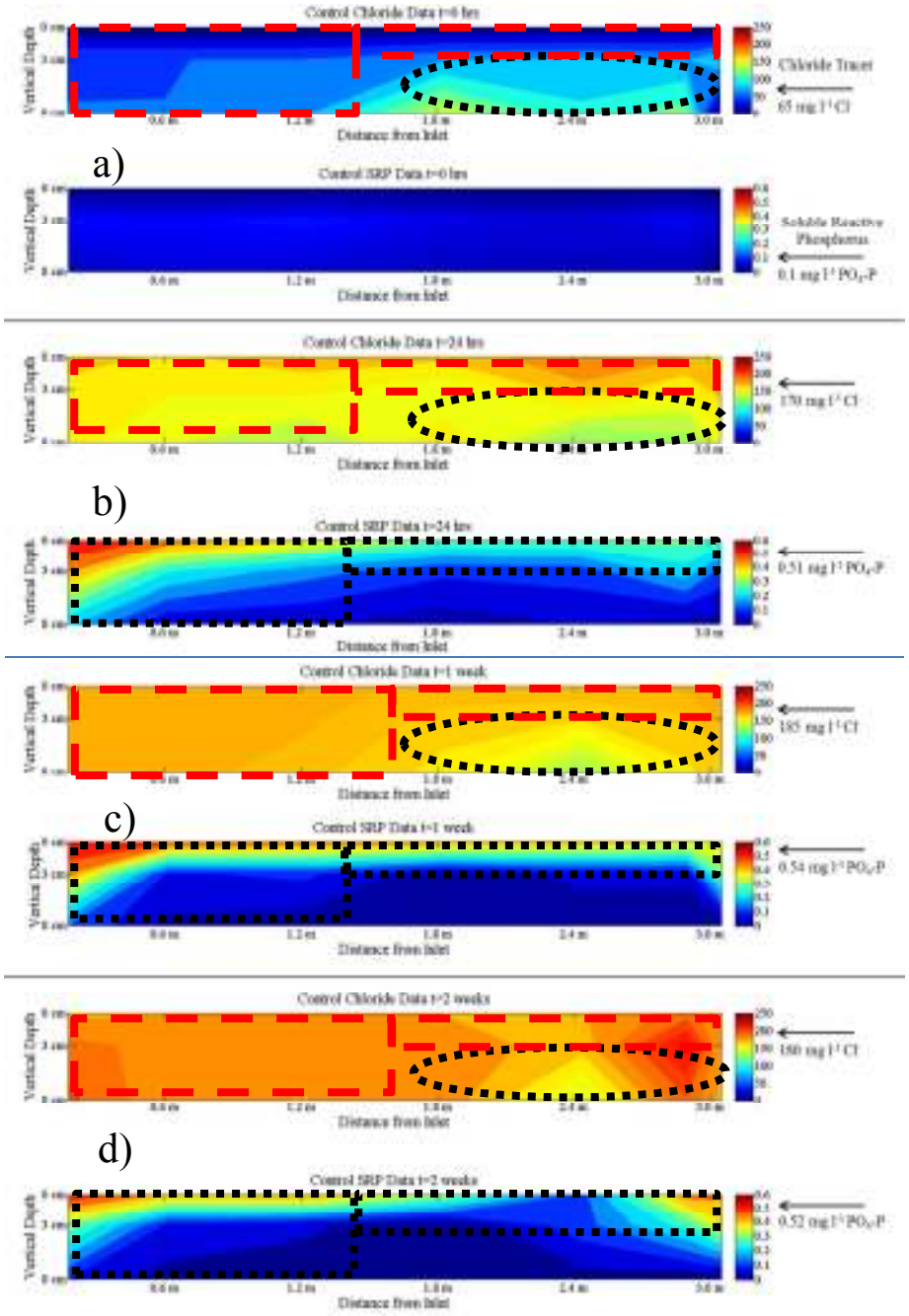

Figure 6.2. Control mesocosm study of chloride tracer and SRP fate and transport for t=0 hrs (a), t=24 hrs (b), t=1 week (c), and t=2 weeks (d). The top contour plots show the chloride tracer concentrations with saturated (red dashed boxes) and unsaturated (black dotted ellipses) regions. The bottom contour plots represent the SRP concentrations and probable areas of removal (black dotted boxes).

The contour plots presented here and in Appendix C provide additional information about how and where the SRP was removed. From Figure 6.2, it is evident that SRP removal

took place in the overlapping area where both the chloride tracer was able to penetrate, and the SRP concentration was lower than the initial value of 0.1 mg L^{-1}. In most instances, this region was within the top 3 cm of soil throughout the length of the mesocosm and within the entire depth of soil at horizontal lengths <1.5 m.

Given that SRP removal is concentrated in certain regions of the mesocosm, this could have caused the variability in the soil analysis. The soil cores were taken from the inlet, middle, and outlet regions and delineated into vertical sections representative of 0-3 cm, 3-8 cm, and 8-15 cm as discussed in Section 3.4.1. A two gram sample from each section was allocated and combined to create a composite sample of the vertical soil layers thus treating the entire soil column as uniform, when there are clear differences in P removal throughout the column. Thus, the large standard deviations observed within each of the nine samples tested could reflect the stratification shown in the soil where more SRP removal took place at the top 3 cm of the mesocosm. There was also lateral variation, such as in the case of the control where more P was extracted off the soil at the inlet than was at the middle or outlet locations (Figure 6.2), which may have been due to horizontal transport.

For the FeP mesocosm, concentrations for chloride and SRP are shown in Figure 6.3. Sub-surface flow within the chloride tracer seemingly did not infiltrate to a depth of 8 cm over a region between 1.2 m and 2.4 m (black dotted ellipse). Generally speaking, for all mesocosms, SRP removal occurred in regions where surface water was able to infiltrate (black dotted boxes), which was generally within the upper 3 cm. In the few instances where water was able to infiltrate below 3 cm (largely at the inlet and outlet), there are

most likely preferential flow paths allowing for the vertical as well as the horizontal migration. As previously noted, lateral K is greater than vertical K, so more research could be done to understand these differences in transport and the implications it may have on treatment in the presence of soil amendments.

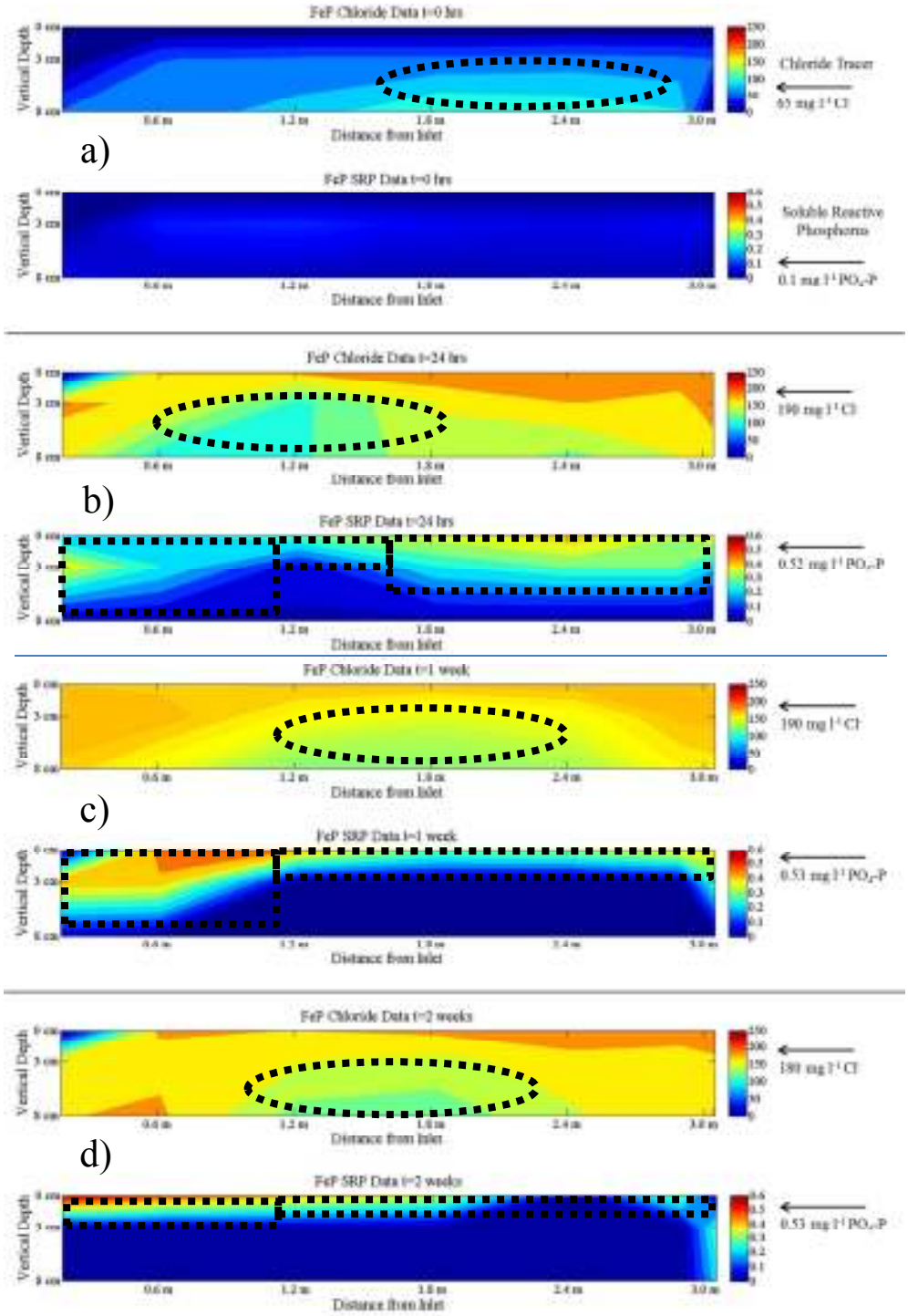

Figure 6.3. FeP mesocosm study of chloride tracer and SRP fate and transport for t=0hrs (a), t=24hrs (b), t=1 week (c), and t=2 weeks (d). The top contour plots show the chloride tracer concentrations unsaturated (black dotted ellipses) regions. The bottom contour plots represent the SRP concentrations and areas of removal (black dotted boxes).

Chapter 7 Conclusions and Future Work

7.1 Summary and Conclusions

The results presented in this research focused on the fate and transport of soluble reactive phosphorus (SRP) in a surface-flow constructed stormwater wetland (CSW). Villanova University's existing CSW was used as the baseline for this study and informed the design of bench-scale laboratory mesocosms. The mesocosms used in this research replicated similar ecology, hydrogeology, and nutrient loadings seen in the existing CSW. A two-phased laboratory mesocosm approach was the method used to study SRP fate and transport.

The phase I objective was to observe and measure SRP pathways through a surface-flow CSW soil profile. A nonvegetated and vegetated mesocosm were employed in this phase. Pore water samples were taken at various vertical and horizontal locations throughout the soil profile, analyzed for SRP, and chloride. A chloride tracer demonstrated within the nonvegetated mesocosms that surface water did not fully saturate the soil column at all depths and horizontal locations over the course of the 24-hr experimental pseudo replicates. Results indicate that the vertical and horizontal hydraulic conductivity prevented equilibrium from occurring within the 24-hr timeframe.

Values from eight, 24 hr replicates within the nonvegetated mesocosm showed decreasing concentrations at each vertical depth (0, 3, and 8 cm) as well as along the lateral flow profile (0.6 and 2.4 m). A two-sample t-test was used to determine that there was a significant difference between the SRP concentrations at t=0 hrs and t=24 hrs for

all eight mesocosm studies. It was also verified that there was a significant difference between the mass SRP going into the mesocosm (123 ± 12 mg PO_4-P) and out (64 ± 29 mg PO_4-P) over all eight, 24-hr experimental replicates (two-sample t-test, $p<0.05$, $R^2=0.75$), confirming that SRP removal had occurred within the soil column of the nonvegetated mesocosm.

The chloride tracer study from the vegetated mesocosm showed that influent water had generally reached the 0 and 3 cm port locations over the full horizontal length of the study; although less infiltration occurred as the water moved from the inlet to the outlet. At the 8 cm location, the chloride tracer did not fully infiltrate at all horizontal locations; however, more surface water reached the 8 cm depth at the inlet region than it did the middle or outlet. A similar trend was seen in the 0 and 3 cm ports where surface water infiltration occurred at the inlet first and then moved towards the outlet. Additionally, a one-way ANOVA analysis was completed on the 0 cm [0.80 ± 0.12 mg L^{-1} PO_4-P (n=53)], 3 cm [0.63 ± 0.14 mg L^{-1} PO_4-P (n=53)], and 8 cm port SRP concentrations [0.30 ± 0.15 mg L^{-1} PO_4-P (n=53)] at the 24 hr mark of all tests to determine whether there was a significant difference in removal over each depth. The resulting analysis showed there was a significant difference between SRP concentrations at each location ($p<0.05$, $R^2=0.69$), while the largest difference occurred between the 0 and 8 cm locations. Less removal of SRP occurred between the 3 and 8 cm depths, which was likely a result of the influent having not reached this location. Results from phase I showed there were both horizontal and vertical flow characteristics that ultimately affected SRP movement through the soil profile over a 24 hr period. Surface water had

not fully infiltrated all horizontal and vertical depths prior to the end of the 24 hr experimental runs. Additionally, more SRP removal was observed at the inlet region of the mesocosm and within the top 3 cm.

There was no significant difference between the mass removal between values between the vegetated (390 mg P or 49 ± 13 mg P wk^{-1}) and nonvegetated (470 mg P or 59 ± 26 mg P wk^{-1}) mesocosms ($p=0.34$, $R^2=0.09$). There was mass SRP removed within both the nonvegetated and vegetated mesocosms, indicating that sorption processes were the main mechanism of SRP removal as opposed to plant uptake.

Phase II consisted of soil amendments mixed into wetland soil taken directly from Villanova University's constructed stormwater wetland (CSW). Two soil amendments were used in phase II: Fe (III) coated sand and Al Water Treatment Residuals (Al WTR). Mesocosms were constructed similarly to phase I. Pore water samples were extracted from each mesocosm and analyzed for SRP and a chloride tracer. There were two objectives of phase II:

1. To quantify pore water soluble reactive phosphorus (SRP) mass removal associated with two soil enhancement strategies (Al WTR and iron (III) coated sand).
2. To analyze physical and chemical characteristics of soil matrices that may relate to SRP mass removal seen in pore water analyses.

Seven mesocosm studies were employed in phase II: control, 5% iron coated sand by dry mass WITH plants (FeP), 5% iron coated sand by dry mass WITHOUT plants (Fe), and 2%, 2% duplicate, 5%, and 8% mix by dry mass of Al WTR. A P sorption isotherm analysis determined that the P sorption capacity of the control mesocosm (390 mg kg^{-1}) was within the range of both the FeP and Fe mesocosms (380 mg kg^{-1}), suggesting SRP

removal would be comparable between these three mesocosms. Conversely, the P sorption capacity increases as more Al WTR was added to the original wetland soil. Both the Al 2 and Al 2D mesocosms showed the same P sorption capacities given the same average inlet concentrations (590 mg kg^{-1}). The Al 5D and Al 8 mesocosm soil matrices provided additional P sorption capacities of 750 and 900 mg kg^{-1}, respectively, suggesting mesocosms amended with Al WTR will provide the greatest SRP removal based on its chemical characteristics. This was not the case.

Soils amended with Fe (III) exhibited additional SRP removal than the control, indicating that removal was not solely based on the chemical characteristics of the soil. When physical characteristics were studied, two things were observed: (1) the FeP and Fe had a greater sand composition and porosity value than the control, which may have assisted with increasing the hydraulic properties of the soil (if only minimally); and (2) after sand was applied to the wetland soil it stuck to the surfaces of the existing soil clods, which may have provided a homogenous distribution of the sand within the soil and additional opportunities for the pore water to come in contact with the amendment, providing more SRP removal.

Quantitative results from the Fe (II) production analysis and qualitative results from the mesocosm de-construction indicated that the Fe mesocosm had reached a more reduced condition than that of either the FeP or the control. The addition of plants within the FeP mesocosm successfully mitigated the development of reduced conditions when compared to the Fe. The addition of plants, however, did not result in significant SRP removal differences in either of the two Phases.

The results from all Al WTR studies indicated that the addition of Al WTR to a CSW did not enhance SRP removal compared to typical wetland soil. Since the soils amended with Al WTR did not provided better removal than the control, it was hypothesized that soil physics and sub-surface water flow hydraulics prevented flow to access all soil so not all the soil and chemical potential was utilized. Several possibilities could result: (1) the hydraulic conductivity of the soil mixture after the residuals were added reduced the infiltration of surface water into the soil column, while also reducing the horizontal movement through the soil; (2) the method by which the residual was added (as-received) resulted in a smaller surface area for sub-surface water to come in contact with; and (3) a combination of soil physics and sub-surface flow hydraulics resulted in less-favorable SRP removal conditions in soil amended with Al WTR.

The method by which the residual was added (as-received clumps) may have affected the possibility for surface and pore water contact. Residuals did not stick to the wetland soil, rather, they formed soil clods that may not have been well-mixed into the soil structure. Variations seen in the P extraction (from the soil matrix) where large standard deviations were observed, further supports the idea that WTR were not well-mixed within the wetland soil. However, this still does not verify the reason for the Al WTR amended soils to exhibit less SRP removal than the control. The hydraulic conductivity of the Al WTR has been documented as low (~10^{-6} cm s^{-1}) which when added to the existing wetland soil reduces the residual hydraulic conductivity from 0.003 cm s^{-1} in a 2% mix to 0.001 cm s^{-1} in an 8% mix. It is presumed that a combination of soil physics and sub-surface flow

hydraulics resulted in less-favorable SRP removal conditions in soil amended with Al WTR.

Overall, the mesocosms amended with Fe (III) coated sand provided the largest mass of SRP removal amongst all added amendments. The pore water analysis for the mesocosms amended with Al WTR showed that the WTR provided less SRP removal than the control; although the initial P sorption capacities were greater in the amended soil than the control. A similar conclusion can be made for the soil amended with Fe (III) coated sand: SRP removal using soil amendments is not solely dependent upon the amendment's chemical characteristics, but is also dependent upon its physical and subsequently hydraulic characteristics.

Results of the phase II study suggested that chemical characteristics of each soil matrix do not solely dictate the SRP removal mechanisms, but physical and hydraulic properties also play a role. Surface-flow constructed stormwater wetlands (CSWs) have both horizontal flow (surface and sub-surface) and vertical infiltration. Phosphorus can move vertically through soil and into the overlying water layer, but pore water advection is potentially more important (Chambers and Odum, 1990). A 2-D numerical modeling program, HYDRUS was used to predict horizontal flow using a representative soil matrix. Hydraulic conductivity values provided by HYDRUS were determined by the soil physical characteristics. Rosetta Lite program (Schaap, et al., 2001) provides soil hydraulic parameters based on the textural classes of the USDA soil triangle. When the actual soil characteristics were input into Rosetta Lite, the K_{satv} values for mesocosms amended with Al WTR decreased as more Al WTR was added which was consistent with

what was determined in the laboratory analysis. While the percent SRP removal still increased with the addition of Al WTR, the decreasing K_{satv} value indicates that the addition of the Al WTR negatively affected the hydraulic characteristics, thus preventing greater SRP removal.

The HYDRUS 2-D horizontal flow-through model showed that horizontal pore water movement over a 24 hr period did not fully saturate the soil profile when surface water was not present. Actual pore water data was used to determine contour plots of SRP and chloride data within each mesocosm when both surface and sub-surface flow was present. These plots were used in attempt to show interactions between both horizontal and vertical sub-surface flow. The surface water had infiltrated the mesocosm by the second week as shown through 3-D tracer plots (Appendix B), but the data showed regions where water had not infiltrated fully. As time progressed and the surface water infiltrated the soil column, SRP removal seemingly took place within the top 3 cm of soil and within the first and last 0.6 m within the mesocosms. In all mesocosms, there existed regions where surface water seemingly did not infiltrate fully and preferential areas where SRP was removed. It did not seem as though the entire soil profile was being utilized for SRP treatment, verifying the necessity to better understand the physical characteristics and application techniques of each soil amendment and the resulting hydraulic properties, especially the lateral hydraulic conductivity of a wetland environment.

7.2 Future Work

This study provided insight into the method of using soil amendments to improve P sorption capabilities within a wetland environment. Several areas of future analysis were determined as a result of the conclusion that Fe (III) coated sand proved to have additional SRP removal properties most likely as a result of its physical characteristics. Conversely, the addition of Al WTR resulted in less SRP removal most likely as a result of its physical characteristics. Future research topics include:

1. Conduct vertical column studies to verify that SRP removal occurs within wetland soils when Al WTR are present in as-received forms.
2. Study the physical changes in Al WTR as a result of saturated conditions. It was hypothesized that over the course of the study, hydraulic properties of the soils amended with Al WTR decreased as Al WTR clumps changed physical forms.
3. Determine hydraulic conductivity in both the vertical and lateral pathways for soils amended with Al WTR.
4. Use Fe (III) coated sand in stormwater control measures where infiltration is desired and soil is not always saturated (bioretention/infiltration)
5. Research different methods of applying Al WTR; can it be coated on sand and mixed into soil; dried; added on top of soil as is?
6. Are there other possible uses of Al WTR in SCMs such as an impermeable liner?

There are opportunities for both amendments to be used in other stormwater control measures. Adding Fe (III) coated sand to a bioretention or infiltration rain garden could

provide additional SRP removal benefits, while reduced conditions are more easily avoided (which would hinder the release of SRP through Fe (III) reduction). Similarly, using Al WTR in a wetland could be valuable if it is added by coating it on sand, drying it to create a more homogenous distribution within the soil, or just sprinkling it on top of the soil. Overall, these future research recommendations are primarily founded in the idea that soil amendments can be used to remove SRP within a wetland environment, but further research must be conducted to verify the practicality of each recommendation.

Works Cited

(USEPA), U. E. P. A., 2002. *2000 National Water Quality Inventory,* Washington, D.C.: U.S. EPA, Office of Water.

Akhtar, M.S., Richards, B.K., Medrano, P.A., deGroot, M., Steenhuis, T.S., 2003. Dissolved phosphorus from undisturbed soil cores: related to adsorption strength, flow rate, or soil structure?. *Soil Science Society of America Journal,* pp. 458-470.

Ann, Y., Reddy, K., Delfino, J., 2000. Influence of chemical amendments on phosphorus. *Ecological Engineering,* p. 157–167.

Ardon, M., Morse, J., Doyle, M. and Bernhardt, E., 2010. The water quality consequences of restoring wetland hydrology to a large agricultural watershed in the souteastern coastal plain. *Ecosystems,* pp. 1060-1078.

Babatunde, A.O.; Zhao, Y.Q.; Burke, A.M.; Morris, M.A.; Hanrahan, J.P., 2009. Characterization of aluminum-based water treatment residuals for potential phosphorus removal in engineered wetlands. *Environmental Pollution,* pp. 2830-2836.

Baker, L.A., 1992. Introduction to nonpoint source pollution in the United States and prospects for wetland use. *Ecological Engineering,* pp. 1-26.

Baldwin, D., 1996. Effects of exposure to air and subsequent drying on the phosphate sorption characteristics of sediments from a eutrophic river. *Limnology and Oceanography,* pp. 1725-1732.

Barko, J., Gunnison, D. and Carpenter, S., 1991. Sediment interactions with submersed macrophyte growth and community dynamics. *Aquatic Botany,* pp. 41-65.

Barth, 1995. Nutrient Movement from the Lawn to the Stream. *Watershed Protection Techniques.,* pp. 239-246.

Bassein, E., Jaffe, P.R., 2009. Measuring in situ reaction rate constants in wetland sediments. *Environmental Monitoring Assessment,* pp. 51-62.

Beek, J., 1978. *Phosphate retention by soil in relation to waste disposal: Ph.D. Thesis,* Wageningen, The Netherlands: s.n.

Boesch, D.F., Brinsfield, R.B., Magnien, R.E., 2001. Chesapeake Bay eutrophication: scientific understanding, ecosystem restoration, and challenges for agriculture. *Journal of Environmental Quality,* pp. 303-320.

Braskerud, B.C., Tonderski, B., Wedding, B., Bakke, R., Blankenberg, A.-G. B., Ulen, B., Koskiaho, J., 2005. Can constructed wetlands reduce the diffuse phosphorus loads to eutrophic water in cold temperate regions?. *Journal of Environmental Quality,* pp. 2145-2155.

Bratieres, K., Fletcher, T. and A. Deletic, Y. Z., 2008. Nutrient and sediment removal by stormwater biofilters: A large-scale design optimisation study. *Water Research,* pp. 3930-3940.

Bratieres, K., Fletcher, T., Deletic, A. and Zinger, Y., 2008. Nutrient and sediment removal by stormwater biofilters: A large-scale design optimisation study. *Water Research,* pp. 3930-3940.

Brooks, S., Taylor, D. and Jardine, P., 1996. Reactive transport of EDTA-complexed cobalt in the presence of ferrihydrite. *Geochimica et Cosmochimica Acta,* pp. 1899-1908.

Campbell, D., Cole, C. and Brooks, R., 2002. A comparison of created and natural wetlands in Pennsylvania, USA. *Wetlands Ecology and Management,* pp. 41-49.

Carleton, J.N, Grizzard, T.J., Godrej, A.N., Post, H.E., Lampe, L., Kenel, P.P., 2000. Performance of a constructed wetlands in treating urban stormwater runoff. *Water Environment Research,* pp. 295-304.

Carleton, J. and Montas, H., 2010. Performance of a Constructed Wetlands in Treating Urban Stormwater Runoff. *Water Research,* pp. 295-304.

Chambers, R. and Odum, W., 1990. Porewater oxidation, dissolved phosphate and the iron curtain: Iron-phosphorus relations in tidal freshwater marshes. *Biogochemistry,* pp. 37-52.

Chavan, P. and Dennet, K., 2008. Behavior of Pilot-Scale Constructed Wetlands in Removing Nutrients and Sediments Under Varying Environmental Conditions. *Water, Air, & Soil Pollution,* pp. 239-250.

Cheung, K.C., Venkitachalam, T.H., 2000. Improving phsphate removal of sand infiltration system using alkaline fly ash. *Chemosphere,* pp. 243-249.

Clesceri, L., Greenberg, A. and Trussell, R., 1990. *Selected physical and chemical standard methods for students.* 17th ed. Washington, D.C.: American Public Health Association.

Das, B., 2010. *Principles of Geotechnical Engineering.* 7th ed. Stamford: Cengage Learning.

del Campillo, M. and Torrent, J., 1992. A rapid acid-oxalate extraction procedure for the determination of active Fe-oxide forms in calcareous soils. *Journal of Plant Nutrition and Soil Science,* pp. 437-440.

Drizo, A., Frost, C., Grace, J. and Smith, K., 1999. Physico-chemical screening of phosphate-removing substrates for use in constructed wetland systems. *Water Resources,* pp. 3595-3602.

Eghball, B., Sander, D. and Skopp, J., 1990. Diffusion, adsorption, and predicted longevity of banded phosphorus-fertilizer in three soils. *Soil Science Society of America Journal,* pp. 1161-1165.

Elliott, H., O'Connor, G., Lu, P. and Brinton, S., 2002. Influence of water treatment residuals on phosphorus solubility and leaching. *Journal of Environmental Quality,* pp. 1362-1369.

Faulkner, S. and Richardson, C., 1989. Physical and chemical characteristics of freshwater wetland soils. In: *Constructed Wetlands for Wastewater Treatment.* Chelsea, Michigan: Lewis Publishers, pp. 41-88.

Fisher, T., Peele, E., Ammerman, J. and Harding, L., 1992. Nutrient limitation of phytoplankton in Chesapeake Bay. *Mar. Ecol. Prog. Ser.,* pp. 51-63.

Forbes, M, Dickson, K, Golden, T, Hudak, P, Doyle, R, 2004. Dissolved Phosphorus Retention of Lightweight Expanded Shale and Masonry Sand Used in Subsurface Flow Treatment Wetlands. *Environmental Science and Technology,* pp. 892-898.

Fozzard, I.R., Doughty, R.,Ferrier, R.C., Letherland, T., Owen, R., 1999. A quality classification for management of Scottish standing waters. *Hydrobiologia,* pp. 433-453.

Freeze, R.A., Cherry, J.A., 1979. *Groundwater.* Edgewood Cliffs, NJ: Prentice-Hall.

Graham, E., 1959. *An Explanation of Theory and Methods of Soil Testing,* s.l.: Missouri Agric. Exp. Stn. Bull..

Grant, R. and Patrick, R., 1970. *Tinicum Marsh as a water purifier,* Washington, DC: The Conservation Foundation.

Guan, B., Yao, Xin; Jiang, J., Tian, Z., An, S., Gu, B., Cai, Y., 2009. Phosphorus removal ability of three inexpensive substrates: Physiochemical properties and application. *Ecological Engineering,* pp. 576-581.

Harvey, J., Chambers, R. and Hoelscher, J., 1995. Preferential flow and segregation of porewater solutes in wetland sediment. *Estuaries,* Volume 18, pp. 568-578.

Hsieh, C.-H., Davis, A. and Needelman, B., 2007. Bioretention column studies of phosphorus removal from urban stormwater runoff. *Water Environment Research,* pp. 177-184.

Hsieh, C., Davis, A. and Needelman, B., 2007. Bioretention column studies of phosphorus removal from urban stormwater runoff. *Water Environmental Resources,* pp. 177-184.

Hsu, P., 1975. Precipitation of phosphate from solution using aluminum salt. *Water Research,* pp. 1155-1161.

Hu, C. and Shan, B., 2009. Phosphorus removal performance and mechanisms of a constructed horizontal subsurface flow wetlands treating reclaimed water. *Environmental Engineering Science,* pp. 1097-1106.

Jin, X.C., Wang, S.R., Pang, Y., Zhao, H.C., Zhou, X.N., 2005. The adsorption of phosphate on different trophic lake sediments. *Colloids and Surfaces A, 254,* pp. 241-248.

Kadlec, Knight, 1996. *Treatment Wetlands.* Boca Raton, FL: Lewis Publishers.

Kalin, L., Hantush, M.M., Izik, S., Yuccekaya, A., Jordan, T., 2012. Nutrient dynamics in flooded wetlands: II. Model application. *Journal of Hydrologic Engineering.*

Kang, S.A, Li, Wei, Lee, E., Phillips, B.L., Lee, Y.J., 2011. Phosphate uptake by TiO2: Batch studies and NMR spectroscopic evidence for multisite adsorption. *Journal of Colloid and Interface Science,* pp. 455-461.

Kang, J., Hesterberg, D. and Osmond, D., 2009. Soil organic matter effects on Phosphorus sorption: A path analysis. *Soil Science Society of America Journal,* pp. 360-366.

Komlos, J. and Traver, R., 2012. Long-term orthophosphate removal in a field-scale storm-water bioinfiltration ran garden. *Journal of Environmental Engineering,* pp. 991-998.

Komlos, J., Welker, A., Punzi, V. and Traver, R., In Review. Feasibility study of as-received and modified (dried/baked) water treatment plant residuals for use in stormwater control measures (SCMs). *Journal of Environmental Engineering.*

Kong, L., Wang, Y.-B., Zhao, L.-N. and Chen, Z.-H., 2009. Enzyme and root activities in surface-flow constructed wetlands. *Chemosphere,* pp. 601-608.

Kuusemets, V. and Mander, U., 2002. Nutrient flows and management of a small watershed. *Landscape Ecology,* pp. 59-68.

Lai, D. and Lam, K., 2009. Phosphorus sorption by sediments in a subtropical constructed wetland receiving stormwater runoff. *Ecological Engineering,* pp. 735-743.

Li, H., Davis, A.P., 2008. Urban particle capture in bioretention media. I: Laboratory and field studies. *Journal of Environmental Engineering,* pp. 409-418.

Liang, Q., 2011. *Simultaneous phosphorus and nitrogen removal using aluminum based water treatment residual.* Master of Science Thesis ed. Fort Collins, Colorado: Colorado State University.

Lucas, W. and Greenway, M., 2008. Nutrient retention in vegetated and nonvegetated bioretention mesocosms. *Journal of Irrigation and Drainage Engineering,* pp. 613-623.

Makris, K.C., El-Shall, H., Harris, W.G., O'Connor, G.A., Obreza, T.A., 2004. Intraparticle phosphorus diffusion in a drinking water treatment residual at room temperature. *Journal of Colloid and Interface Science,* pp. 417-423.

McKeague, J. and Day, J., 1966. Dithionite- and oxalate-extractable Fe and Al as aids in differentiating various classes of soils. *Canadian Journal of Soil Science,* pp. 13-22.

Min, J., Perkins, D. and Jawitz, J., 2010. Wetland-groundwater interactions in subtropical depressional wetlands. *WEtlands,* pp. 997-1006.

Mitsch, W.J., Cronk, J.K., Wu, X., Nairn, R. W., Hey, D.L., 1995. Phosphorus Retention in Constructed Freshwater Riparian Marshes. *Ecological Applications,* pp. 830-845.

Mitsch, W., 1992. Landscape design and the role of created, restored, and natural riparian wetlands in controlling nonpoint source pollution. *Ecological Engineering,* pp. 27-47.

Mitsch, W. and Gosselink, J., 2000. *Wetlands.* New York, NY: John Wiley & Sons, Inc..

Nair, P.S., Logan, T.J., Sharpley, A.N., Sommers, L.E., Tabatabai, M.A., Yuan, T.I., 1984. Interlaboratory comparison of a standardized phosphorus adsorption procedure. *Journal of Environmental Quality,* pp. 211-215.

Nairn, R.W., Mitsch, W.J., 2000. Phosphorus removal in created wetland ponds receiving river overflow. *Ecological Engineering,* pp. 107-126.

Nairn, R. and Mitsch, W., 2000. Phosphorus removal in created wetland ponds receiving river overflow. *Ecological Engineering,* pp. 107-126.

Neori, A., 2000. Bioactive Chemicals and Biological-Biochemical Activities and Their Functions in Rhizospheres of Wetland Plants. *The Botanical Review,* pp. 350-378.

Noguchi, S., Tsuboyama, Y., Sidle, R. and Hosada, I., 2001. Subsurface runoff characteristics from a forest hillslope soil profile including macropores. *Hydrological Processes,* pp. 2131-2149.

Novak, J., 2004. Dissolved Phosphorus Retention and Release from a Coastal Plain In-Stream Wetland. *Journal of Environmental Quality,* pp. 394-401.

NRC, 2008. *Committee on Reducing Stormwater Discharge Contributions to Water Pollution, Water Science and Technology Board, division on Earth and Life Studies,* Washington D. C.: National Research Council of the National Academies, The National Academies Press.

O'Conner, G., Elliott, H. and Lu, P., 2001. Soil Crop Science Society. *Florida Proc.,* pp. 67-73.

Odum, H., Ewel, K., Mitsch, W. and Ordway, J., 1977. *Recycling treated sewage through cypress wetlands in Florida,* University of Florida: Center for Wetlands.

Odum, W., 1988. Comparitive ecology of tidal freshwater and salt marshes. *Ann. Rev. Ecol. Syst.,* pp. 147-176.

O'Neill, S. and Davis, A., 2012. Water treatment residual as a bioretention amendment for phosphorus. I: evaluation studies. *Journal of Environmental Engineering,* pp. 318-327.

Pant, H. and Reddy, K., 2003. Potential internal loading of phosphorus in a wetland constructed in agricultural land. *Water Research,* pp. 965-972.

Petru, B., Ahn, C. and Chescheir, G., 2013. Alteration of soil hydraulic properties during the construction of mitigation wetlands in the Virginia Piedmont. *Ecological Engineering,* pp. 140-150.

Reddy, K. and D'Angelo, E., 1994. Soil processes regulating water quality in wetlands. In: *Global Wetlands: Old and New.* Elsevier, Amsterdam: s.n., pp. 309-324.

Reddy, K., White, J., Wright, A. and Chua, T., 1999. Influence of phosphorus loading on microbial processes in soil and water column of wetlands. In: *Phosphorus biogeochemistry in subtropical exosystems.* Boca Raton, Fl: CRC/Lewis Pub., pp. 249-273.

Richardson, C. J., 1985. Mechanisms controlling phosphorus retention capacity in freshwater wetlands. *Science,* pp. 1424-1427.

Rosenquist, S., Cully Hession, W., Eick, M. J. and Vaughan, D., 2010. Variability in adsorptive phosphorus removal by structural stormwater best management practices. *Ecological Engineering,* pp. 664-671.

Sade, R., Litaor, M. and Shenker, M., 2010. Evaluation of groundwater and phosphorus transport in fractured altered wetland soils. *Journal of Hydrology,* pp. 133-142.

Schaap, M., Leij, F. and van Genuchten, M., 2001. Rosetta: a computer program for estimating soil hydraulic parameters with hierarchical pedotransfer functions. *Journal of Hydrology,* pp. 163-176.

Schoumans, O., 2000. *Determination of the degree of phosphate saturation in non-calcerous soils,* Raleigh: North Carolina State University.

Schultz, G. and Ruppel, C., 2002. Constraints on hydraulic parameters and implications for groundwater flux across the upland-estuary interface. *Journal of Hydrology,* pp. 255-269.

Schwertmann, U., 1964. Differentiating the iron oxidation of the base using photochemical extraction of acidic ammonium-oxide solution. *Z. Pflanzenernaehr,* pp. 194-202.

SERA-IEG, 2009. *Methods of Phosphorus Analysis,* s.l.: Southern Extension/Research Activity-Information Exchange Group 17; Virginia Tech University.

Serra, T., Fernando, H. and Rodriquez, R., 2004. Effects of emergent vegetation on lateral diffusion in wetlands. *Water Research,* pp. 139-147.

Sharpley, A.N., Daniel, T., Sims, J.T., Lemunyon, J., Stevens, R., Parry, R., 1999. *Agricultural phosphorus and eutrophication,* Washington, DC: U.S. Department of Agriculture.

Sims, J., Simard, R. and Joern, B., 1998. Phosphorus loss in agricultural drainage: Historical perspective and current research. *Journal of Environmental Quality,* pp. 277-293.

Stookey, L., 1970. Ferrozine-A new spectrophotometric reagent for iron. *Analytical Chemistry,* pp. 779-781.

Sundaravadivel, M. and Vigneswaran, S., 2001. Constructed Wetlands for Wastewater Treatment. *Critical Reviews in Environmental Science and Technology,* pp. 351-409.

Tanner, C., Sukias, J. and Upesdell, M., 1999. Substratum phosphorus accumulation during maturation of gravel-bed constructed wetlands. *Water Science Technology,* pp. 147-154.

Urbonas, B. and Doerfer, J., 2004. Some observations on atmospheric dust: Fallout in the Denver, Colorado area. *Stormwater,* pp. 46-50.

USEPA, 2005. *National management measures to control non point source pollution from urban areas,* Washington D.C.: United States Environmental Protection Agency.

Vadas, P., Mallarino, A. and McFarland, A., 2006. *The importance of sampling depth when testing soils for their potential to supply phosphorus to surface runoff,* Washington D.C.: Agricultural Research Service, United States Department of Agriculture.

Vohla, C., Alas, R., Nurk, K., Baatz, S., Mander, U., 2007. Dynamics of phosphorus, nitrogen and carbon removal in a horizontal subsurface flow constructed wetland. *Science of the Total Environment,* p. 66–74.

Vymazal, J., 2007. Removal of nutrients in various types of constructed wetlands. *Science of the Total Environment,* pp. 48-65.

Wadzuk, B.M, Rea, M., Woodruff, G., Flynn, K., Traver, R.G., 2010. Water-Quality Performance of a Constructed Stormwater Wetland for All Flow Conditions. *Journal of the American Water Resources Association,* pp. 385-394.

Weiler, M. and McDonnell, J., 2007. Conceptualizing lateral preferential flow and flow networks and simulating the effects on gauged and ungauged hillslopes. *Water Resources Research,* p. 43.

White, J., Reddy, K. and Majer-Newman, J., 2006. Hydrologic and vegetation effects on water column phosphorus in wetland mesocosms. *Soil Science Society of America Journal,* pp. 1242-1251.

Wolf, A. and Baker, D., 1990. Colorimetric method for phosphorus measurement in ammonium oxalate soil extracts. *Commun. in Soil Science and Plant Anal.,* pp. 2257-2263.

Xu, S. and Jaffe, P., 2006. Effects of plants on the removal of hexavalent chromium in wetland sediments. *Journal of Environmental Quality,* pp. 334-341.

Xu, S., Leri, A., Myneni, S. and Jaffe, P., 2004. Uptake of bromide by two wetland plants (Typha latifolia L. and Phragmites australis (Cav.) Trin. ex Steud. *Environmental Science & Technology,* pp. 5642-5648.

Zazo, J., Paull, J. and Jaffe, P., 2008. Influence of plants on the reduction of hexavalent chromium in wetland sediments. *Environmental Pollution,* pp. 29-35.

Zhang, T., Wang, X. and Jin, X., 2007. Variations of alkaline phosphatase activity and P fractions in sediments of a shallow Chinese eutrophic lake. *Environmental Pollution,* pp. 288-294.

APPENDIX A: Phase I Raw Data

Table A.0.1Non-vegetated raw SRP concentrations all tests 1-8.

Non-Vegetated (mg L^{-1} PO_4-P)					
t=0 hrs	t=24 hrs	t=0 hrs	t=24 hrs	t=0 hrs	t=24 hrs
0.09	0.90	0.17	0.85	0.09	0.37
0.24	0.93	0.28	0.86	0.15	0.40
0.86	0.91	0.17	0.84	0.12	0.46
0.06	0.71	0.14	0.88	0.13	0.67
0.69	0.93	0.26	0.91	0.22	0.59
0.88	1.03	0.17	0.98	0.24	0.65
0.01	0.87	0.20	0.81	0.11	0.34
0.01	0.96	0.03	0.75	0.10	0.54
0.17	0.83	0.14	0.65	0.09	0.37
0.22	0.80	0.11	0.63	0.13	0.32
0.16	0.83	0.10	0.67	0.08	0.36
0.02	0.90	0.12	0.71	0.09	0.54
0.19	0.88	0.17	0.85	0.24	0.78
0.57	0.97	0.13	0.83	0.19	0.70
0.02	0.86	0.09	0.78	0.15	0.56
0.01	0.77	0.07	0.68	0.11	0.61

Table A.0.2. Non-vegetated raw SRP concentrations by horizontal port location all tests 1-8

Non-Vegetated (mg L^{-1} PO_4-P)			
0.6 m		2.4 m	
t=0 hrs	t=24 hrs	t=0 hrs	t=24 hrs
0.09	0.90	0.17	0.83
0.24	0.93	0.22	0.80
0.86	0.91	0.16	0.83
0.06	0.71	0.02	0.90
0.69	0.93	0.19	0.88
0.88	1.03	0.57	0.97
0.01	0.87	0.02	0.86
0.01	0.96	0.01	0.77
0.17	0.85	0.14	0.65
0.28	0.86	0.11	0.63
0.17	0.84	0.10	0.67
0.14	0.88	0.12	0.71
0.26	0.91	0.17	0.85
0.17	0.98	0.13	0.83
0.20	0.81	0.09	0.78
0.03	0.75	0.07	0.68
0.09	0.37	0.09	0.37
0.15	0.40	0.13	0.32
0.12	0.46	0.08	0.36
0.13	0.67	0.09	0.54
0.22	0.59	0.24	0.78
0.24	0.65	0.19	0.70
0.11	0.34	0.15	0.56
0.10	0.54	0.11	0.61

Table A.0.3 Non-vegetated raw SRP concentrations by vertical port location all tests 1-8.

Non-Vegetated (mg L^{-1} PO_4-P)					
0 cm		3 cm		8 cm	
t=0 hrs	t=24 hrs	t=0 hrs	t=24 hrs	t=0 hrs	t=24 hrs
0.09	0.90	0.17	0.85	0.09	0.37
0.24	0.93	0.28	0.87	0.15	0.40
0.86	0.91	0.17	0.84	0.12	0.46
0.06	0.71	0.14	0.88	0.13	0.67
0.69	0.93	0.26	0.91	0.22	0.59
0.88	1.03	0.17	0.98	0.24	0.65
0.01	0.87	0.20	0.81	0.11	0.34
0.01	0.96	0.03	0.75	0.10	0.54
0.19	1.01	0.14	0.76	0.09	0.35
0.17	0.83	0.14	0.65	0.09	0.37
0.22	0.80	0.11	0.63	0.13	0.32
0.16	0.83	0.10	0.67	0.08	0.36
0.02	0.90	0.12	0.71	0.09	0.54
0.19	0.88	0.17	0.85	0.24	0.78
0.57	0.97	0.13	0.84	0.19	0.70
0.02	0.86	0.09	0.78	0.15	0.56
0.01	0.78	0.07	0.68	0.11	0.61
0.12	0.89	0.14	0.60	0.11	0.29

Table A.0.4 Vegetated raw SRP concentrations all tests 1-8

Vegetated (mg L^{-1} PO_4-P)							
t=0 hrs	t=24 hrs	t=0 hrs	t=24 hrs	t=0 hrs	t=24 hrs	t=0 hrs	t=24 hrs
0.06	0.66	0.53	0.85	0.56	0.77	0.13	0.80
0.17	0.71	0.60	0.93	0.49	0.88	0.05	0.79
0.67	0.91	0.59	0.96	0.35	0.64	0.14	0.59
0.70	0.86	0.09	0.78	0.31	0.82	0.02	0.76
0.79	0.99	0.22	0.80	0.34	0.81	0.07	0.92
0.83	0.91	0.59	0.75	0.28	0.76	0.12	0.83
0.86	0.73	0.55	0.47	0.08	0.70	0.04	0.73
0.79	0.83	0.13	0.82	0.20	0.89	0.09	0.74
0.07	0.81	0.46	0.82	0.13	0.87	0.27	0.85
0.21	0.81	0.56	0.79	0.17	0.33	0.04	0.64
0.57	0.78	0.59	0.89	0.14	0.69	0.12	0.30
0.62	0.80	0.11	0.91	0.07	0.58	0.14	0.47
0.46	0.91	0.22	0.76	0.02	0.75	0.10	0.62
0.60	1.01	0.57	0.89	0.13	0.78	0.13	0.69
0.50	1.00	0.54	0.72	0.06	0.71	0.03	0.66
0.78	0.84	0.40	0.75	0.21	0.68	0.02	0.67
0.11	0.89	0.38	0.82	0.15	0.79	0.11	0.75
0.18	0.84	0.49	0.80	0.10	0.74	0.03	0.62
0.57	0.79	0.43	0.72	0.11	0.59	0.14	0.57
0.39	0.83	0.09	0.94	0.06	0.76	0.13	0.55
0.21	0.73	0.22	0.88	0.02	0.70	0.12	0.68

Vegetated (mg L^{-1} PO_4-P) cont'd							
t=0 hrs	t=24 hrs	t=0 hrs	t=24 hrs	t=0 hrs	t=24 hrs	t=0 hrs	t=24 hrs
0.13	0.65	0.13	0.64	0.03	0.36		0.17
0.04	0.75	0.11	0.53	0.07	0.40		0.26
0.01	0.70	1.72	0.41	0.02	0.42		0.35
0.17	0.62	0.10	0.56	0.07	0.40		0.21
0.07	0.72	0.07	0.60	0.08	0.49		0.28
0.17	0.54	0.04	0.46	1.21	0.46		0.22
0.14	0.52	0.01	0.46	0.08	0.42		0.06
0.12	0.45	0.04	0.55	0.03	0.51		0.11
0.06	0.67	0.15	0.48	0.01	0.26		0.15
0.07	0.62	0.07	0.31	0.06	0.15		0.09
0.01	0.80	1.31	0.53	0.05	0.20		0.15
0.12	0.59	0.07	0.47	0.06	0.21		0.09
0.08	0.57	0.05	0.54	0.01	0.34		0.06
0.15	0.65	0.03	0.44	1.59	0.33		0.11
0.15	0.52	0.04	0.30	0.10	0.41		0.08
1.93	0.34	0.04	0.31	0.06	0.28		
0.12	0.25	0.10	0.35	0.01	0.31		
0.06	0.48	0.08	0.36	0.06	0.15		
0.07	0.39	1.59	0.26		0.15		
0.01	0.48	0.09	0.27		0.24		
0.04	0.55	0.03	0.12		0.18		

Table A.0.5 Vegetated raw SRP concentrations by vertical port location all tests 1-8 at t=24hrs

Vegetated (mg L^{-1} PO_4-P)

t=24hrs

0 cm Values	3 cm Values	8 cm Values	0 cm Values	3 cm Values	8 cm Values
0.66	0.75	0.56	0.47	0.57	0.15
0.71	0.78	0.60	0.82	0.55	0.20
0.91	0.71	0.46	0.82	0.68	0.21
0.86	0.68	0.46	0.79	0.65	0.34
0.99	0.79	0.55	0.89	0.75	0.33
0.91	0.74	0.48	0.91	0.70	0.41
0.73	0.59	0.31	0.76	0.62	0.28
0.83	0.76	0.53	0.89	0.72	0.31
0.81	0.70	0.47	0.72	0.54	0.15
0.81	0.80	0.54	0.75	0.52	0.15
0.78	0.79	0.44	0.82	0.45	0.24
0.80	0.59	0.30	0.80	0.67	0.18
0.91	0.76	0.31	0.72	0.62	0.17
1.01	0.92	0.35	0.94	0.80	0.26
1.00	0.83	0.36	0.88	0.59	0.35
0.84	0.73	0.26	0.77	0.57	0.21
0.89	0.74	0.27	0.88	0.65	0.28
0.84	0.85	0.12	0.64	0.52	0.22
0.79	0.64	0.36	0.82	0.34	0.06
0.83	0.30	0.40	0.81	0.25	0.11
0.73	0.47	0.42	0.76	0.48	0.15
0.85	0.62	0.40	0.70	0.39	0.09
0.93	0.69	0.49	0.89	0.48	0.15
0.96	0.66	0.46	0.87	0.55	0.09
0.78	0.67	0.42	0.33	0.64	0.06
0.80	0.75	0.51	0.69	0.53	0.11
0.75	0.62	0.26	0.58	0.41	0.08

Table A.0.6. P sorption isotherm values for t=24hrs and t=48hrs.

	t=24hrs		t=24 hrs		t=48hrs	
Initial Conc of P in solution (mgP/L)	I.D.	Conc. Of P Sorbed (mg/g)	I.D.	Conc. Of P Sorbed (mg/g)	I.D.	Conc. Of P Sorbed (mg/g)
0	set 1		set 2		set 3	
0.5	set 1	0.01	set 2	0.01	set 3	0.01
1.5	set 1	0.03	set 2	0.03	set 3	0.03
5	set 1	0.11	set 2	0.11	set 3	0.11
10	set 1	0.21	set 2	0.20	set 3	0.21
25	set 1	0.39	set 2	0.40	set 3	0.41
50	set 1	0.52	set 2	0.40	set 3	0.44

Table A.0.7. Raw data from oxalate analysis in phase I. Values are for non-vegetated and vegetated data. Both t=0hrs and t=24hrs data are presented.

	P_{ox} (mg kg^{-1}) t=0 hrs		P_{ox} (mg kg^{-1}) t=24 hrs	
Sample #	Non-Vegetated	Vegetated	Non-Vegetated	Vegetated
1	244	194	240	230
2	223	276	284	268
3	214	259	223	238
4	236	231	262	200
5	-	274	236	251
6	-	243	219	244
Avg	229	246	244	238
Stdev	13	31	25	23

APPENDIX B: Phase II

Raw Data

Temperature/RH

P Sorption Isotherms

Chloride tracer 3D graphs

Flow graphs

Hydrometer analyses

Table B.0.1. Raw SRP data for control mesocosm study.

Control				
Time (weeks)	% SRP Removed	Mass SRP Removed (mg P)	Mass SRP IN (mg P)	Mass SRP OUT (mg P)
0.143	64%	44	68	25
1	44%	199	454	255
2	23%	106	465	359
3	29%	136	474	339
4	11%	51	455	404
5	27%	117	434	317
6	33%	175	528	353
7	23%	114	505	391
8	29%	105	357	252
9	18%	63	358	295
10	6%	25	407	382
11	26%	114	444	330
12	21%	90	432	342

Table B.0.2. Raw SRP data for FeP mesocosm study.

FeP				
Time (weeks)	% SRP Removed	Mass SRP Removed (mg P)	Mass SRP IN (mg P)	Mass SRP OUT (mg P)
0.143	42%	28	66	38
1	34%	149	435	286
2	44%	204	465	261
3	51%	225	443	218
4	44%	175	400	225
5	45%	235	542	400
6	35%	162	521	286
7	43%	201	465	303
8	27%	110	471	270
9	35%	159	400	290
10	31%	134	458	299
11	31%	134	430	296
12	38%	157	416	259

Table B.0.3. Raw SRP data for Fe mesocosm study.

Fe				
Time (weeks)	% SRP Removed	Mass SRP Removed (mg P)	Mass SRP IN (mg P)	Mass SRP OUT (mg P)
0.143	77%	53	69	16
1	58%	250	431	181
2	36%	169	471	301
3	52%	232	450	218
4	18%	76	428	352
5	44%	192	438	246
6	55%	283	517	234
7	46%	247	540	294
8	45%	204	457	253
9	51%	245	474	229
10	23%	110	473	363

Table B.0.4. Raw SRP data for Al 2 mesocosm study.

Al 2				
Time (weeks)	% SRP Removed	Mass SRP Removed (mg P)	Mass SRP IN (mg P)	Mass SRP OUT (mg P)
0.143	56%	37	66	29
1	26%	122	465	343
2	14%	58	422	364
3	16%	64	389	325
4	18%	82	459	377

Table B.0.5. Raw SRP data for Al 2D mesocosm study.

Al 2D				
Time (weeks)	% SRP Removed	Mass SRP Removed (mg P)	Mass SRP IN (mg P)	Mass SRP OUT (mg P)
0.143	43%	29	66	38
1	28%	115	403	289
2	23%	100	428	329
3	22%	96	442	346
4	22%	95	438	343

Table B.0.6. Raw SRP data for Al 5D mesocosm study.

Al 5D				
Time (weeks)	% SRP Removed	Mass SRP Removed (mg P)	Mass SRP IN (mg P)	Mass SRP OUT (mg P)
0.143	91%	50	55	5
1	31%	125	400	275
2	28%	85	300	215
3	18%	66	378	312
4	21%	83	389	306
5	17%	64	370	306
6	20%	87	444	357
7	18%	74	417	343
8	13%	54	425	372

Table B.0.7. Raw SRP data for Al 8 mesocosm study.

Al 8				
Time (weeks)	% SRP Removed	Mass SRP Removed (mg P)	Mass SRP IN (mg P)	Mass SRP OUT (mg P)
0.143	99%	71	72	1
1	33%	145	433	288
2	24%	99	411	312
3	25%	103	415	312
4	25%	112	443	331

Table B.0.8. Raw SRP data for Al 5 mesocosm study.

Al 5				
Time (weeks)	% SRP Removed	Mass SRP Removed (mg P)	Mass SRP IN (mg P)	Mass SRP OUT (mg P)
0.143	99%	89	90	1
1	37%	168	459	291
2	98%	464	473	9
3	79%	380	481	101
4	61%	271	441	170

Table B.0.9. Fe (II) concentrations for control mesocosm over a 12 week study.

	mM Fe (II)												
Sample Name	0 hrs	1 wk	2 wks	3 wks	4 wks	5 wks	6 wks	7 wks	8 wks	9 wks	10 wks	11 wks	12 wks
C 73	0.06	0.33	0.39	0.01	1.13	0.69							
C 78	0.01					0.29	1.70	0.60	0.63	0.48	0.81	0.59	0.50
C 23	0.10	0.22	0.43	0.15	0.79	1.55	0.80	2.87	7.25	6.71	11.43	5.66	7.00
C 28	0.22	0.42	0.38	0.02	0.39	0.85	1.09	0.89	1.41	1.44	3.18	2.73	2.18
C 43	0.10	0.52	0.89	0.28	0.71	0.89	2.57	1.08	0.96	1.30	6.31	7.04	3.82
C 48	0.24	0.03	0.16	0.11	0.37	0.47	1.54	0.50	0.70	0.80	1.67	1.33	1.84
C 63	0.10	0.22	0.35	0.22	0.46	0.39	2.37	0.24	0.17	0.34	0.30	0.61	0.87
C 68	0.36	0.84	0.79	0.63	1.15	1.29	4.12	0.82	1.43	0.52	0.66	1.00	2.47
C 83	0.22	0.06	0.31	0.26	0.72	0.30	7.93	0.67	1.71	1.82	10.75	8.96	0.11
C 88	0.16	0.43	0.57	0.37	0.89	0.97	3.93	0.98	1.34	2.50	14.75	6.29	10.98
C 93	0.05	0.13	0.31	0.25	2.05	0.23	8.04	6.43	5.36	1.68	0.75	0.89	1.13
C 98	0.10	0.27	0.28	0.35	0.54	0.55	0.87	1.05	0.40	0.41	0.61	1.29	2.14
C Out 3	0.01	0.02	0.03	0.31	0.05	0.15	0.15	0.18	0.11	0.11	0.15	0.34	0.14
C out 8		0.11	0.61	0.46	0.74	0.44	0.26	1.56	0.66	0.11	0.40	0.38	0.11
Average	0.13	0.28	0.42	0.26	0.77	0.65	2.72	1.37	1.70	1.40	3.98	2.86	2.56
StdDev	0.10	0.23	0.24	0.17	0.49	0.42	2.64	1.67	2.14	1.76	5.10	3.02	3.16
n	14	14	14	14	14	14	14	14	14	14	14	14	14

Table B.0.10. Fe (II) concentrations for FeP mesocosm over a 12 week study.

	mM Fe (II)												
Sample Name	0 hrs	1 wk	2 wks	3 wks	4 wks	5 wks	6 wks	7 wks	8 wks	9 wks	10 wks	11 wks	12 wks
FeP 73	0.01	0.16	0.37	0.22	0.50	0.97	2.08	1.01	3.42	2.29	3.22	3.36	2.16
FeP 78	0.23	0.08	0.43	1.20	1.05	1.23	2.09	1.51	1.25	1.39	1.38	1.56	1.12
FeP 23	0.07					0.25	2.49	1.37	1.95	3.13	7.43	0.57	4.17
FeP 28	0.45					0.91	1.75	1.58	3.09	0.51	0.51	1.81	1.82
FeP 43	0.30	0.01	0.51	0.43	0.85	0.85	3.94	1.30	7.91	7.44	5.76	2.17	5.17
FeP 48	0.25					1.23	1.79	1.58	1.17	1.88	1.07	1.20	1.92
FeP 63	0.05	0.01	0.40	0.29	0.43	0.58	0.62						
FeP 68	0.42	0.01	0.57	0.69	0.92	0.93	1.14	1.33	1.72	1.12	2.44	0.81	1.40
FeP 83	0.15	0.11	0.31	0.25	0.77	0.88	1.78	1.91	6.01	4.49	5.02	4.08	2.43
FeP 88	0.21	0.20	0.69	0.61	0.92	1.38	2.00	1.50	2.97	1.71	1.87	2.00	2.46
FeP 93	0.50	0.06	0.44	0.33	0.76	0.49	4.24	2.10	3.32	6.31	6.32	1.14	0.74
FeP 98	0.36	0.20	0.58	0.37	0.55	1.05	1.55	1.92	4.09	2.11	2.97	2.19	2.56
FeP Out 3	0.04	0.35		0.01	0.33	0.10	0.12	0.70	0.50	0.11	0.31	0.33	0.11
FeP Out 8		0.03	0.75	0.88	2.92	0.59	1.58	1.30	0.99	0.41	0.14	0.32	0.11
Average	0.23	0.11	0.51	0.48	0.91	0.82	1.94	1.47	2.95	2.53	2.96	1.66	2.01
StdDev	0.17	0.11	0.14	0.34	0.71	0.37	1.10	0.38	2.12	2.27	2.45	1.13	1.46
n	14	14	14	14	14	14	14	14	14	14	14	14	14

Table B.0.11. Fe (II) concentrations for Fe mesocosm over a 12 week study.

	mM Fe (II)										
Sample Name	0 hrs	1 wk	2 wks	3 wks	4 wks	5 wks	6 wks	7 wks	8 wks	9 wks	10 wks
Fe 73	0.15	0.06	0.26	2.95	3.56		1.33	7.25	39.95	6.50	51.02
Fe 78	0.01	0.72	0.14	0.27	0.28	0.34	0.69	0.50	0.54	0.47	0.60
Fe 23	1.25	0.21	0.03	0.18				7.25	39.00	8.58	35.80
Fe 28	0.13	0.54	0.42	0.70	0.87	0.44	0.59	0.99	0.56	0.48	1.18
Fe 43	0.24	0.25	0.37	0.69	2.70	5.53	4.87	7.17	19.97	35.60	54.54
Fe 48	0.29	0.11	0.50	0.66	0.79	0.79	0.61	0.85	1.38	0.72	0.88
Fe 63	0.25	0.29	0.52	0.36	1.43	0.87	6.36	2.58	11.00	11.47	31.17
Fe 68	0.32	0.37	0.71	0.77	0.88	0.83	0.99	1.19	1.00	0.99	0.94
Fe 83	0.05	0.17	0.37	0.53	1.03	1.21	1.43	3.62	6.65	4.83	32.00
Fe 88	0.35	0.59	0.85	1.19	1.19	2.24	0.91	0.94	2.61	1.12	1.65
Fe 93	0.37	0.22	0.07	0.45	0.44	0.76	6.77	1.41	2.52	24.92	7.75
Fe 98	0.31	0.28	0.29	0.56	0.50	0.45	0.50	0.60	3.16	0.92	1.52
Fe Out 3	0.41	1.65	0.33	0.01	0.36	0.09	0.12	0.28	0.17	0.37	0.11
Fe out 8	0.30	0.57	0.57	0.52	1.26	1.75	0.15	0.98	0.99	0.45	1.11
Average	0.32	0.43	0.39	0.70	1.18	1.27	1.95	2.54	9.25	6.96	15.73
StdDev	0.29	0.40	0.23	0.71	0.95	1.47	2.38	2.68	13.90	10.69	20.49
n	14	14	14	14	14	14	14	14	14	14	14

Table B.0.12. Raw data from oxalate extractions in control mesocosm study.

Sample ID	Mass Amt (g)	a = Conc P (mg/L)	Pox (mg/kg)	a = Conc Fe (mg/L)	Feox (mg/kg)	a = Conc Al (mg/L)	Alox (mg/kg)
C t=0_1	1.3	5.5	547.3	84.6	8462.2	10.9	1093.9
C t=0_2	1.3	2.8	281.7	66.2	6623.4	15.6	1561.8
C t=0_3	1.3	2.4	243.9	73.3	7330.6	16.0	1596.2
C t=0_4	1.3	2.5	248.8	73.6	7359.7	15.1	1506.0
C t=0_5	1.3	2.7	271.0	65.1	6511.0	14.1	1411.8
C t=0_6	1.3	4.0	402.2	91.5	9153.6	15.3	1526.7
Control t=0 ALL Averages		3.3	332.5	75.7	7573.4	14.5	1449.4
Control t=0 Std. Deviation		1.2	120.2	10.4	1041.4	1.9	185.0
N		6.0	9.0	9.0	12.0	12.0	15.0
C t=4 Comp Inlet	1.3	6.4	638.4	90.3	9034.5	11.2	1116.0
C t=4 Comp Inlet	1.3	3.4	337.9	70.1	7009.4	16.2	1617.9
C t=4 Comp Inlet	1.3	3.0	303.8	61.6	6163.3	13.6	1356.5
C t=4 Comp Inlet AVERAGES		4.3	426.7	74.0	7402.4	13.6	1363.5
C t=4 Comp Middle	1.3	6.0	598.1	97.5	9749.4	9.8	978.1
C t=4 Comp Middle	1.3	3.4	336.8	77.9	7787.9	14.3	1427.5
C t=4 Comp Middle	1.3	2.8	281.9	65.6	6561.2	11.7	1167.2
C t=4 Comp Middle AVERAGES		4.1	405.6	80.3	8032.8	11.9	
C t=4 Comp Outlet	1.2	3.8	380.4	55.0	5498.6	6.0	602.8
C t=4 Comp Outlet	1.3	2.2	222.8	53.6	5361.5	10.6	1064.2
C t=4 Comp Outlet	1.3	1.9	190.7	44.2	4420.3	8.8	880.5
C t=4 Comp Outlet AVERAGES		2.6	264.7	50.9	5093.5	8.5	849.2
Control t=4 ALL Averages		3.7	365.6	68.4	6842.9	11.3	1134.5
Control t=4 Std. Deviation		1.5	154.9	17.5	1753.0	3.1	305.5
N		9.0	9.0	9.0	9.0	9.0	9.0
C t=12 Comp Inlet	1.3	6.7	670.8	78.9	7893.5	10.1	1006.6
C t=12 Comp Inlet	1.3	4.2	420.9	67.6	6755.7	16.0	1599.3
C t=12 Comp Inlet	1.3	4.1	406.3	61.7	6170.5	13.7	1371.6
C t=12 Comp Inlet AVERAGES		5.0	499.3	69.4	6939.9	13.3	1325.8
C t=12 Comp Middle	1.3	5.1	505.1	69.1	6909.1	8.0	803.2
C t=12 Comp Middle	1.3	2.6	259.3	57.1	5705.1	12.0	1203.9
C t=12 Comp Middle	1.3	2.4	237.3	52.3	5234.0		
C t=12 Comp Middle AVERAGES		3.3	333.9	59.5	5949.4	10.0	1003.5
C t=12 Comp Outlet	1.3	4.9	492.6	68.1	6812.2	7.9	789.9
C t=12 Comp Outlet	1.3	3.0	304.3	62.9	6290.9	12.8	1275.7
C t=12 Comp Outlet	1.3	2.8	280.0	55.4	5535.2	10.7	1072.1
C t=12 Comp Outlet AVERAGES		3.6	359.0	62.1	6212.8	10.5	1045.9
Control t=12 ALL Averages		4.0	397.4	63.7	6367.4	11.4	1140.3
Control t=12 Std. Deviation		1.4	142.8	8.2	824.0	2.8	279.2
N		9.0	9.0	9.0	9.0	9.0	9.0

Table B.0.13. Raw data from oxalate extractions in FeP mesocosm study.

Sample ID	Mass Amt (g)	a = New Conc P (mg/L)	Pox (mg/kg)	a = New Conc Fe (mg/L)	Feox (mg/kg)	a = New Conc Al (mg/L)	Alox (mg/kg)
FeP t=0 _1	1.25	5.2	519	75.4	7544	8.3	831
FeP t=0 _2	1.25	3.0	304	72.6	7259	13.1	1308
FeP t=0 _3	1.25	1.7	169	61.2	6124	12.6	1255
FeP t=0 _4	1.25	1.7	169	59.0	5897	11.9	1193
FeP t=0 _5	1.25	3.1	305	68.8	6883	11.1	1110
FeP t=0 Sample 1 AVERAGES		2.93	293.16	67.42	6741.59	11.39	1139.27
FeP t=0 _6	1.251	5.8	577	92.4	9242	9.2	923
FeP t=0 _7	1.25	3.1	314	76.9	7693	13.4	1336
FeP t=0 _8	1.251	1.9	194	68.1	6813	13.5	1346
FeP t=0 _9	1.251	2.0	201	66.8	6684	13.2	1318
FeP t=0 _10	1.25	3.2	318	75.4	7541	11.6	1163
FeP t=0 Sample 2 AVERAGES		3.21	320.61	75.95	7594.54	12.17	1217.37
FeP t=0 _11	1.25	3.1	307	77.5	7748	11.1	1105
FeP t=0 ALL Averages		3.07	306.89	72.21	7220.75	11.72	1171.68
FeP t=0 Std. Deviation		1.34	134.29	9.12	911.86	1.71	170.58
N		11.00	11.00	11.00	11.00	11.00	11.00
FeP t=12 Comp Inlet	1.25	7.3	730	89.0	8903	10.0	997
FeP t=12 Comp Inlet	1.25	4.5	449	82.4	8236	14.9	1494
FeP t=12 Comp Inlet	1.25	4.8	475	82.8	8276	14.1	1405
FeP t=12 comp Inlet AVERAGES		5.51	551.25	84.71	8471.43	12.99	1299.00
FeP t=12 Comp Middle	1.25	2.3		66.0	6601	7.0	697
FeP t=12 Comp Middle	1.25	4.2	417	77.2	7718	14.1	1411
FeP t=12 Comp Middle	1.25	4.1	414	76.2	7618	11.9	1190
FeP t=12 comp Middle AVERAGES		3.52	415.40	73.12	7312.50	10.99	1099.11
FeP t=12 Comp Outlet	1.25	5.9	589	77.1	7706	8.0	804
FeP t=12 Comp Outlet	1.25	3.6	362	74.8	7481	13.0	1301
FeP t=12 Comp Outlet	1.25	3.7	370	73.3	7334	11.8	1184
FeP t=12 comp Outlet AVERAGES		4.40	440.28	75.07	7507.20	10.96	1096.06
FeP t=12 ALL Averages		4.48	475.67	77.64	7763.71	11.65	1164.72
FeP t=12 Std. Deviation		1.43	124.98	6.54	654.37	2.79	279.16
N		9.00	9.00	9.00	9.00	9.00	9.00

Table B.0.14. Raw data from oxalate extractions in Fe mesocosm study.

Sample ID	Mass Amt (g)	a = New Conc P (mg/L)	Pox (mg/kg)	a = New Conc Fe (mg/L)	Feox (mg/kg)	a = New Conc Al (mg/L)	Alox (mg/kg)
Fe t=0 _1	1.25	5.9	588	83.8	8385	8.6	855
Fe t=0 _2	1.25	3.0	300	69.8	6976	12.6	1259
Fe t=0 _3	1.25	2.2	215	64.6	6463	12.3	1227
Fe t=0 _4	1.25	2.2	220	65.8	6583	13.6	1358
Fe t=0 _5	1.25	3.0	302	65.8	6580	10.9	1085
Fe t=0 Sample 1 AVERAGES		3.25	324.87	69.97	6997.32	11.57	1156.82
Fe t=0 _6	1.251	6.0	598	93.6	9355	9.8	979
Fe t=0 _7	1.25	3.4	338	86.0	8600	14.7	1472
Fe t=0 _8	1.249	2.2	222	67.0	6703	13.1	1312
Fe t=0 _9	1.25	2.8	280	82.3	8230	16.4	1642
Fe t=0 _10	1.25	2.7	272	69.6	6955	11.3	1133
Fe t=0 Sample 2 AVERAGES		3.42	341.91	79.69	7968.61	13.08	1307.75
Fe t=0 _11	1.25	3.4	337	85.7	8571	11.6	1158
Fe t=0 ALL Averages		3.34	333.76	75.82	7581.91	12.26	1225.53
Fe t=0 Std. Deviation		1.35	135.19	10.49	1049.21	2.22	221.52
N		11.00	11.00	11.00	11.00	11.00	11.00
Fe t=10 Comp Inlet	1.251						
Fe t=10 Comp Inlet	1.251	3.8	383	87.2	8717	15.8	1582
Fe t=10 Comp Inlet	1.25	4.0	400	86.1	8609	14.0	1401
Fe t=10 comp Inlet AVERAGES		3.91	391.38	86.63	8663.24	14.92	1491.53
Fe t=10 Comp Middle	1.251	6.5	651	112.4	11236	9.9	993
Fe t=10 Comp Middle	1.251	3.9	394	98.4	9844	14.6	1458
Fe t=10 Comp Middle	1.25	3.7	368	93.2	9317	13.0	1295
Fe t=10 comp Middle AVERAGES		4.71	470.76	101.32	10132.46	12.49	1248.89
Fe t=10 Comp Outlet	1.251	8.0	802	109.5	10951	11.5	1146
Fe t=10 Comp Outlet	1.251	4.0	401	96.6	9659	15.0	1505
Fe t=10 Comp Outlet	1.25	4.6	455	93.9	9391	14.8	1480
Fe t=10 comp Outlet AVERAGES		5.53	552.89	100.01	10000.57	13.77	1376.83
Fe t=10 ALL Averages		4.82	481.71	97.16	9715.70	13.58	1357.53
Fe t=10 Std. Deviation		1.58	158.37	9.52	951.95	2.00	200.12
N		9.00	9.00	9.00	9.00	9.00	9.00

Table B.0.15. Raw data from oxalate extractions in Al 2 mesocosm study.

Sample ID	Mass Amt (g)	a = New Conc P (mg/L)	Pox (mg/kg)	a = New Conc Fe (mg/L)	Feox (mg/kg)	a = New Conc Al (mg/L)	Alox (mg/kg)
Al 2 t=0 Inlet	1.25	5.6	557	87.6	8759	22.8	2281
Al 2 t=0 Inlet	1.25	3.4	341	77.0	7701	32.4	3243
Al 2 t=0 Inlet	1.25	2.7	270	64.7	6472	39.1	3908
Al 2 t=0 Inlet	1.25	2.8	279	68.0	6795	36.2	3616
Al 2 t=0 Inlet	1.25	3.8	385	82.7	8272	30.7	3068
Al 2 t=0 Inlet AVERAGES		3.66	366.50	76.00	7599.93	32.23	3223.24
Al 2 t=0 Outlet	1.25	5.8	579	78.6	7861	26.9	2688
Al 2 t=0 Outlet	1.25	4.1	411	77.9	7791	42.8	4279
Al 2 t=0 Outlet	1.25	2.9	289	74.4	7439	34.0	3399
Al 2 t=0 Outlet	1.25	3.1	313	86.7	8672	37.2	3724
Al 2 t=0 Outlet	1.25	4.3	429	80.6	8055	36.0	3598
Al 2 t=0 Outlet AVERAGES		4.04	404.33	79.64	7963.51	35.37	3537.49
Al 2 t=0 Outlet	1.25	3.9	392	81.1	8113	35.0	3500
Al 2 t=0 ALL Averages		3.86	386.06	78.12	7811.88	33.91	3391.20
Al 2 t=0 Std. Deviation		1.05	105.01	7.06	705.90	5.59	559.00
N		11.00	11.00	11.00	11.00	11.00	11.00
Al 2 t=4 Comp Inlet	1.25	6.2	618	87.5	8755	23.0	2300
Al 2 t=4 Comp Inlet	1.25	4.2	416	79.4	7944	37.7	3766
Al 2 t=4 Comp Inlet	1.25	4.3	433	77.9	7792	35.5	3552
Al 2 t=4 comp Inlet AVERAGES		4.89	489.23	81.64	8163.73	32.06	3205.98
Al 2 t=4 Comp Middle	1.25	7.5	751	92.9	9292	21.6	2155
Al 2 t=4 Comp Middle	1.25	4.9	490	92.5	9254	34.6	3456
Al 2 t=4 Comp Middle	1.25	5.3	533	91.4	9141	35.9	3595
Al 2 t=4 comp Middle AVERAGES		5.91	591.42	92.29	9228.94	30.69	3068.73
Al 2 t=4 Comp Outlet	1.25	6.2	616	81.2	8122	25.0	2496
Al 2 t=4 Comp Outlet	1.25	4.3	434	77.1	7709	41.6	4156
Al 2 t=4 Comp Outlet	1.25	4.9	491	75.5	7550	46.3	4631
Al 2 t=4 compOutlet AVERAGES		5.14	513.88	77.94	7793.99	37.61	3761.06
Al 2 t=4 ALL Averages		5.32	531.51	83.96	8395.55	33.45	3345.26
Al 2 t=4 Std. Deviation		1.11	110.91	7.12	711.73	8.54	853.98
N		9.00	9.00	9.00	9.00	9.00	9.00

Table B.0.16. Raw data from oxalate extractions in Al 2D mesocosm study.

Sample ID	Mass Amt (g)	a = New Conc P (mg/L)	Pox (mg/kg)	a = New Conc Fe (mg/L)	Feox (mg/kg)	a = New Conc Al (mg/L)	Alox (mg/kg)
Al 2D t=0 Inlet	1.25	2.6	260	67.9	6792	29.1	2907
Al 2D t=0 Inlet	1.25	3.0	301	74.1	7410	35.3	3532
Al 2D t=0 Inlet	1.25	3.6	361	99.3	9934	39.3	3935
Al 2D t=0 Inlet	1.25	3.4	341	109.9	10994	34.1	3408
Al 2D t=0 Inlet	1.25	3.2	316	72.4	7243	34.0	3399
Al 2D t=0 Inlet AVERAGES		3.16	315.87	84.74	8474.46	34.36	3436.15
Al 2D t=0 Outlet	1.25	7.2	716	86.2	8622	36.3	3630
Al 2D t=0 Outlet	1.25	4.4	443	85.8	8578	58.2	5821
Al 2D t=0 Outlet	1.25	4.0	403	94.5	9448	75.6	7557
Al 2D t=0 Outlet	1.25	4.3	428	99.2	9915	79.3	7930
Al 2D t=0 Outlet	1.25	5.1	507	75.9	7589	73.8	7375
Al 2D t=0 Outlet AVERAGES		4.99	499.28	88.30	8830.42	64.63	6462.76
Al 2D t=0 Outlet	1.25	3.8	379	97.2	9725	41.9	4186
Al 2 t=0 ALL Averages		4.05	404.95	87.50	8749.93	48.80	4880.06
Al 2 t=0 Std. Deviation		1.25	124.80	13.61	1361.23	19.13	1912.75
N		11.00	11.00	11.00	11.00	11.00	11.00
Al 2D t=4 Comp Inlet	1.25	6.0	604	68.7	6873	26.3	2630
Al 2D t=4 Comp Inlet	1.25	3.3	333	68.4	6841	33.8	3380
Al 2D t=4 Comp Inlet	1.25	4.0	400	75.3	7534	40.2	4019
Al 2D t=4 Comp Inlet AVERAGES		4.46	445.92	70.83	7082.61	33.43	3342.90
Al 2D t=4 Comp Middle	1.25	4.3	435	66.8	6681	38.6	3858
Al 2D t=4 Comp Middle	1.25	4.1	413	74.7	7468	49.5	4951
Al 2D t=4 Comp Middle	1.25	4.7	469	72.3	7228	54.6	5457
Al 2D t=4 Comp Middle AVERAGES		4.39	438.81	71.26	7125.76	47.56	4755.56
Al 2D t=4 Comp Outlet	1.25	7.2	722	89.1	8912	35.7	3569
Al 2D t=4 Comp Outlet	1.25	4.4	444	85.0	8503	55.3	5532
Al 2D t=4 Comp Outlet	1.25	4.8	482	86.8	8678	52.3	5228
Al 2D t=4 Comp Outlet AVERAGES		5.49	549.00	86.98	8697.88	47.76	4776.33
Al 2 t=4 ALL Averages		4.78	477.91	76.35	7635.42	42.92	4291.60
Al 2 t=4 Std. Deviation		1.17	116.99	8.51	851.33	10.36	1035.94
N		9.00	9.00	9.00	9.00	9.00	9.00

Table B.0.17. Raw data from oxalate extractions in Al 5D mesocosm study.

Sample ID	Mass Amt (g)	a = New Conc P (mg/L)	Pox (mg/kg)	a = New Conc Fe (mg/L)	Feox (mg/kg)	a = New Conc Al (mg/L)	Alox (mg/kg)
Al 5D t=0 Inlet	1.25	5.6	565	75.5	7549	83.9	8388
Al 5D t=0 Inlet	1.25	3.6	355	69.2	6918	60.9	6087
Al 5D t=0 Inlet	1.25	3.5	347			55.8	5577
Al 5D t=0 Inlet	1.25	5.3	532	94.7	9468	73.9	7395
Al 5D t=0 Inlet	1.25	8.8		79.8	7979	56.9	5687
Al 5D t=0 Inlet AVERAGES		5.35	449.80	79.79	7978.68	66.27	6626.62
Al 5D t=0 Middle	1.25	5.2	520	84.5	8454	76.6	7661
Al 5D t=0 Middle	1.25	3.3	325	80.1	8006	156.8	15676
Al 5D t=0 Middle	1.25	3.2	324	80.2	8021	55.7	5572
Al 5D t=0 Middle	1.25	4.1	413	75.7	7566	59.0	5899
Al 5D t=0 Middle	1.25	7.3	725	83.0	8300	45.1	4509
Al 5D t=0 Middle AVERAGES		4.61	461.46	80.70	8069.59	78.63	7863.19
Al 5D t=0 Outlet	1.25	7.6	757	66.5	6648	134.8	13480
Al 5D t=0 Outlet	1.25	3.6	361	61.1	6106	65.7	6573
Al 5D t=0 Outlet	1.25	4.1	405	60.7	6072	78.5	7848
Al 5D t=0 Outlet	1.25	7.0	701	62.5	6252	137.1	13713
Al 5D t=0 Outlet	1.25	10.1		66.4	6639	86.9	8691
Al 5D t=0 Outlet AVERAGES		6.47	555.88	63.43	6343.48	100.61	10061.19
Al 5D t=0 ALL Averages		5.48	486.93	74.27	7427.15	81.84	8183.67
Al 5D t=0 Std. Deviation		2.19	158.64	10.18	1017.51	33.98	3397.82
N		15.00	11.00	11.00	11.00	11.00	11.00
Al 5D t=4 Comp Inlet	1.25	6.2	619	79.2	7916	76.6	7656
Al 5D t=4 Comp Inlet	1.25	6.0	602	76.0	7602	80.2	8020
Al 5D t=4 Comp Inlet	1.25	8.8	879	83.9	8387	33.8	3377
Al 5D t=4 comp Inlet AVERAGES		7.00	699.65	79.68	7968.19	63.51	6350.93
Al 5D t=4 Comp Middle	1.25	8.8	876	85.6	8562	160.5	16052
Al 5D t=4 Comp Middle	1.25	7.6	765	81.9	8187	145.6	14556
Al 5D t=4 Comp Middle	1.25	11.0	1104	86.7	8674	85.8	8584
Al 5D t=4 compMiddle AVERAGES		9.15	915.10	84.74	8474.40	130.64	13063.73
Al 5D t=4 Comp Outlet	1.25	7.9	787	76.6	7661	136.7	13669
Al 5D t=4 Comp Outlet	1.25	8.3	830	81.6	8162	160.1	16006
Al 5D t=4 Comp Outlet	1.25	10.7	1073	88.6	8861	72.7	7272
Al 5D t=4 comp Outlet AVERAGES		8.96	896.49	82.28	8228.09	123.16	12315.54
Al 5D t=4 ALL Averages		8.37	837.08	82.24	8223.56	105.77	10576.73
Al 5D t=4 Std. Deviation		1.74	173.60	4.41	440.72	45.64	4564.03
N		9.00	9.00	9.00	9.00	9.00	9.00
Al 5D t=8 Comp Inlet	1.25	6.7	672	76.6	7658	92.6	9261
Al 5D t=8 Comp Inlet	1.25	6.2	617	83.5	8354	90.5	9048
Al 5D t=8 Comp Inlet	1.25	4.5	446	79.5	7951	57.3	5730
Al 5D t=8 comp Inlet AVERAGES		5.78	578.44	79.88	7987.56	80.13	8012.99
Al 5D t=8 Comp Middle	1.25	6.2	617	77.3	7734	88.2	8824
Al 5D t=8 Comp Middle	1.25	5.5	553	83.8	8378	80.3	8028
Al 5D t=8 Comp Middle	1.25	8.7	869	75.7	7565	52.4	5242
Al 5D t=8 comp Middle AVERAGES		6.80	679.77	78.92	7892.12	73.65	7364.76
Al 5D t=8 Comp Outlet	1.25	6.2	625	79.9	7988	84.8	8477
Al 5D t=8 Comp Outlet	1.25	5.9	592	77.8	7777	80.7	8072
Al 5D t=8 Comp Outlet	1.25	9.0	897	74.6	7464	52.7	5271
Al 5D t=8 comp Outlet AVERAGES		7.05	704.69	77.43	7743.15	72.73	7273.34
Al 5D t=8 ALL Averages		6.54	654.30	78.74	7874.28	75.50	7550.36
Al 5D t=8 Std. Deviation		1.44	144.37	3.24	324.36	16.58	1657.73
N		9.00	9.00	9.00	9.00	9.00	9.00

Table B.0.18. Raw data from oxalate extractions in Al 8 mesocosm study.

Sample ID	Mass Amt (g)	a = New Conc P (mg/L)	Pox (mg/kg)	a = New Conc Fe (mg/L)	Feox (mg/kg)	a = New Conc Al (mg/L)	Alox (mg/kg)
Al 8 t=0 Inlet	1.25	6.6	664	70.3	7031	55.4	5539
Al 8 t=0 Inlet	1.25	4.0	396	64.3	6427	78.2	7816
Al 8 t=0 Inlet	1.25	3.4	341	64.6	6458	56.5	5654
Al 8 t=0 Inlet	1.25	3.7	369	61.6	6160	75.5	7548
Al 8 t=0 Inlet	1.25	4.6	458	65.0	6504	93.5	9350
Al 8 t=0 Inlet AVERAGES		4.46	445.81	65.16	6516.04	71.81	7181.40
Al 8 t=0 Outlet	1.25	7.4	739	86.2	8616	64.4	
Al 8 t=0 Outlet	1.25	5.8	578	71.2	7122	133.5	13346
Al 8 t=0 Outlet	1.25	6.2	619	63.9	6393	170.2	17021
Al 8 t=0 Outlet	1.25	6.5	651	70.5	7052	175.8	17580
Al 8 t=0 Outlet	1.25	5.6	557	65.5	6553	118.6	11863
Al 8 t=0 Outlet AVERAGES		6.29	629.02	71.47	7147.02	132.50	14952.65
Al 8 Combo Air Dry t=0	1.25	4.8	483	66.3	6626	78.7	7874
Al 8 t=0 ALL Averages		5.32	532.45	68.13	6812.86	100.03	10359.17
Al 8 t=0 Std. Deviation		1.32	131.91	6.73	672.82	43.43	4405.07
N		11.00	11.00	11.00	11.00	11.00	9.00
Al 8 t=4 Inlet	1.25	6.9	691	61.6	6163	46.0	4601
Al 8 t=4 Inlet	1.25	4.3	430	73.5	7349	61.1	6113
Al 8 t=4 Inlet	1.25	4.6	462	66.3	6627	74.3	7429
Al 8 t=4 comp Inlet AVERAGES		5.28	527.65	67.13	6712.92	60.48	6047.85
Al 8 t=4 Middle	1.25	8.9	888	73.6	7363	94.1	9414
Al 8 t=4 Middle	1.25	6.4	635	71.7	7174	154.0	15399
Al 8 t=4 Middle	1.25	6.8	677	68.7	6865	159.9	15990
Al 8 t=4 comp Middle AVERAGES		7.34	733.56	71.34	7134.10	136.01	13601.07
Al 8 t=4 Outlet	1.25	8.0	802	78.7	7866	67.5	6748
Al 8 t=4 Outlet	1.25	6.1	607	70.4	7036	120.8	12079
Al 8 t=4 Outlet	1.25	5.9	590	70.3	7026	112.8	11278
Al 8 t=4 comp Outlet AVERAGES		6.66	666.12	73.09	7309.28	100.35	10035.29
Al 8 t=4 ALL Averages		6.42	642.44	70.52	7052.10	98.95	9894.73
Al 8 t=4 Std. Deviation		1.46	146.21	4.83	483.34	40.72	4072.37
N		9.00	9.00	9.00	9.00	9.00	9.00

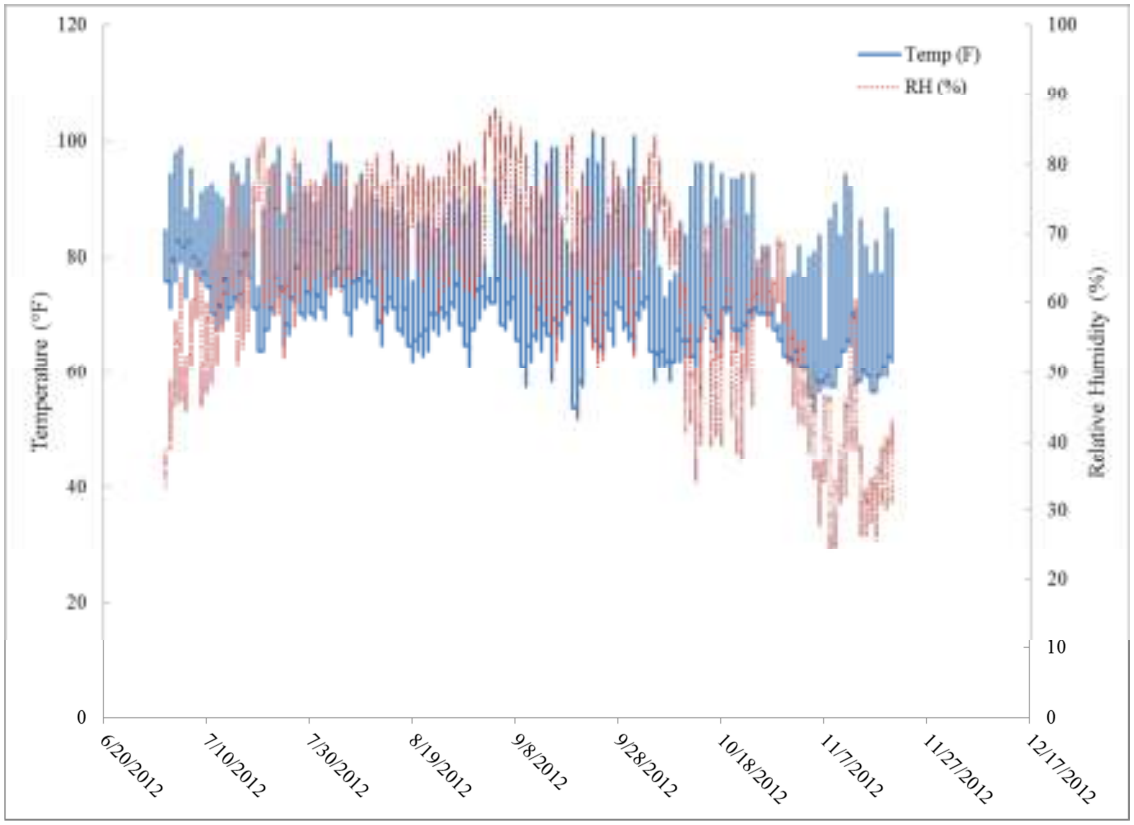

Figure B.1. Temperature and relative humidity data from phase II study.

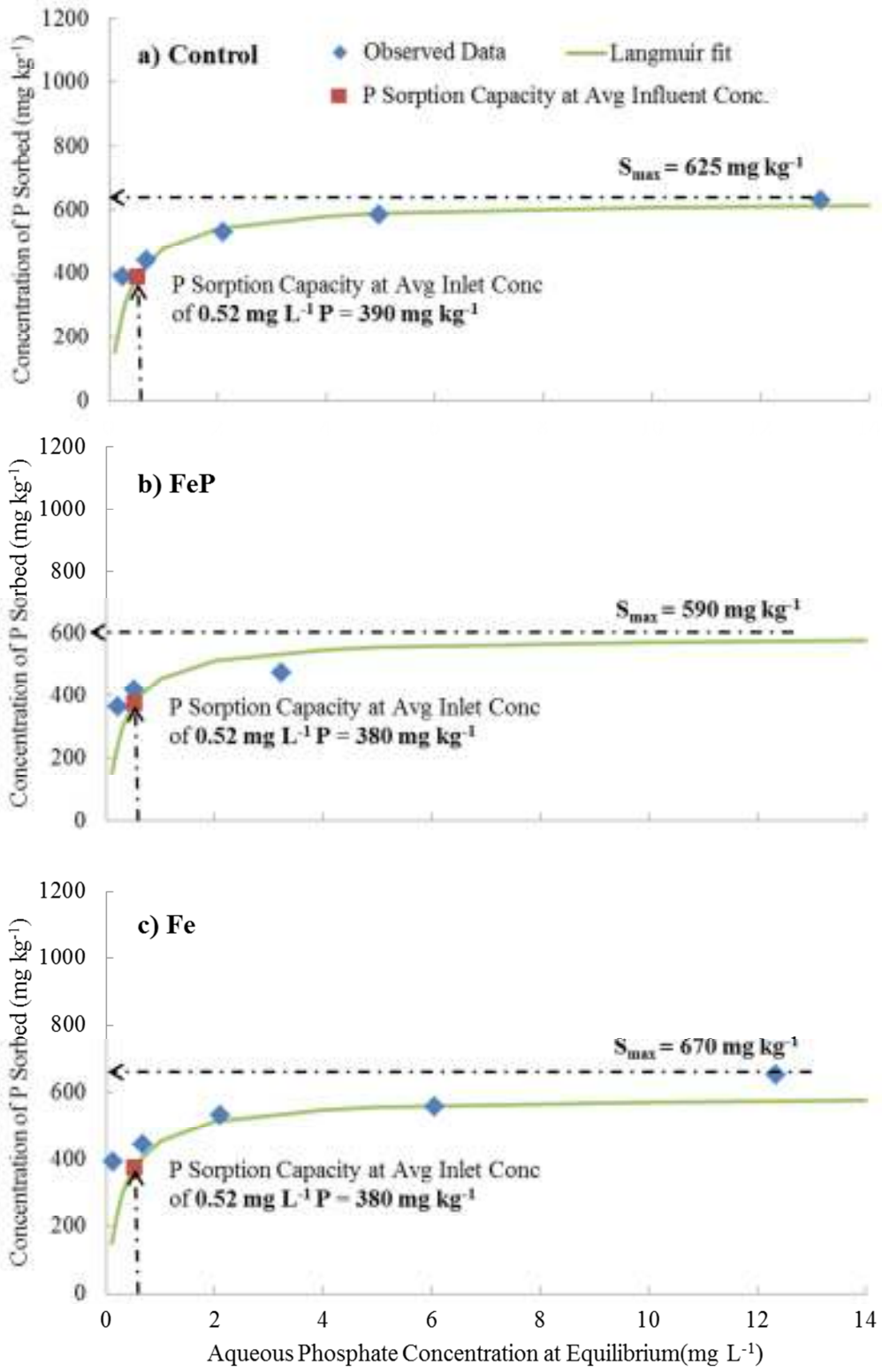

Figure B.2. P sorption isotherm data for the control (a), FeP (b), and Fe (c) mesocosms.

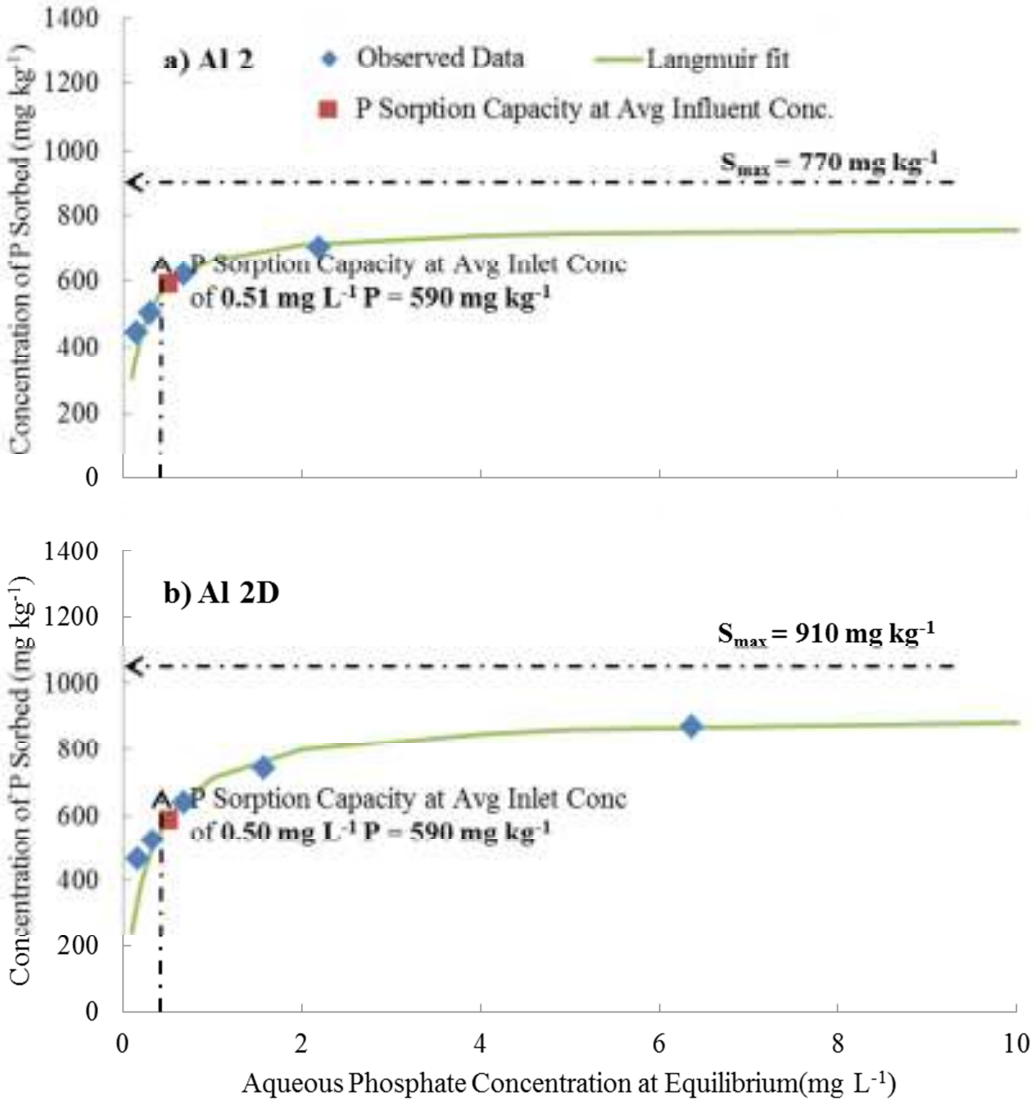

Figure B.3. P sorption isotherm data for the Al 2 (a) and Al 2D (b) mesocosms.

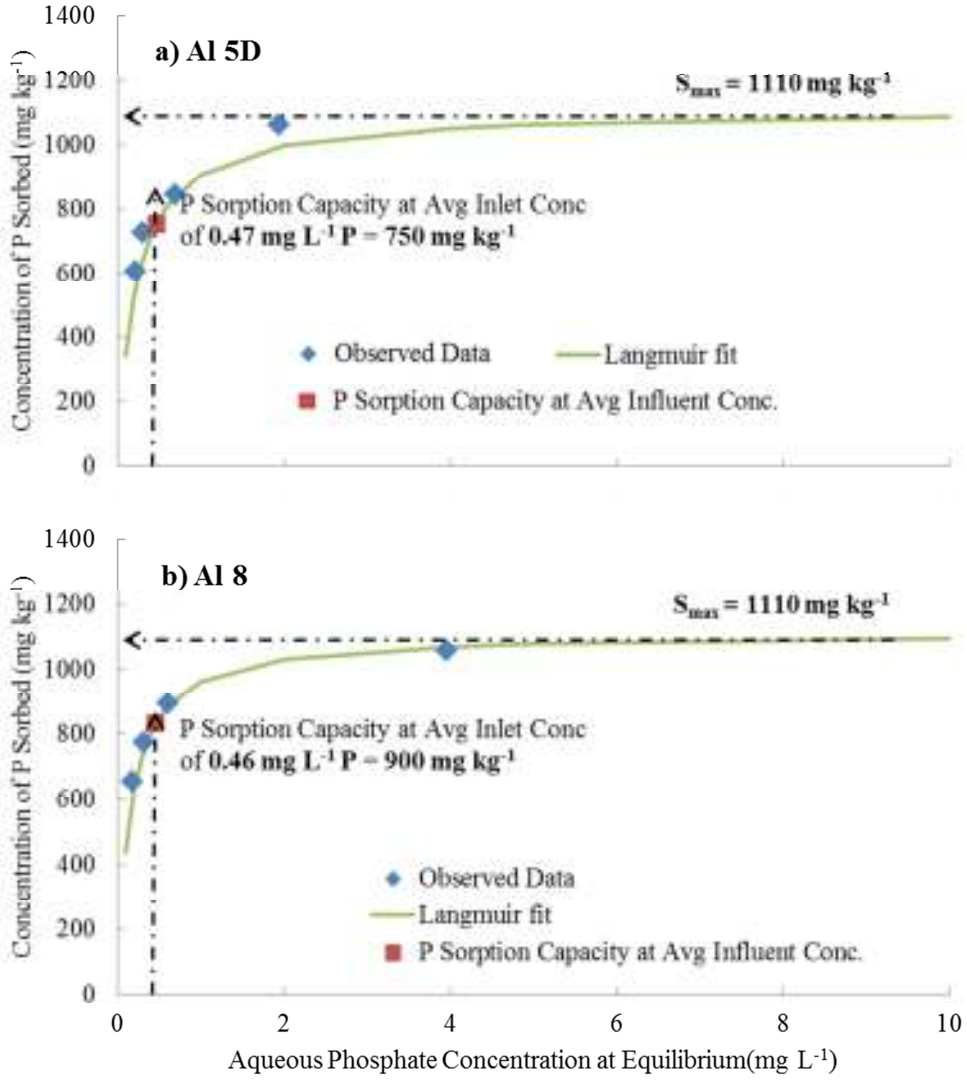

Figure B.4. P sorption isotherm data for the Al 5D (a) and Al 8 (b) mesocosms.

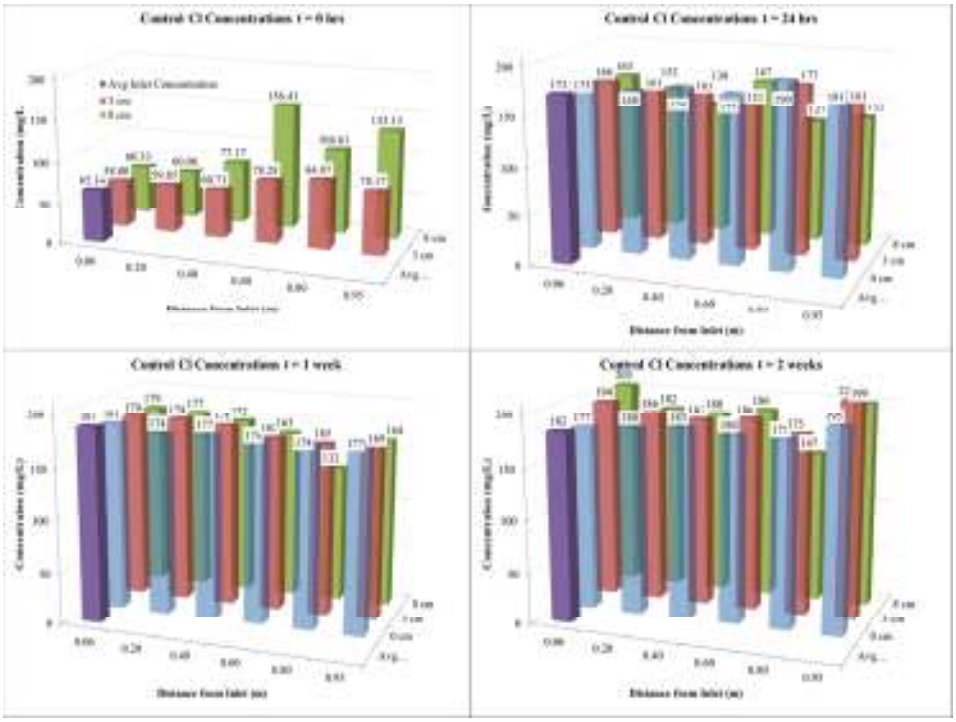

Figure B.5. Chloride tracer study, 3D graphs showing equilibrium had fully been reached by week two for the control mesocosm.

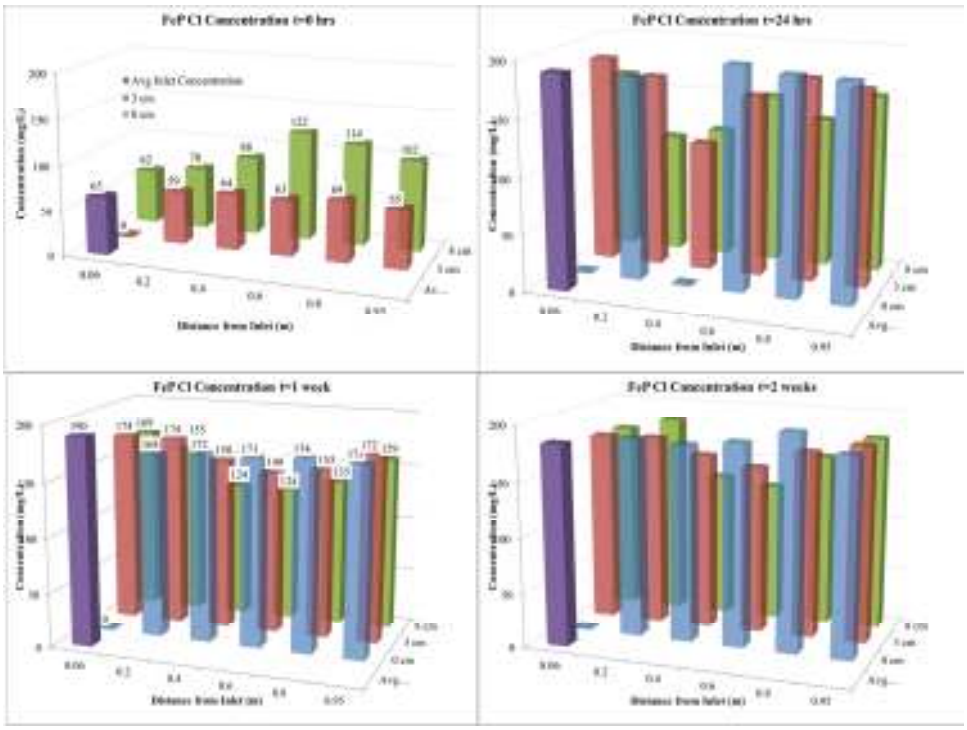

Figure B.6. Chloride tracer study, 3D graphs showing equilibrium had fully been reached by week two for the FeP mesocosm.

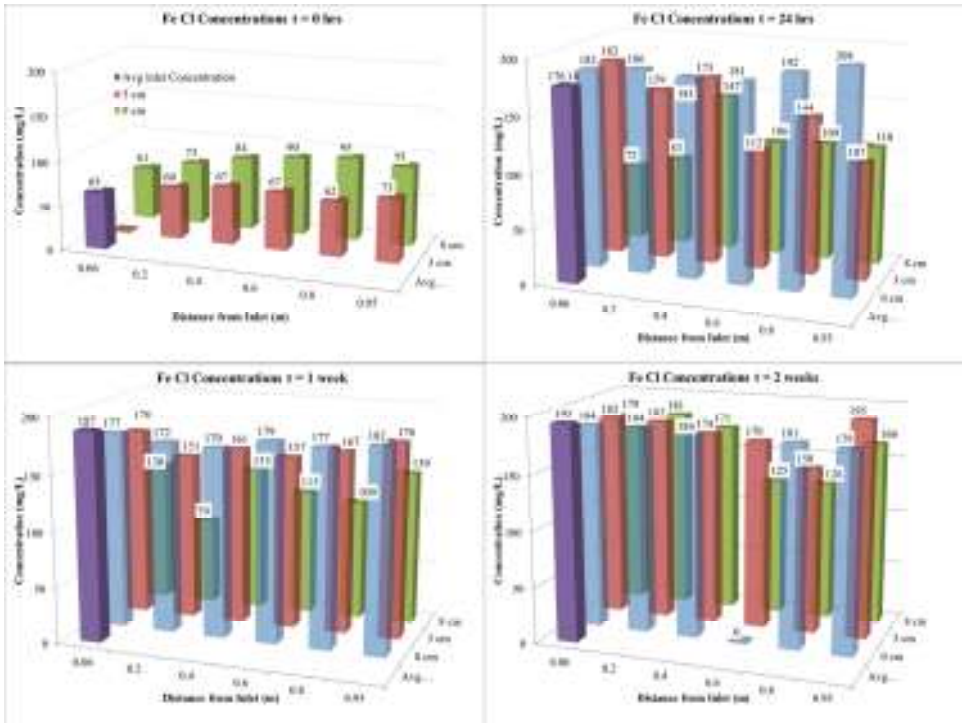

Figure B.7. Chloride tracer study, 3D graphs showing equilibrium had fully been reached by week two for the Fe mesocosm.

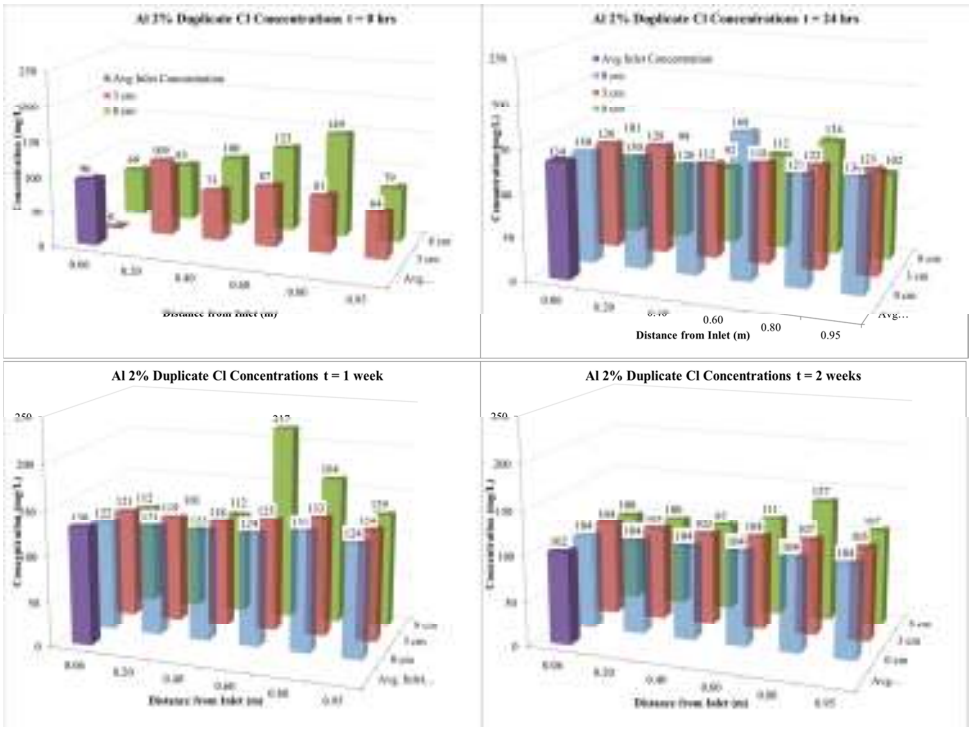

Figure B.8. Chloride tracer study, 3D graphs showing equilibrium had fully been reached by week two for the Al 2 mesocosm.

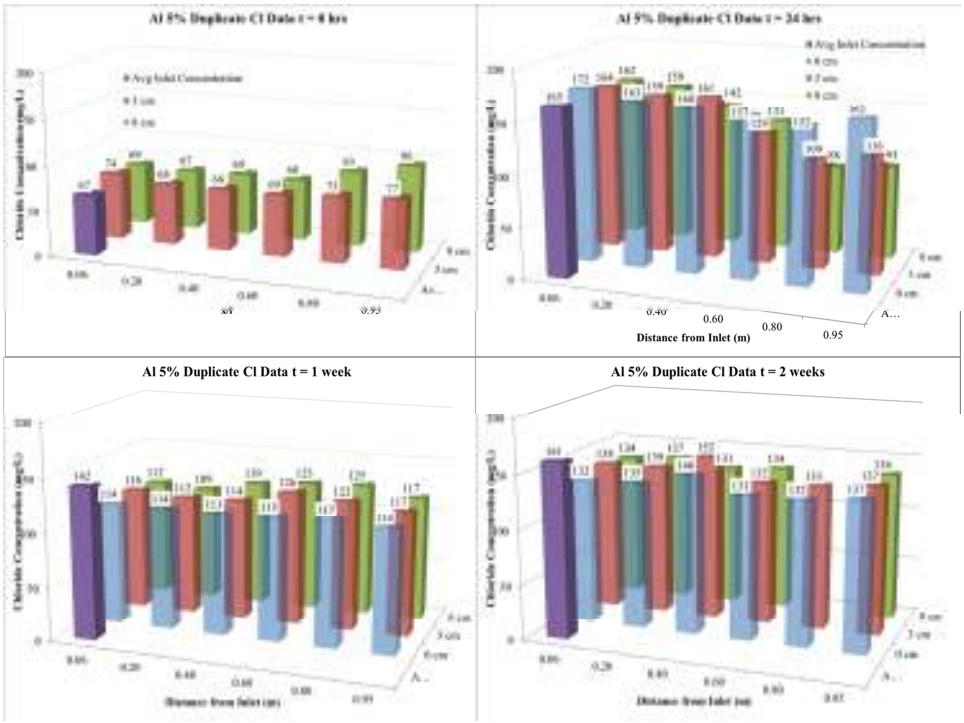

Figure B.9. Chloride tracer study, 3D graphs showing equilibrium had fully been reached by week two for the Al 5D mesocosm.

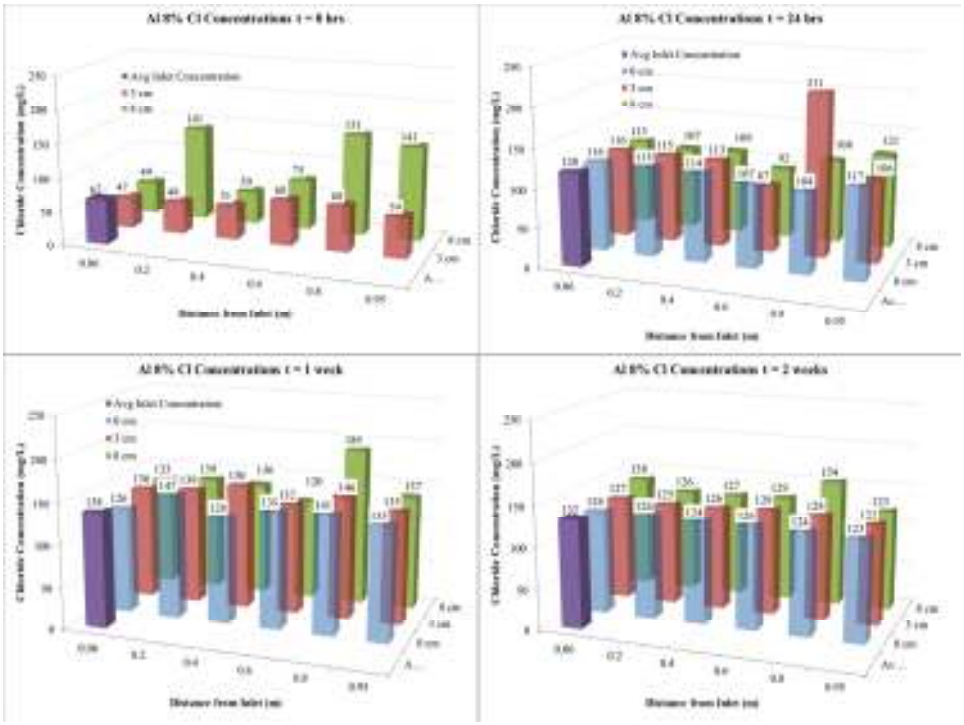

Figure B.10. Chloride tracer study, 3D graphs showing equilibrium had fully been reached by week two for the Al 8 mesocosm.

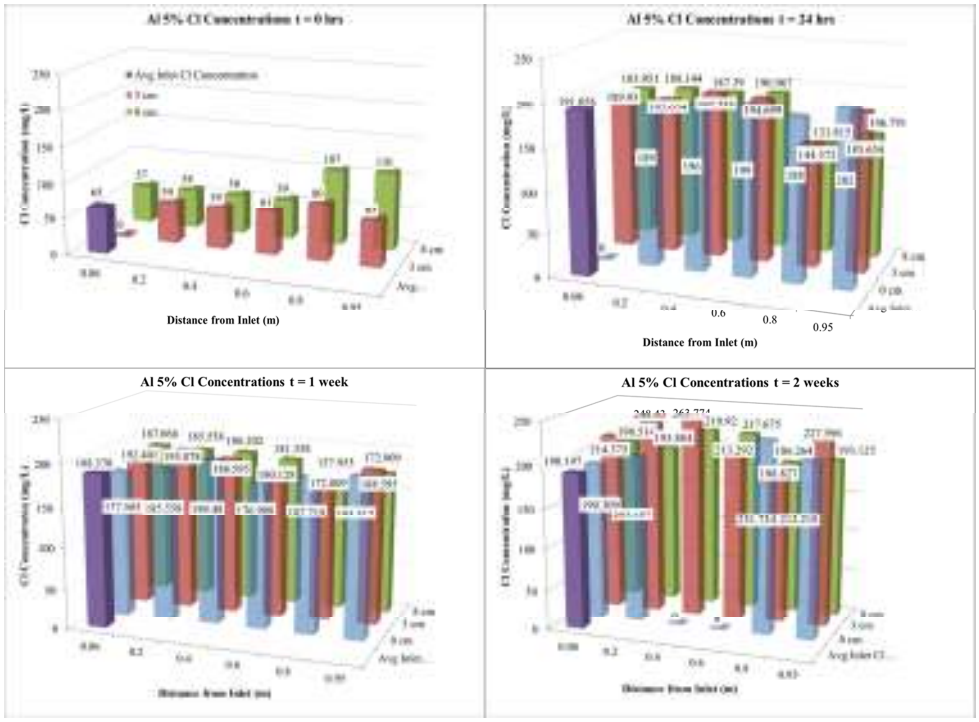

Figure B.11. Chloride tracer study, 3D graphs showing equilibrium had fully been reached by week two for the Al 5 mesocosm.

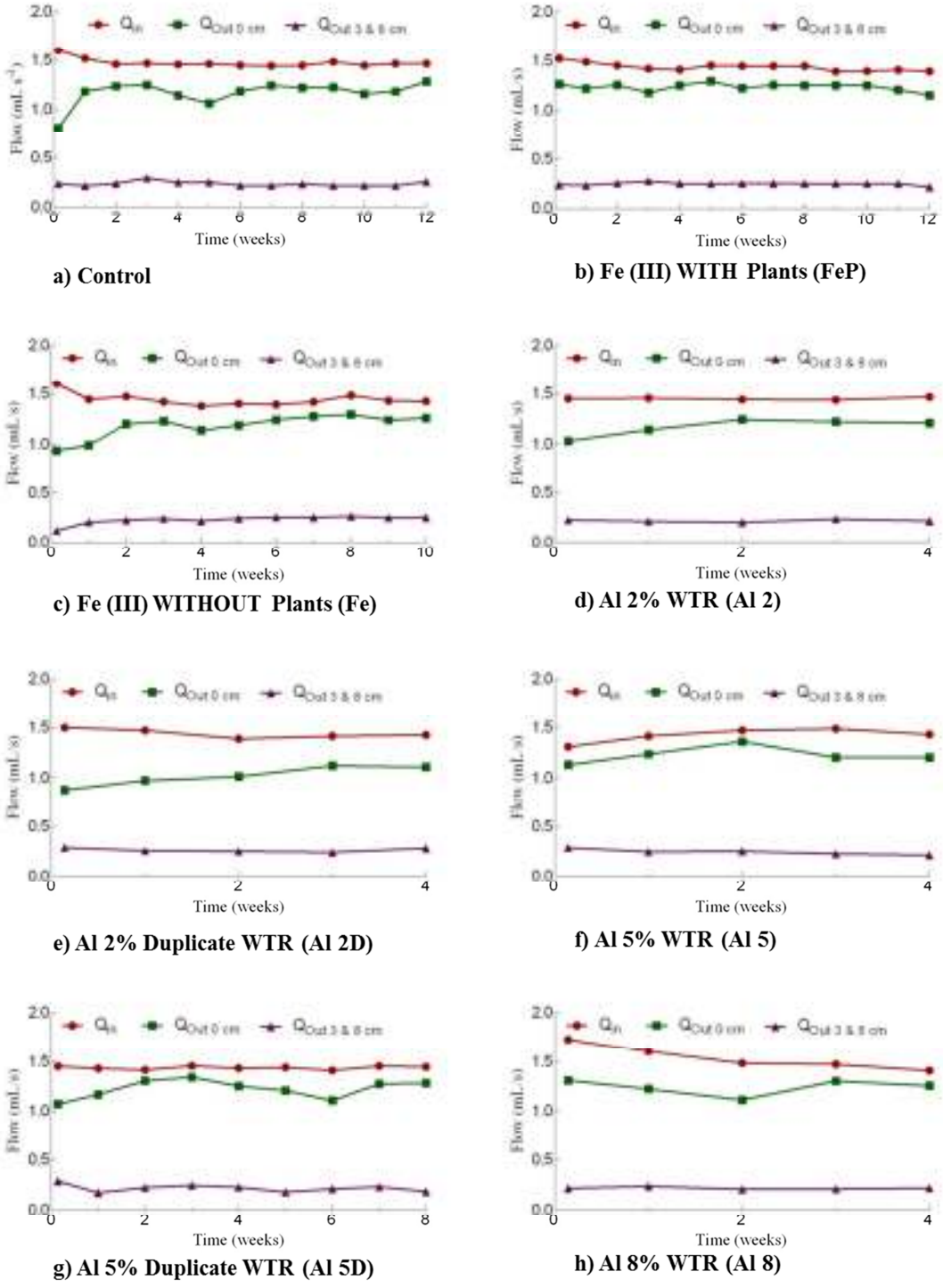

Figure B.12. Typical flow rates for all mesocosm studies (a,b,c,d,e,f) over respective durations.

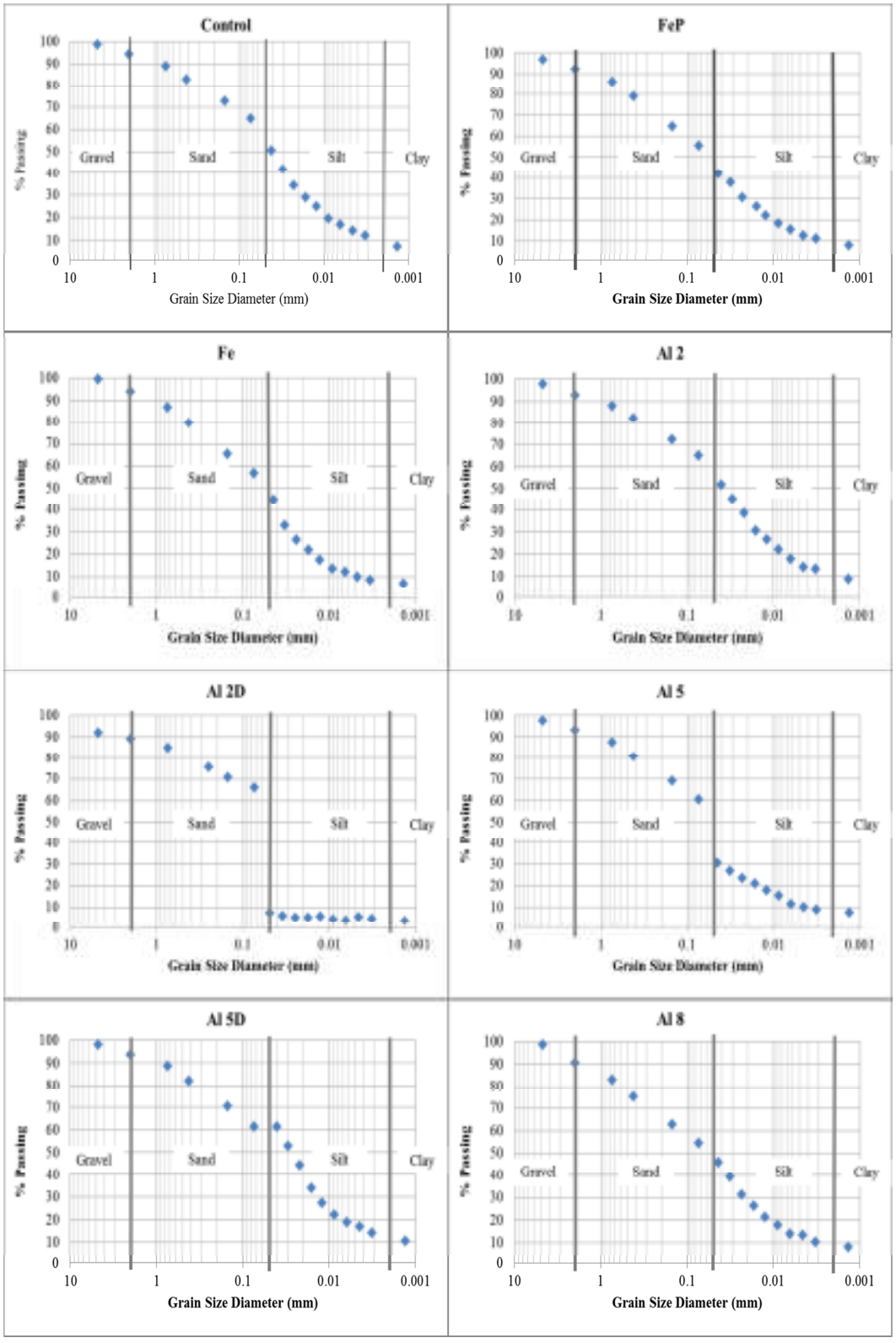

Figure B.13. Results from the hydrometer and grain size analysis for each mesocosm initial soil sample.

APPENDIX C: Model Results

Additional contour plots of SRP and chloride data: Phase II

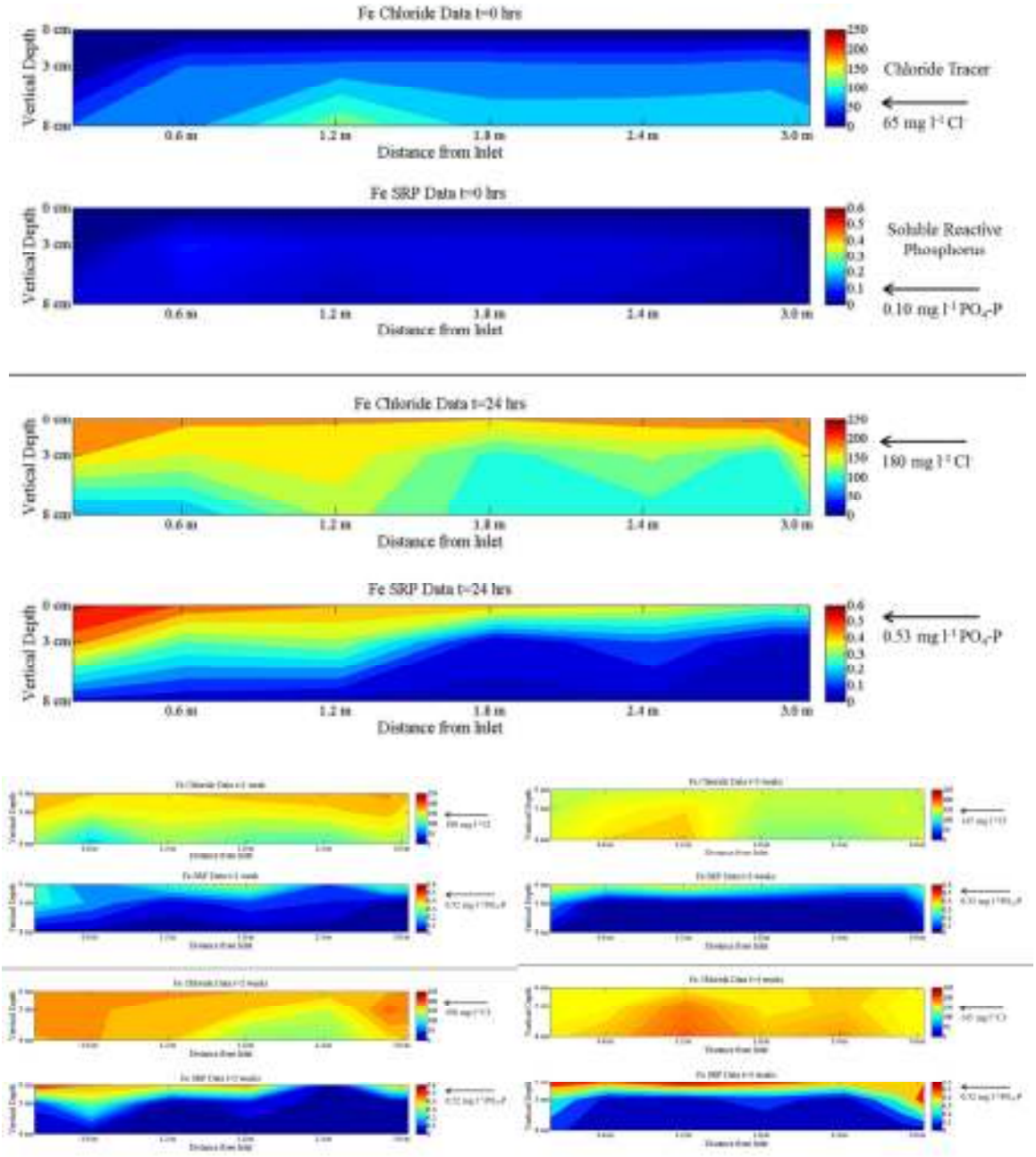

Figure C.1. Contour plot of actual SRP and chloride concentrations at each port location over a four week period for the Fe mesocosm. Top contour plot is of chloride results and bottom contour represents SRP removal.

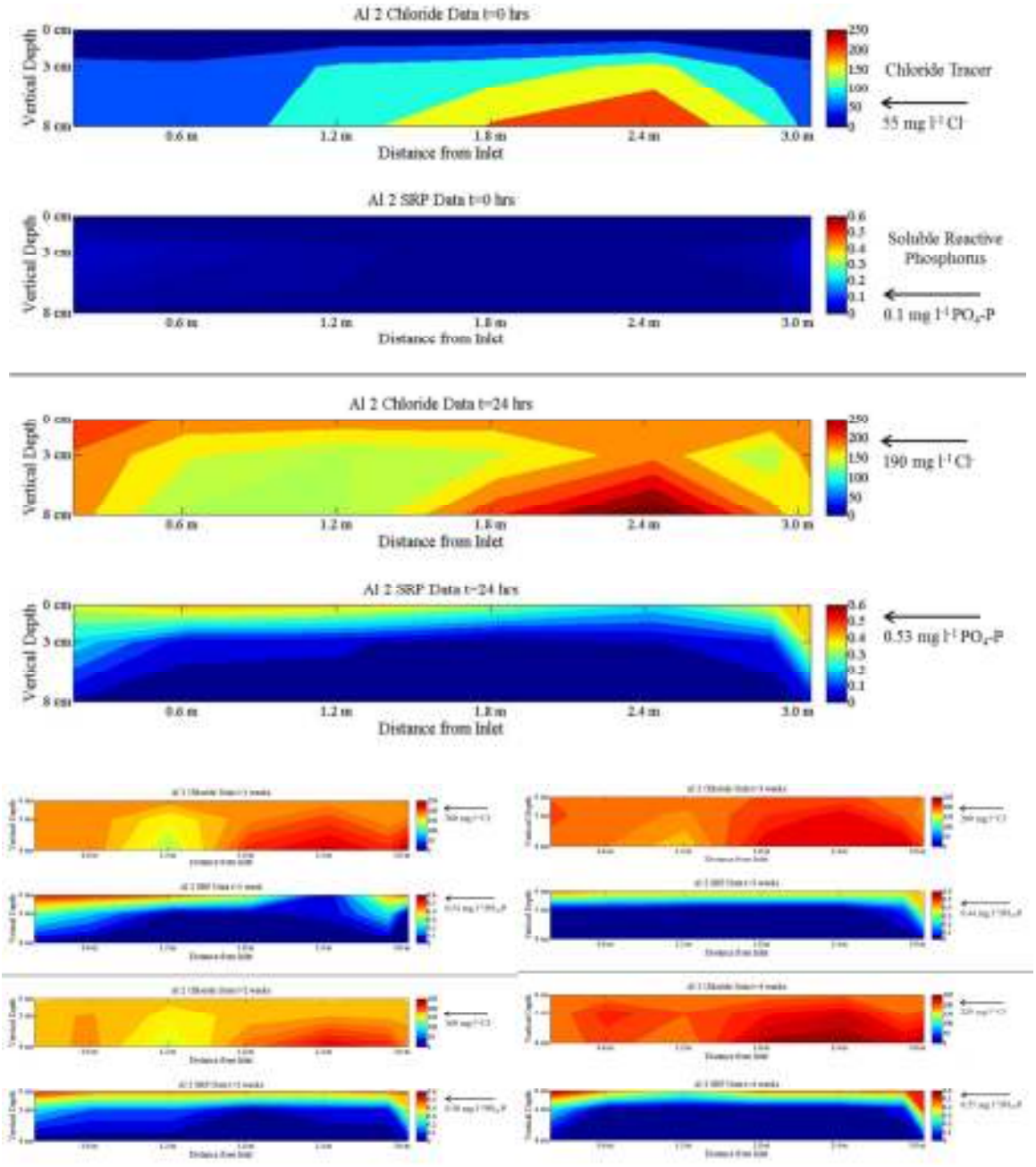

Figure C.2. Contour plot of actual SRP and chloride concentrations at each port location over a four week period for the Al 2 mesocosm. Top contour plot is of chloride results and bottom contour represents SRP removal.

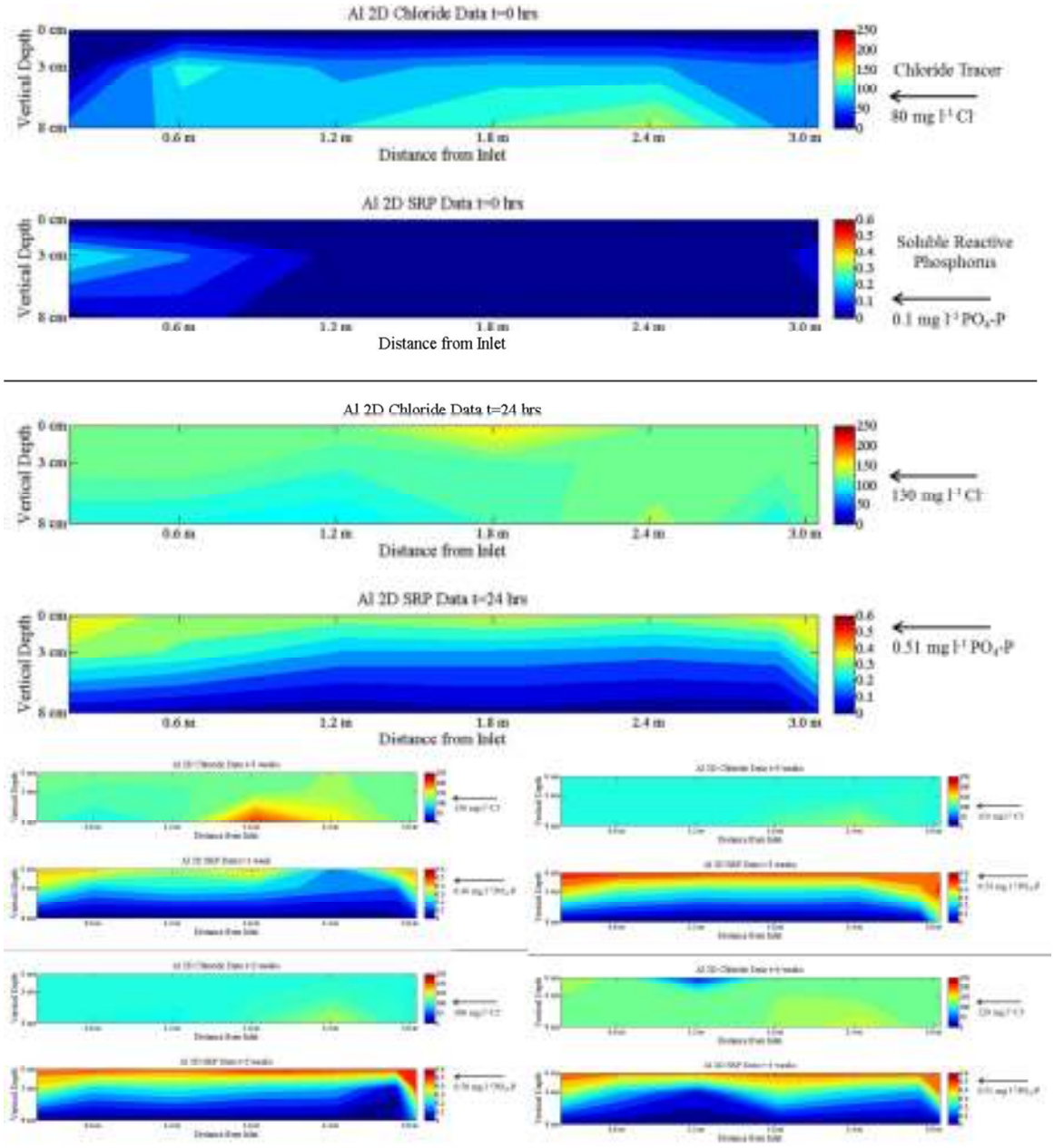

Figure C.3 Contour plot of actual SRP and chloride concentrations at each port location over a four week period for the Al 2D mesocosm. Top contour plot is of chloride results and bottom contour represents SRP removal.

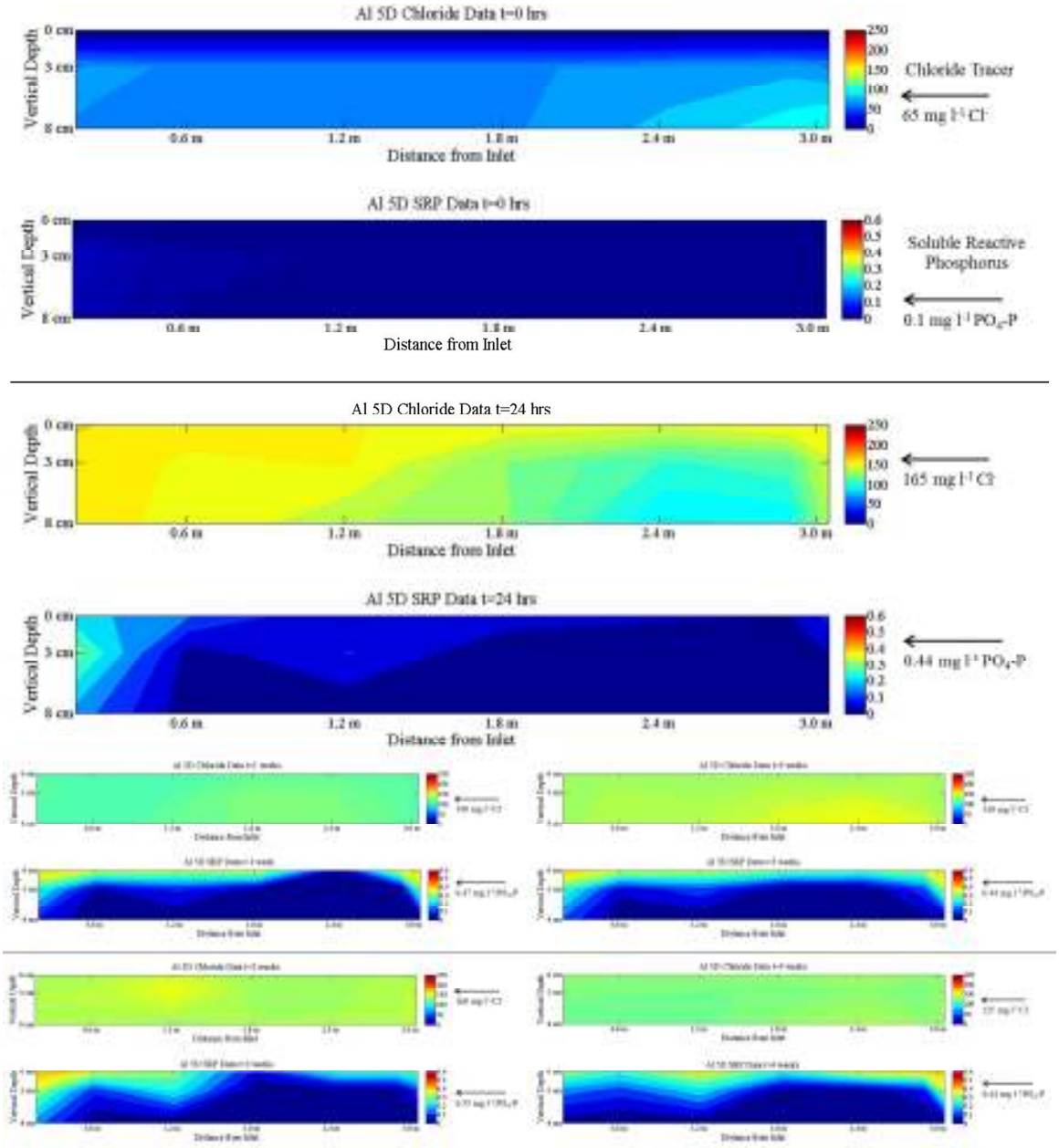

Figure C.4. Contour plot of actual SRP and chloride concentrations at each port location over a four week period for the Al 5D mesocosm. Top contour plot is of chloride results and bottom contour represents SRP removal.

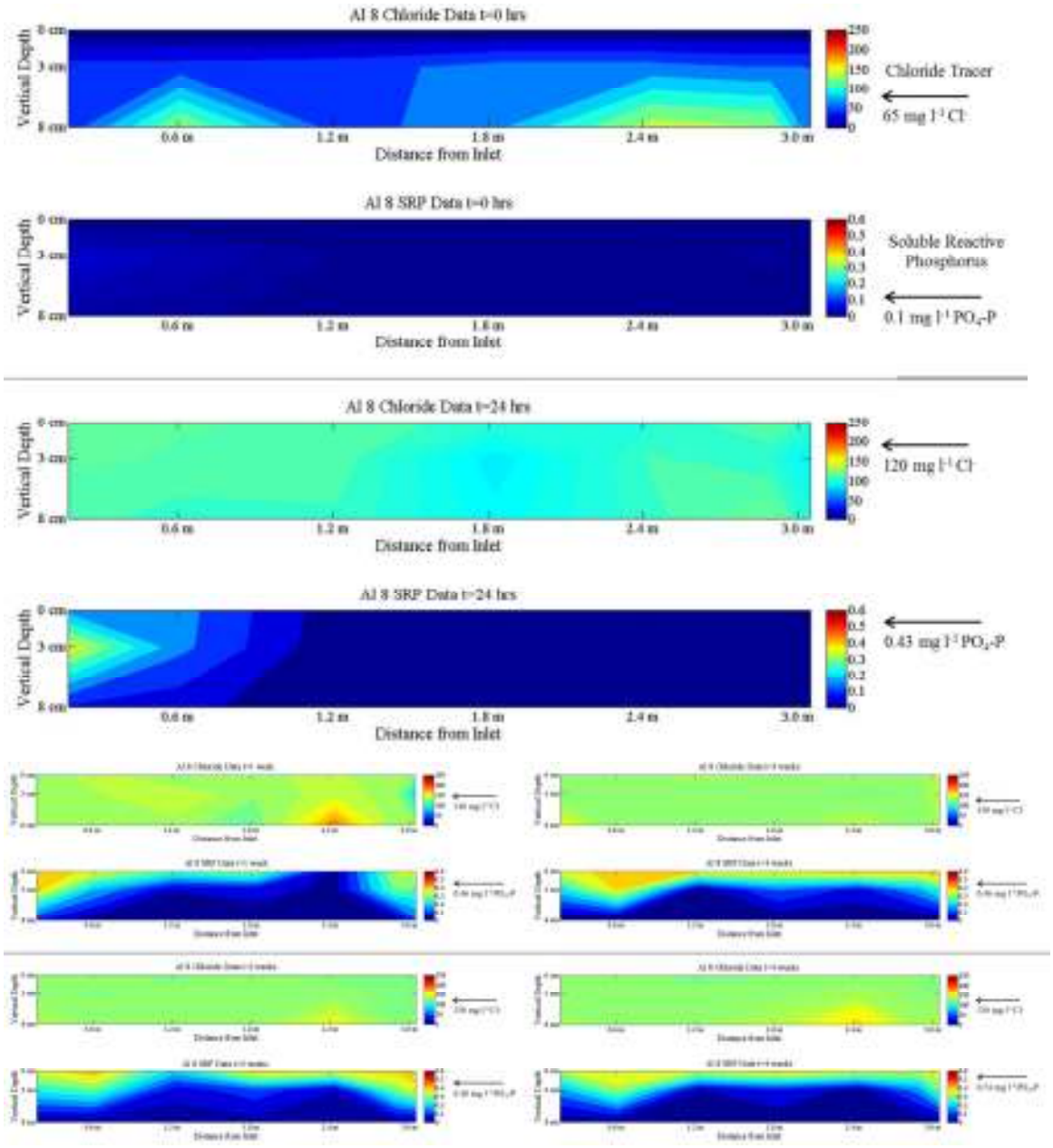

Figure C.5 Contour plot of actual SRP and chloride concentrations at each port location over a four week period for the Al 8 mesocosm. Top contour plot is of chloride results and bottom contour represents SRP removal.

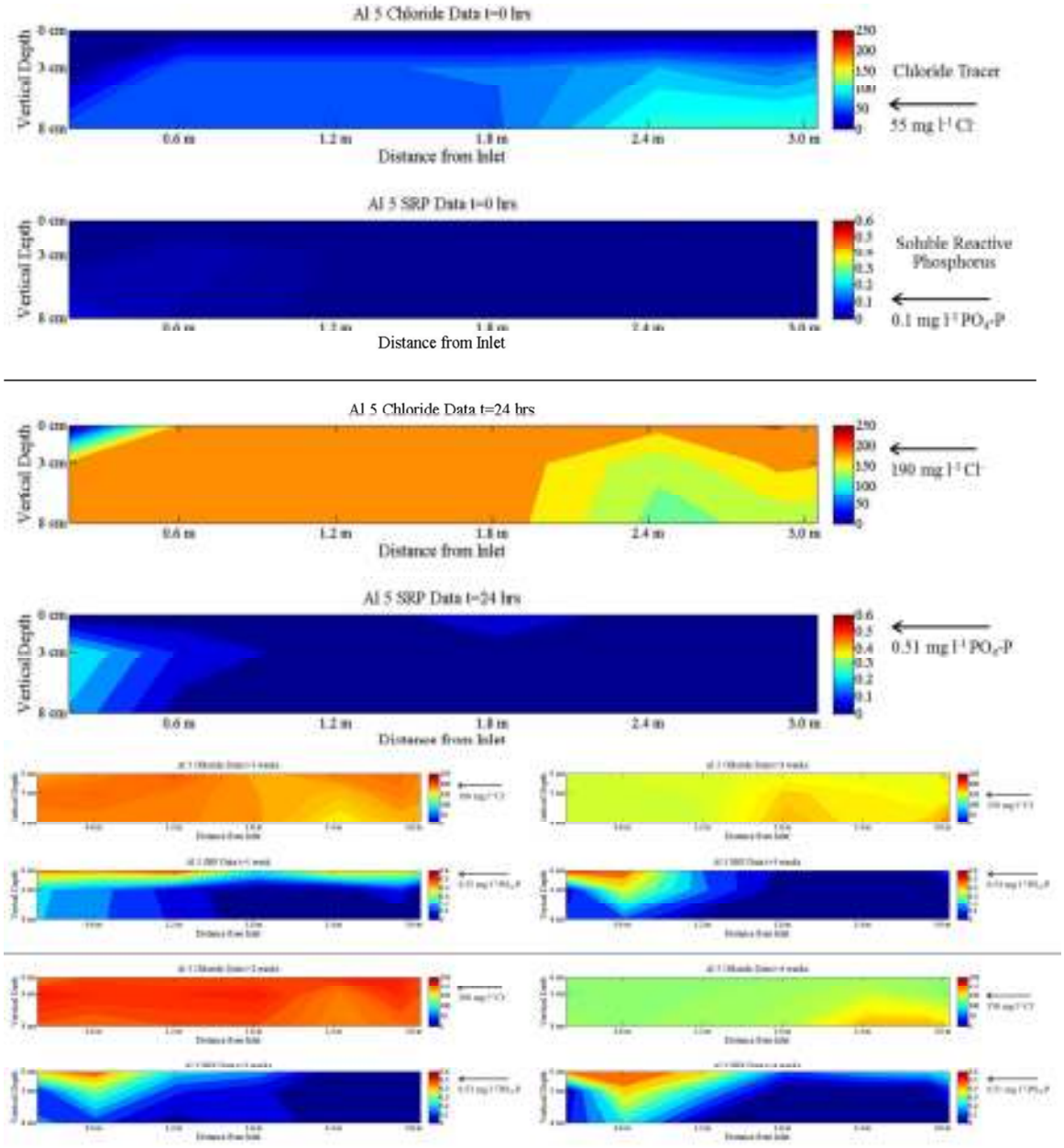

Figure C.6. Contour plot of actual SRP and chloride concentrations at each port location over a four week period for the Al 5 mesocosm. Top contour plot is of chloride results and bottom contour represents SRP removal.